5-2015

Single-Walled Carbon Nanotube Arrays for High Frequency Applications

Asmaa Elkadi
University of Arkansas, Fayetteville

Single-Walled Carbon Nanotube Arrays for High Frequency Applications

Single-Walled Carbon Nanotube Arrays for High Frequency Applications

A dissertation submitted in partial fulfillment
of the requirements for the degree of
Doctor of Philosophy in Electrical Engineering

by

Asmaa Elkadi
Cairo University
Bachelor of Science in Electronics and Communications Engineering, 2004
Cairo University
Master of Science in Electronics and Communications Engineering, 2008

May 2015
University of Arkansas

This dissertation is approved for recommendation to the Graduate Council

Dr. Samir M. El-Ghazaly, Professor
Dissertation Director

Dr. Hameed A. Naseem, Professor
Committee Member

Dr. Douglas Spearot, Associate Professor
Committee Member

Abstract

This dissertation presents a thorough analysis of semiconducting Single-Walled Carbon Nanotube-based devices, followed by a test structure fabrication and measurements.

The analysis starts by developing an individual nanotube model, which is then generalized for many nanotubes and adding the parasitic elements. The parasitic elements appear when forming the device electrodes degrade the overall performance.

The continuum model of an individual nanotube is developed. A unique potential function is presented to effectively describe the electron distribution in the carbon nanotube subsequently facilitating solving Schrödinger's equation to obtain the energy levels, and to generalize the model for many nanotubes.

It is shown that the overall energy band gap is inversely proportional to the number of nanotubes due to the coupling between the nanotubes. The coupling is then enhanced by applying an external transverse electric field, which controls the energy band gap. The electric field is represented as a function of the number of nanotubes per device showing that the higher the number of nanotubes, the lower the value of the electric field needed to alter the energy band gap. An electromagnetic model is developed for the contact where a detailed parametric study of the length, thickness, and conductivity of the contact area is presented. The overlap length between the nanotube and the metal of the contact appears to be the dominating factor.There is a clear inverse proportionality between overlap length and contact resistance to reach a minimum value after an effective overlap length. An equation is developed to describe the conductance as a function of the number of nanotubes per device.

A four-electrode test structure is fabricated using both photolithography and electron-beam-lithography. The carbon nanotubes are deposited using the dielectrophoresis method for many devices simultaneously to provide a sheet resistance as low as 10 KΩ/□. The I-V characteristics

are measured with and without change in the transverse electric field. It shows a change in the current reflecting the changes in the energy band gap discussed earlier. There are many applications for the results presented in this dissertation such as optimizing devices operating in the THz frequency range.

Acknowledgment

الْحَمْدُ لِلَّهِ الَّذِي هَدَانَا لِهَٰذَا وَمَا كُنَّا لِنَهْتَدِيَ لَوْلَا أَنْ هَدَانَا اللَّهُ ۖ الأعراف الآية: 43

All the praises and thanks be to Allah, Who has guided us to this, and never could we have found guidance, were it not that Allah had guided us. Qur'an 7:43

I am extremely grateful to my advisor Dr. Samir El-Ghazaly for his continuous mentoring and guidance throughout my Ph.D. work. Thank you for being the teacher who cares as a real father.

I would like to thank my committee members Dr. Hameed Naseem, Dr. Shui-Qing (Fisher) Yu, and Dr. Douglas Spearot for their time and fruitful discussions on my research.

Dr. Magda El-Shenawee, thank you for your continuous support and for always giving me sincere advices.

I don't believe there are any words that could be put together to thank my Mom for making me the person I am today. You have always been the support throughout the hardships of the journey. Love you, Mom!

To my friends Ayat Shaban, Asmaa Abdel Khalek, Samah Johnson, Sabina Koukourinkova, and Mona Adel; thanks for being the sisters I have never had and for being always by my side. I don't know how my life would have been without having you.

Finally, Thanks to Dr. Madan Dubey for approving my manuscripts for publication. Research was sponsored by the Army Research Laboratory under Cooperative Agreement Number W911NF-10-2-0072. The views and conclusions contained in this are those of the authors and should not be interpreted as representing the official policies, either expressed or implied, of the Army Research Laboratory or the U.S. Government. The U.S. Government is authorized to

Table of Contents

Chapter I Introduction

1. Electronic Band structure of SWCNT **1**
2. Growth Techniques **4**
3. Separation **5**
4. Alignment **6**
5. Dissertation Structure **7**

Chapter II Aligned semiconducting single-walled carbon nanotubes: Semi-analytical solution

1. Introduction **12**
2. Theoretical Background **14**
3. Model for s-SWCNT **17**
    A. Analytical potential function **17**
    B. Solving Schrödinger equation **18**
4. Coupling Between Two Carbon Nanotubes **20**
    A. Without electric field **20**
    B. With applied transverse electric field **25**
5. Conclusion **28**

Chapter III A. Electronic Properties of Double-Walled Carbon Nanotube

1. Introduction **37**
2. Analytical Potential Function **38**
3. Simulations and Results **40**
4. Conclusion **42**

B. Energy Band Gap Study of Semiconducting Single Walled Carbon Nanotube Bundle

1. Introduction **47**
2. Analytical Potential Function **49**
3. Simulations and Discussions **50**
4. Conclusion **60**

Chapter IV Single-Walled-Carbon-Nanotube Contact Resistance: Analysis and RF Performance

1. Introduction **65**
2. Model **66**
   - A. Electrostatic Analysis **67**
   - B. RF Analysis **73**
3. Results **76**
4. Conclusion **77**

Chapter V A. Fabrication Technique of Highly Dense Aligned Semiconducting Single-Walled Carbon Nanotubes Devices

1. Introduction **81**
2. Fabrication Technique **82**
3. Results and Discussion **84**
4. Conclusion **85**

B. Arrays of Single-Walled Carbon Nanotubes in RF Devices: Analysis and Measurements

1. Introduction **89**

2. Model **91**

A. Individual SWCNT **91**

B. Arrays of SWCNTs **94**

1. Resistive Elements **94**

2. Capacitive Elements **98**

3. Measurements and Discussions **101**

A. Fabrication **101**

B. Measurements **103**

4. Conclusion **106**

Chapter VI Tuning the Energy Band Gap of Aligned Arrays of semiconducting single-walled carbon nanotubes for THz Applications

1. Introduction **113**

2. Analytical Potential Function **114**

3. Quantum Cascaded Laser Analogy **116**

4. The Current **119**

5. Measurements **123**

6. Conclusion **127**

Chapter VII Conclusion **131**

List of Publications

[1] **"Aligned semiconducting single-walled carbon nanotubes: Semi-analytical solution"**
A Elkadi, E Decrossas, SQ Yu, HA Naseem, SM El-Ghazaly,
Journal of applied physics 114 (11), 114306, 1, 2013.

[2] **"Arrays of Single-Walled Carbon Nanotubes in RF Devices: Analysis and Measurements"**
A Elkadi, S El-Ghazaly,
IEEE Transactions on Electromagnetic Compatibility.

[3] **"Single-Walled-Carbon-Nanotube Contact Resistance: Analysis and RF Performance"**
A Elkadi, S El-Ghazaly, Under Revision.

[4] **"Controlling the energy band gap of aligned semiconducting single-walled carbon nanotubes for THz modulator"**
A Elkadi, E Decrossas, SQ Yu, HA Naseem, SM El-Ghazaly
7th European Microwave Integrated Circuits Conference (EuMIC), 2012.

[5] **"Fabrication Technique of Highly Dense Aligned Semiconducting Single-Walled Carbon Nanotubes Devices"**
A Elkadi, E Decrossas, SM El-Ghazaly,
IEEE Photonics Conference (IPC), 485 – 486, 1, 2012.

[6] **"Carbon nanotube based prototype as THz time domain sources/detectors"**
E Decrossas, **A Elkadi**, SM El-Ghazaly,
37th Infrared, Millimeter, and Terahertz Waves (IRMMW-THz), 2012.

[7] **"Electronic Properties of Double Walled Carbon Nanotube"**
A Elkadi, S El-Ghazaly,
Middle East Conference on Antennas and Propagation (MECAP-2012), 2012.

[8] **"Energy Band Gap Study of Semiconducting Single Walled Carbon Nanotube Bundle"**
A Elkadi, E Decrossas, S El-Ghazaly,
IEEE International Symposium on Electromagnetic Compatibility-EMC 2013-Denver CO.

[9] "On the Contact Resistance of Single-Walled Carbon Nanotubes in RF devices"
A Elkadi, S El-Ghazaly
IEEE International Microwave Symposium, Tampa, FL, June 2014.

[10] **"Modeling of Carbon Nanotubes-Metal Contact Losses in Electronic Devices"**
A Elkadi, S El-Ghazaly,
IEEE International Symposium on Electromagnetic Compatibility - EMC 2014, Raleigh NC 2014.

Chapter I. Introduction

Carbon nanotubes have attracted the attention of researchers due to their substantial properties along their axis such as one dimensional confined carriers and photons and high electrical conductivity. In addition, carbon nanotubes have tremendous mechanical properties such as high thermal conductivity and tensile strength [1]. Single-walled carbon nanotubes can be regarded as a rolled graphene sheet and it is either semiconducting or metallic based on its chiral angle determined by rolling indices (*m, n*). A semiconducting single-walled carbon nanotube (s-SWCNT) has a typical diameter of 0.5 to 2 nm, and its energy gap is inversely proportional to its diameter in the range of 1.4 to 0.35 eV [2].

Aligned s-SWCNTs demonstrated promising responses in various devices [3]-[5]. It led researchers to compare the enhanced properties of aligned multi s-SWCNTs to individual ones. Studying aligned s-SWCNTs theoretically is a complex problem due to the lack of a well-defined potential function of individual s-SWCNT. The electronic structure of the nanotube will be discussed followed by the fabrication aspects that might hinder the performance of the carbon nanotube-based devices.

1. Electronic Band structure of SWCNT

Carbon nanotube is a rolled single atomic layer of carbon. Based on the way this atomic layer is rolled, it will define the boundary conditions and hence the properties of the carbon nanotube. Fig. 1 shows the different chiral vector $\vec{C} = n\vec{a}_1 + m\vec{a}_a$ the nanotube could take. The common types are either armchair or zigzag.

The one dimensional energy dispersion relation of SWCNT is defined by

$$E\ (k) = \pm V_{pp\pi}\sqrt{1 + 4\cos\left(\frac{k_x\sqrt{3a}}{2}\right)\cos\left(\frac{k_y a}{2}\right) + 4\cos^2\left(\frac{k_y a}{2}\right)} \quad (1)$$

where $a = \sqrt{3}a_{c-c}$, $a_{c\text{-}c}$ is the lattice constant and $V_{pp\pi}$ is the nearest neighbor overlap integral between carbon atoms*(2.5-3 eV).*[6]

A. Armchair SWCNT

The periodic boundary conditions are satisfied by

$$e^{ik_x N_x\sqrt{3}a} = 1 \Rightarrow k_x N_x\sqrt{3}a = 2m\pi \quad \therefore k_x = \frac{m}{N_x}\frac{2\pi}{\sqrt{3}a}, m = 1,2,\ldots..N_x$$

Substitute in (1)

$$\therefore E = \sqrt{|h_o|^2} = \pm V_{pp\pi}\sqrt{1 \pm 4\cos\left(\frac{m\pi}{N_x}\right)cos\left(\frac{ka}{2}\right) + 4cos^2\left(\frac{ka}{2}\right)}$$

where $h_o = V_{pp\pi}\left\{e^{ik_x a/\sqrt{3}} + 2e^{-ik_x a/2\sqrt{3}}cos\left(\frac{k_y a}{2}\right)\right\}$, $a = 1.42\text{Å}\sqrt{3}$ is the lattice constant, and $V_{pp\pi} = 2.7eV$ is the hopping integral constant. Hence $-\pi < ka < \pi$

B. Zigzag SWCNT

The periodic boundary condition are satisfied by

$$e^{ik_y N_y a} = 1 \Rightarrow k_y N_y a = 2m\pi \quad \therefore k_y = \frac{m}{N_y}\frac{2\pi}{a}, m = 1,2,\ldots..N_y$$

Substitute in (1)

$$\therefore E = \sqrt{|h_o|^2} = \pm t\sqrt{1 \pm 4\cos\left(\frac{\sqrt{3}k\ \ a}{2}\right)cos\left(\frac{m\pi}{N_y}\right) + 4cos^2\left(\frac{ka}{2}\right)}$$

hence $\frac{-\pi}{\sqrt{3}} < ka < \frac{\pi}{\sqrt{3}}$

Zigzag Carbon nanotubes have special characteristic that if $N_y=3n$, where n is integer, the carbon nanotube will behave like metallic one. Otherwise it will be semiconducting carbon nanotube.

Fig. 1 (a) shows the schematic of carbon nanotubes with different chiralities.

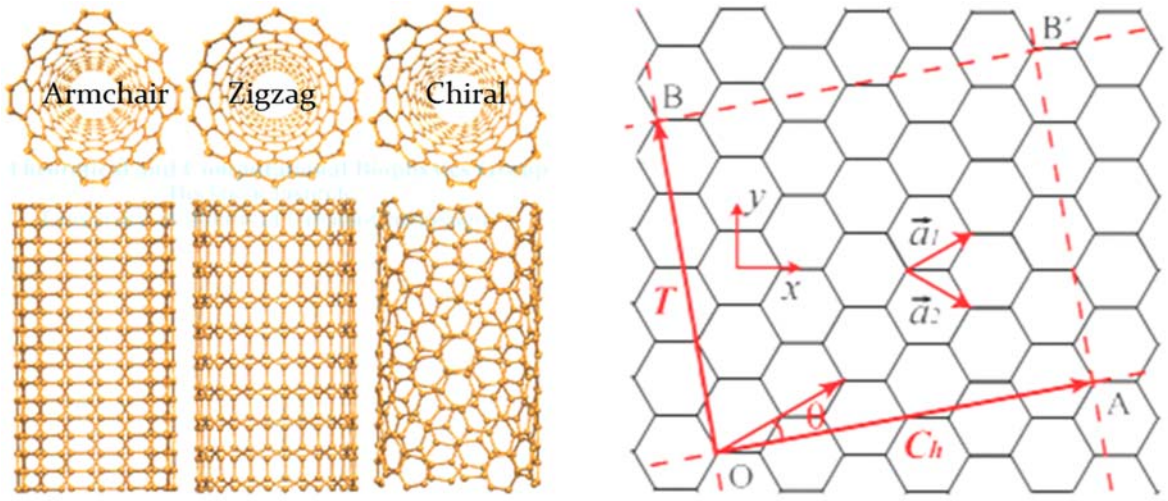

(a) (b)

Fig. 1 (a) Carbon nanotubes of different chiralities (b) schematic of how graphene sheet can be rolled to form the different carbon nanotubes. [7]

Fig.2 shows some examples of the dispersion relation of semiconducting and metallic SWCNTs. It can be inducted from Fig.2 (a) that the Zigzag SWCNTs is semiconducting when the difference between their chiral numbers is not dividable by three and the armchair nanotubes are always metallic.

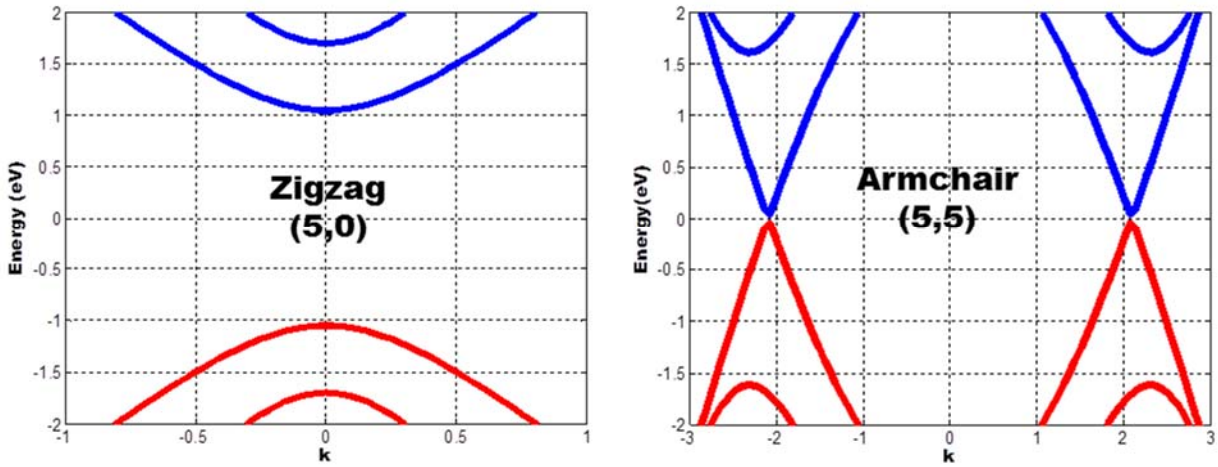

(a) (b)

Fig. 2 Example of the dispersion relation of (a) semiconducting SWCNT(b) metallic SWCNT

For electronic applications the main difference between semiconducting carbon nanotubes and metallic ones is its conductivity. The conductivity of the metallic ones is three orders of magnitude higher than the semiconducting ones. In addition, the metallic carbon nanotube's conductivity is constant while the semiconducting carbon nanotube can be modulated by a bias voltage. Semiconducting ones are used for FET devices and metallic ones for interconnects.

2. Growth Techniques

Producing carbon nanotubes as a mass production is very challenging and there many methods are under research. In this section, we are exploring some of the growth techniques that are already well established.

A. Arc discharge

When two graphite rods are connected to a power supply in hot plasma chamber, and applying high current, carbon vaporizes and forms carbon nanotubes. Arc discharge technique is one of the

first methods known for producing carbon nanotubes and it can produce SWCNT and MWNTs (Multi-walled Carbon nanotubes) with few structural defects. The main known disadvantage is that the produced carbon nanotubes are short with random size and direction [8].

B. Laser ablation

When a graphite rod is shined with intense laser pulses, carbon gas will be produced from which the carbon nanotubes form. Various conditions should be tried until finding one that produces remarkable amounts of SWCNTs. Laser ablation is one of the best methods because its parameters can be controlled to produce precise SWCNTs but it needs very expensive laser source [9].

C. Chemical vapor deposition (CVD)

In this method a substrate is placed in oven with temperature equals 600 ^{o}C, and slowly methane gas is added. As the gas decomposes it carbon atoms are free hence it recombines to form of carbon nanotubes. This is the most used method for mass production and substrate direct use but it is mostly MWCNTs and it might have a lot of defects [10].

All the produced carbon nanotubes are mix between metallic and semiconducting SWCNTs in addition to MWCNTs. In order to have a specific type of the carbon nanotubes a separation technique has to be used.

3. Separation

Having the SWCNTs grown in the powder form makes it hard to separate them. Nanointegris manufacturer has introduced the idea of putting them in an aqueous solution and adding mix of ionic surfactant materials. So each surfactant material convolutes the different carbon nanotubes' types based on its polarity. This makes the overall solution is mix different density materials. Then spinning this solution with high revolution speed, these materials will spate to form layers, where

the highly dense will be in the bottom and the lightly dense on the top. Then they can be sucked separately and getting a very high purity metallic and semiconducting SWCNTs.

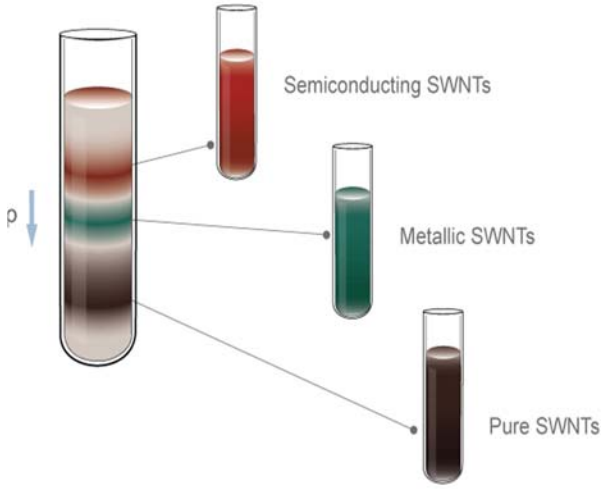

Fig.3 Carbon nanotube solutions after separation-Nanointegris [11]

4. Alignment

The carbon nanotubes are sold in the form or powder or aqueous solution. In order to use in devices, it has to be deposited on a substrate. Alignment of carbon nanotubes plays a vital role in designing electronic devices and optimizing their operation. Ren *et al.* have used aligned metallic SWCNT to develop THz polarizer. THz signals polarized parallel to the carbon nanotubes are absorbed, while signals polarized perpendicular to the alignment direction are transmitted. Wang *et al.* have used partially aligned s-SWCNTs in a FET transistor, where the performance is a function of the number of nanotubes per device [12]. Aligned carbon nanotubes have been used in many devices. The measured results were not to highly accurate with respect to electron transport physics in carbon nanotubes due to the lack of comprehensive theoretical model. Carbon nanotubes modeling can be prepared either by electromagnetic theory or by photonics.

Transmission line model for the carbon nanotubes in the gigahertz range was presented by Burke [13]. Transmission line is not an efficient tool in THz frequency range. Hence, in our model, we are applying the photonics properties in modeling carbon nanotubes in order to enhance and synthesize better devices in the THz range.

There are different techniques used to align an aqueous solution of carbon nanotubes on a substrate. Langmuir-Blodgett technique is considered the mechanical method where a substrate is slowly dipped into a solution of well-dispersed highly dense carbon nanotubes and then is slowly (1cm/min) pulled out.[14] The second method uses gas flow of linear velocity (10cm/s) while the solution of dispersed CNTs is being drop-wise deposited onto a substrate. The flow simultaneously spreads the drops, dries them and aligns the nanotubes along the flow direction [15]. Finally, using an AC electric field aligns the individual nanotubes between the electrodes, thereby producing high-quality electrical CNT devices which is known as dielectrophoresis method [16].

5. Dissertation Structure

This dissertation is composed of six chapters containing previously published papers. Chapter two discusses the theoretical background of the Thomas Fermi model applied in this work. Then an analytical approach is introduced to obtain the potential function of one s-SWCNT that describes the carrier charge density. The unique potential function proposed facilitates solving the problem as a cylindrical quantum well. Hence, integrating the potential function into Schrödinger's equation facilitates obtaining the probability wave functions and the energy band gap of one s-SWCNT. Extending the model to contain two s-SWCNTs is then realized by two methods, analytically and numerically. The analytical solution uses the double quantum well analogy. The numerical solution is obtained by implementing the model in COMSOL Multiphysics simulator. Results obtained using the two methods are in good agreement. The coupling effect of two aligned s-

SWCNTs reduces the energy band gap of the system. A specific case where an external electric field is applied across the aligned s-SWCNTs is studied to show the variation of the energy band gap as a function of the applied electric field.

Chapter three is divided into two sections that describe general cases of nanotube configurations.

The first part, an analytical approach is adapted to obtain the potential function of DWNT. The expression for the potential function of DWNT's carrier charge density. Schrodinger model is built in ComSol Multiphysics simulator. Therefore, the probability wave functions are obtained and the energy band gap is calculated. The second part, in order to enhance the performance of future carbon based devices, it is essential to improve simulated model closer to experiments. Thus, two different approaches can be considered to develop new models. An efficient model based on experimental observations considering fabrication technique, nanotube defects, parasitic effects are developed by imposing new constraints. The approach utilized with the emergence of new technologies and growth techniques, semiconducting carbon nanotube highly uniform can now be produced allowing models to predict the behaviour of a device more accurately justifying this approach. The developed model at high frequency considers either metallic or semiconducting nanotubes depending on the applications. The presented model predicts the energy band gap of a bundle of aligned s-SWCNTs arranged in semi-random order considering different radii and distances separating nanotube. A typical diameter of s-SWCNT is in the order of 1.4-2.1nm, and the minimum distance between s-SWCNTs is the graphite interlayer distance 0.34 nm. The effective potential function is implemented in the Schrödinger equation to determine the ground state wave function and the energy band gap variations. Finally, the energy band tuning is demonstrated after applying an external electric field across the bundle.

Chapter four discusses the observed discrepancies between simulated data and experimental results of fabricated devices that obstruct the development of SWCNT-based devices into practical and large-scale integrated circuits. The contact resistance and fringe capacitance between nanotubes and metallic electrodes are important factors degrade carbon-based devices. Although palladium provides the highest on-current in SWCNT due to its matching work function, carbon-based devices contact resistances have been reported to be on the order of a few KΩ. These values are higher than the ones for the Ohmic contacts formed in conventional semiconductor devices. A perfect ohmic contact could not be formed at the nano-scale level due to the chemical reactivity between the SWCNT and the metal. Instead, an overlap area of a lower conductivity forms between the SWCNT and the metal which creates an extra barrier due to the hybridization between the carbon atoms and the metal. The chapter presents a physical insight to understand this phenomena. A scheme for calculating the contact resistance and the fringe capacitance for individual SWCNT-based devices is presented, with full parametric study. The results are presented which includes an independent verification of the model.

Chapter five is divided into two parts. The first part, alignment of the nanotubes to optimize the performance of electronic devices and consider mass production manufacture is developed. The method based on AC dielectrophoresis technique to align semiconducting single-walled carbon nanotubes (s-SWCNTs) is applied to several devices at once. In addition, the resulting density of s-SWCNTs per device has exceeded the ones reported in the literature and the enhancement of the sheet resistance is observed compared to recent publications. The second part presents a physical insight into the processes affecting the contact resistance and the fringe capacitance of an individual SWCNT-based device. Then a method to calculate their values is presented. Understanding arrays of nanotubes is one of the key contributions of this paper. Thanks to their

ability to retain their interesting quantum properties, nanotube arrays may provide a large current carrying capacity and low impedance. The resultant parasitic-element models of the individual nanotube are embedded into a model for multiple SWCNT-based devices using a quantitative physics-based RC model to estimate the frequency dependence of such a device. A test structure is presented with a verification of the model followed by discussion and future insight.

Chapter six discusses the effective potential function of an individual s-SWCNT, this it is generalized for aligned s-SWCNTs. Then an analogy between Quantum Cascaded Lasers (QCL) and system of aligned s-SWCNTs is discussed. The current-voltage characteristics of an individual nanotube and an array of nanotubes is discussed. The measurements are then compared to the theory.

References

[1] A. Jorio, G. Dresselhaus, and M. Dresselhaus, *Carbon Nanotubes: Advanced Topics in the Synthesis, Structure, Properties and Applications* (Springer, 2008), Vol. 111.

[2] S. Rotkin and S. Subramoney, *Applied Physics of Carbon Nanotubes: Fundamentals of Theory, Optics and Transport Devices* (Springer, 2005).

[3] L. Ren, C. Pint, L. Booshehri, W. Rice, X. Wang, D. Hilton, K. Takeya, I. Kawayama, M. Tonouchi, R. Hauge *et al.*, " Carbon nanotube terahertz polarizer," *Nano Lett.* **9**, 2610–2613 (2009).

[4] E. Decrossas, A. Elkadi, and S. El-Ghazaly, " Carbon nanotube based prototype as THz time domain sources/detectors," in*37th International Conference on Infrared, Millimeter, and Terahertz Waves (IRMMW-THz)* (IEEE, 2012), pp. 1–2.

[5] A. Elkadi, E. Decrossas, S.-Q. Yu, H. A. Naseem, and S. M. El-Ghazaly, " Controlling the energy band gap of aligned semiconducting single-walled carbon nanotubes for THz modulator," in *7th European Microwave Integrated Circuits Conference (EuMIC)* (IEEE, 2012), pp. 270–273.

[6] J. M. Marulanda and A. Srivastava., Carrier density and effective mass calculations in carbon nanotubes. *Physica Status Solidi (b) 245(11),* 2008*,* pp. 2558-2562.

[7] Jeroen W. G. Wilder; Liesbeth C. Venema; Andrew G. Rinzler; Richard E. Smalley; Cees Dekker, Electronic structure of atomically resolved carbon nanotubes**,** Nature 391, 6662, 59-62 (1998)

[8] Iijima, Sumio . Helical microtubules of graphitic carbon. *Nature* 354 (6348) 56–58, 1991**.**

[9] Guo, Ting; Nikolaev, Pavel; Rinzler, Andrew G.; Tomanek, David; Colbert, Daniel T.; Smalley, Richard E. Self-Assembly of Tubular Fullerenes. *J. Phys. Chem.* 99(27): 10694–10697, 1995**.**

[10] N. Ishigami; Ago, H; Imamoto, K; Tsuji, M; Iakoubovskii, K; Minami, N. Crystal Plane Dependent Growth of Aligned Single-Walled Carbon Nanotubes on Sapphire. *J. Am. Chem. Soc.* 130 (30): 9918–9924, 2008.

[11] NanoIntergris IsoNanotubes-S ™ SWCNTs (Available: http://www.nanointegris.com/skin/frontend/default/nano/downloads/NanoIntegris%20Brochure%20ENG.pdf)

[12] J. Wang, Y. Chen and W. J. Blau. Carbon nanotubes and nanotube composites for nonlinear optical devices.*Journal of Materials Chemistry 19(40),* pp. 7425-7443. 2009.

[13] P.J. Burke, "Luttinger liquid theory as a model of the gigahertz electrical properties of carbon nanotubes," Nanotechnology, IEEE Transactions on, vol. 1, pp. 129-144, Sep. 2002.

[14] Li, Xiaolin, et al. Langmuir-Blodgett assembly of densely aligned single-walled carbon nanotubes from bulk materials. *Journal of the American Chemical Society* 129.16, pp. 4890-4891, 2007.

[15] Hedberg, James, Lifeng Dong, and Jun Jiao. Air flow technique for large scale dispersion and alignment of carbon nanotubes on various substrates. *Applied Physics Letters* 86.14 (143111), 2005.

[16] J. Li, Q. Zhang, N. Peng and Q. Zhu, "Manipulation of carbon nanotubes using AC dielectrophoresis," *Appl. Phys. Lett*., vol. 86, pp. 153116, Apr. 2005.

Chapter II. Aligned semiconducting single-walled carbon nanotubes: Semi-analytical solution

Abstract

This paper presents a semi-analytical model to study coupling between adjacent semiconducting single-walled carbon nanotubes (s-SWCNT) and its effect on the energy band gap. A potential function is proposed to describe the charge density distribution of s-SWCNT based on the continuum model. The potential function is then used in solving Schrödinger'sequation to obtain the ground state probability wave function for one s-SWCNT and aligned bundle of s-SWCNTs. Then, a parametric study of energy band gap is developed by varying the distance between adjacent s-SWCNTs and applying transverse electric field across the bundle axis. The energy band gap of aligned s-SWCNTs is 10% less than one s-SWCNT. When the distance (*d*) between the adjacent s-SWCNTs is increased, the change of the energy band gapvanishes. By applying transverse electric field, the energy band gap may reduce by as much as 20% and vanishes with the increase of *d*.

1. Introduction

Carbon nanotubes have attracted the attention of researchers due to their substantial properties along their axis such as one dimensional confined carriers and photons and high electrical conductivity. In addition, carbon nanotubes have tremendous mechanical properties such as high thermal conductivity and tensile strength [1]. Single-walled carbon nanotubes can be regarded as a rolled graphene sheet and it is either semiconducting or metallic based on its chiral angle

determined by rolling indices (*m, n*). A semiconducting single-walled carbon nanotube (s-SWCNT) has a typical diameter of 0.5 to 2 nm, and its energy gap is inversely proportional to its diameter in the range of 1.4 to 0.35 eV [2].

Aligned s-SWCNTs demonstrated promising responses in various devices [3]-[5]. It led researches to compare the enhanced properties of aligned multi s-SWCNTs to individual ones. Studying aligned s-SWCNTs theoretically is a complex problem due to the lack of a well-defined potential function of individual s-SWCNT. Two adjacent s-SWCNTs were studied by Kim *et al* [6]. using first principle *ab initio* method. It was mentioned that their method could be extended to three aligned s-SWCNTs.

Alignment of carbon nanotubes plays a vital role in designing electronic devices and optimizing their operation. Ren *et al.* have used aligned metallic SWCNT to develop THz polarizer. THz signals polarized parallel to the carbon nanotubes are absorbed, while signals polarized perpendicular to the alignment direction are transmitted. [3] Wang *et al.* have used partially aligned s-SWCNTs in a FET transistor, where the performance is a function of the number of nanotubes per device [7]. Aligned carbon nanotubes have been used in many devices. The measured results were not to highly accurate with respect to electron transport physics in carbon nanotubes due to the lack of comprehensive theoretical model. Carbon nanotubes modeling can be prepared either by electromagnetic theory or by photonics. Transmission line model for the carbon nanotubes in the gigahertz range was presented by Burke [8]. Transmission line is not an efficient tool in THz frequency range. Hence, in our model, we are applying the photonics properties in modeling carbon nanotubes in order to enhance and synthesize better devices in the THz range.

This paper is organized as follows: Section II discusses the theoretical background of the Thomas Fermi model applied in this work. In Sec. III , an analytical approach is introduced to obtain the

potential function of one s-SWCNT that describes the carrier charge density. Having a well-defined potential function facilitates solving the problem as a cylindrical quantum well. Hence, integrating the potential function into Schrödinger's equation facilitates obtaining the probability wave functions and the energy band gap of one s-SWCNT. Extending the model to contain two s-SWCNTs is then realized by two methods, analytically and numerically. The analytical solution uses the double quantum well analogy. The numerical solution is obtained by implementing the model in COMSOL Multiphysics simulator [9]. Results obtained using the two methods are in good agreement. The coupling effect of two aligned s-SWCNTs reduces the energy band gap of the system. Section IV describes a specific case where an external electric field is applied across the aligned s-SWCNTs. The study of the energy band gap variation as a function of the applied electric field is presented.

2. Theoretical Background

The continuum approach introduced by Zuloaga [10] is applied to an individual s-SWCNT, where the surface charge density of graphene describes the positive charge on its wall and an electron gas surrounds it, as shown in the inset of Fig. 1(a) . A generalization of Thomas-Fermi (TF) model is then used to calculate the charge distribution for individual s-SWCNT. In this model, the equilibrium electron density distribution is combined with Poisson's equation to compute the potential function which is then inserted in Schrödinger's equation. The equilibrium electron density is calculated by minimizing the overall system energy function [10]

$$n(r) = \left(\frac{3}{5C_F}\, V_{eff}(r)\right)^{\frac{3}{2}} \tag{1}$$

where V_{eff} is the electrostatic potential produced by the positive ion core and C_F is TF energy coefficient. Poisson's equation is given by

$$\nabla^2 V_{eff}(r) = -4\pi\rho(r) \tag{2}$$

where the total charge is $\rho(r) = -n(r) + n_+(r)$ and the positive charge is only located on the s-SWCNT's surface:$n_+(r) = \sigma * \delta(r - R_t)$, hence $\nabla^2 V_{eff}(r) = 4\pi n(r)$. Substituting Eq. (1) in Eq. (2) results in Thomas Fermi's differential equation

$$\nabla^2 V_{eff}(r) = 4\pi \left(\frac{3}{5C_F} V_{eff}(r) \right)^{\frac{3}{2}}. \tag{3}$$

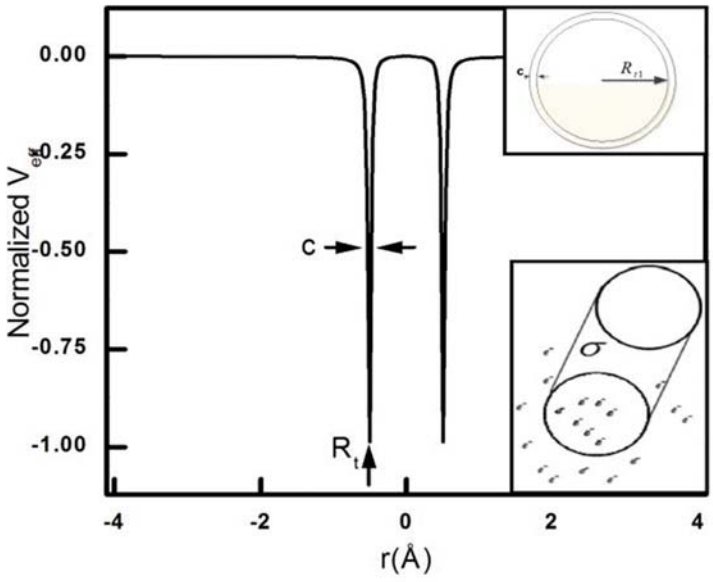

(a)

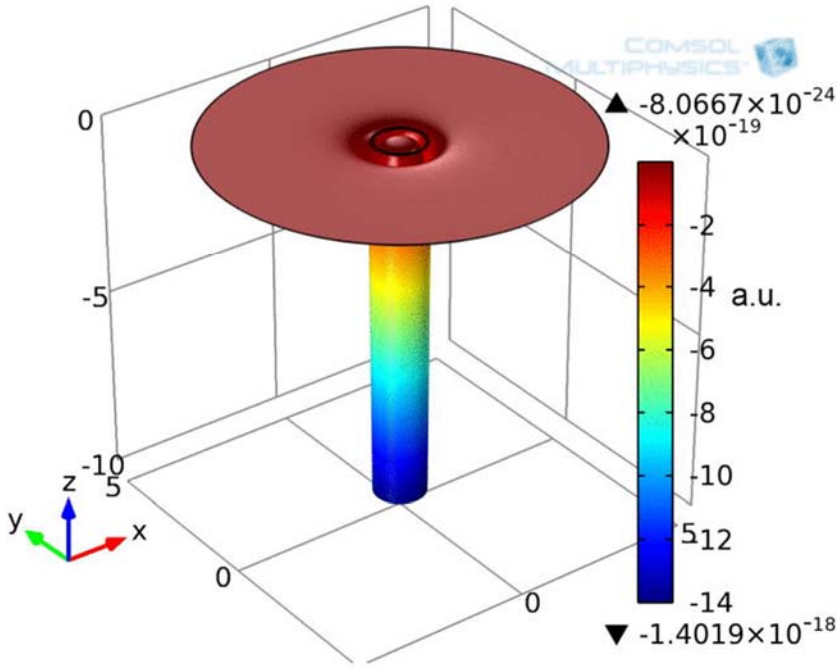

(b)

Fig. 1 Normalized Potential function V_{eff} (a) 2D with inset shows the continuum model of s-SWCNT (b) 3D plot obtained from COMSOL Multiphysics simulator (a.u.) ($R_t = 0.7$ nm).

3. Model for s-SWCNT

A. Analytical potential function

Semi-analytical solution of TF differential equation is obtained by substituting asymptotic form [11] of $V_{eff} = \frac{A}{r^b}$, and calculating the constants A and b. The analytical potential function is proposed to be in the form

$$V_{eff}(r) = \frac{-B \times c_2 r^2}{\left(r^2 - R_t^2\right)^2 + c^2 r^2} \tag{4}$$

where R_t is the nanotube's radius, $c = \frac{R_t}{11.446}$ represents the effective s-SWCNT's wall thickness [12], and $B = 8.75$ eV is the potential well depth [2]. The 2D and 3D plots of the potential function is shown in Figs. 1(a) and 1(b) , respectively. The results agree with TF equation solved numerically [10], [13]. The potential function is symmetrical around the tube axis and localized around the tube wall. A comparison is presented in Fig. 2 between the normalized electron charge distribution calculated by substituting Eq. (4) in Eq. (1) and the numerical data produced by Zuloaga [10]. According to the derivative of the potential function, it results in a huge number due to very small nanotube wall thickness. That is an acceptable approximation for the discontinuity on the carbon nanotube wall that encounters the positive localized charge on the wall. After having a well-defined potential function describing the s-SWCNTs, this potential function is inserted in Schrödinger's equation to obtain the wave function for the system ground state wave function.

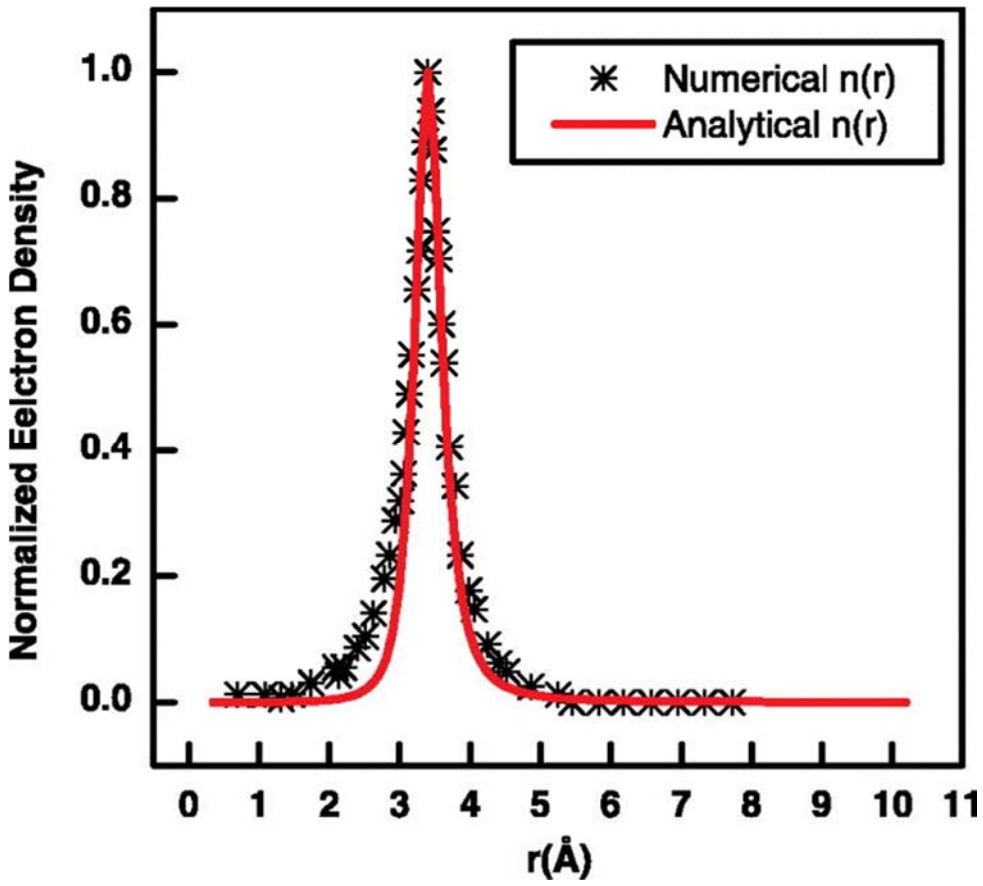

Fig. 2. Electron charge distribution calculated using the proposed potential function compared with the one calculated numerically by Zuloaga [10]. ($R_t = 0.32\,nm$).

B. Solving Schrödinger equation

For this problem, Schrödinger equation is formulated as follows:

$$(-\frac{\hbar^2}{2m^*}\nabla^2 + V_{eff}(r))\Psi(r,\phi,z) = E\Psi(r,\phi,z) \quad (5)$$

where $\hbar$ is Planck's constant and m^* is the effective mass [14]. The general solution of Schrödinger differential equation in cylindrical coordinates is

$$\Psi(r,\phi,z) = y(r)cos\, m\phi\, exp(ik_z z) \quad (6)$$

where $y(r)$ is the radial component , $m = 0, \pm1, \pm2, \ldots$ is the azimuthal number, and k_z is the axial wave vector. Taking into account the large aspect ratio of the s-SWCNT, where the length is

three orders of magnitude larger than the diameter, the *z*-component is considered propagating. Therefore, Eq. (5) is reduced to

$$\frac{\partial^2 y}{\partial r^2} + \frac{1}{r}\frac{\partial y}{\partial r} + \left(\frac{2m^*}{\hbar}\left(E - V_{eff}(r)\right) - \frac{m^2}{r^2}\right) y = 0 \tag{7}$$

To obtain the analytical expression of the wave function, Frobenius method is used, the details are given in Appendix A . The resultant radial component of the wave function of the ground state is

$$y_0(r) = J_0(k_r r) + C_1\left(K^* \frac{Bc^2}{k_r^2 R_t^4}\right) J_4(\alpha k_r r) - C_2 J_2\left(\beta\sqrt{K^* B c^2}\left(\frac{r}{R_t}\right)^2\right) \tag{8}$$

where $J_i(x)$ is Bessel function of the first kind, $K* = 2m * \hbar 2$, the quantized radial wave number $k_r = \sqrt{\frac{E_0}{K^*}}$, $E_0 = B - E$ and B is the highest energy value an electron can take in a carbon atom. E are the energy states obtained from the eigenvalue solution of Eq. (8) . Fig. 3 presents the probability wave function for the ground energy state and the second energy level for single s-SWCNT.

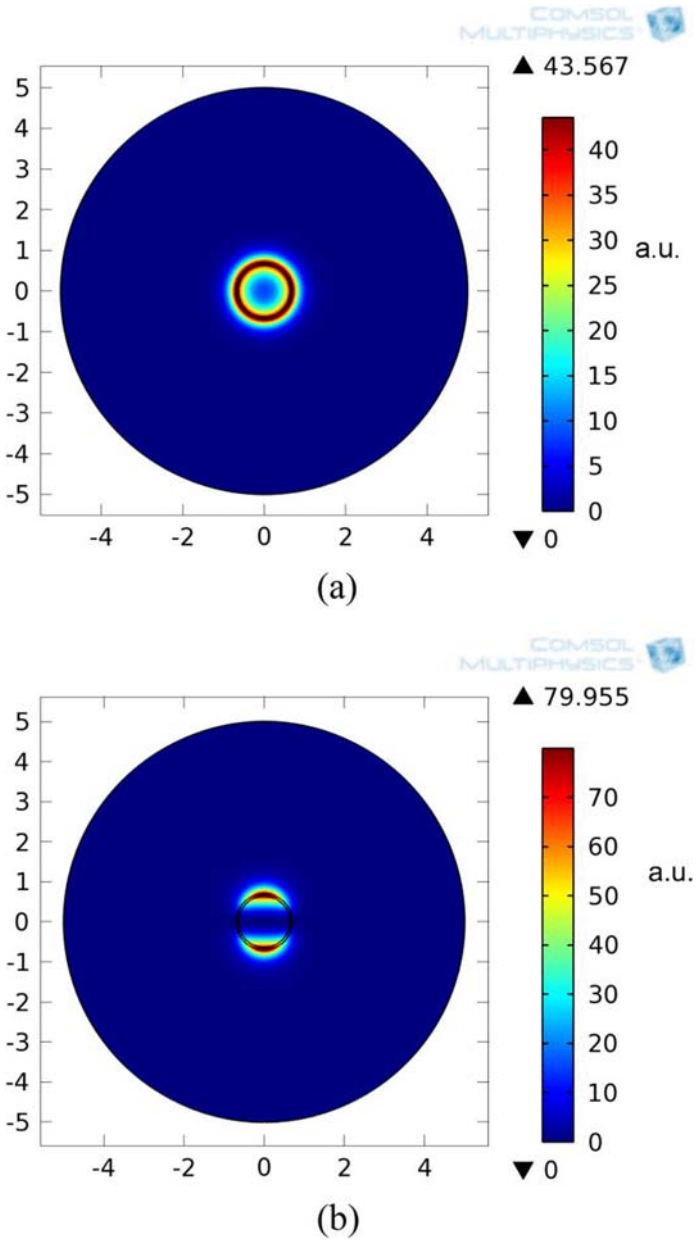

Fig. 3 Probability wave function (a) ground state (b) second energy level (a.u.) ($R_{t\,1} = 0.7\,nm$, and $E_{\,0} = 0.285\,eV$, $E_{\,1} = 0.6\,eV$).

4. Coupling between Two Carbon Nanotubes

A. Without electric field

In this section, the coupling between two adjacent aligned s-SWCNTs is studied as a function of the wall-to-wall distance (*d*) separating them. Fig. 4 describes the coupling between two s-SWCNTs, following the same analogy of double quantum wells. [15]As the potential function is highly localized around the carbon nanotube wall and that is represented by the positive charge $n_+ = \sigma * \delta(r - R_t)$, the potential of each carbon nanotube, a repeated shifted version around the center of each carbon nanotube. Hence, the total potential function V_{tot} , plotted in Fig. 4 , is the superposition of the potential function of each individual s-SWCNT, $V_{tot} = V_{eff1} + V_{eff2}$. The overall potential function replaces the individual s-SWCNT potential function in Eq. (5) . The model is general and can be applied for any semiconducting carbon nanotubes regardless of their chiralities or diameter because it uses the potential function proposed in Eq. (4) and the wave function obtained in Eq. (8) . The energy band gap changes by coupling effect between aligned s-SWCNTs

$$E_g(coupled) = E_g + 2\bar{V}_1 \pm \bar{V}_{12} \tag{9}$$

where $\bar{V}_1 = \langle \Psi_1 \mid V_{eff2}(r) \mid \Psi_1 \rangle = \langle \Psi_2 \mid V_{eff1}(r) \mid \Psi_2 \rangle$ is the shift integral, and $\bar{V}_{12} = \langle \Psi_1 \mid V_{eff2}(r) \mid \Psi_2 \rangle = \langle \Psi_2 \mid V_{eff1}(r) \mid \Psi_1 \rangle$ is the transfer integral. The coupling between s-SWCNTs produces a splitting in the ground levels in both directions; higher and lower than the original ground state. Hence the new lowest state is what defines the system energy band gap. The difference between the energy band gap of individual s-SWCNT and the energy band gap of the coupled system is

$$\Delta E = E_g(coupled) - E_g(one\ s - SWCNT) \tag{10}$$

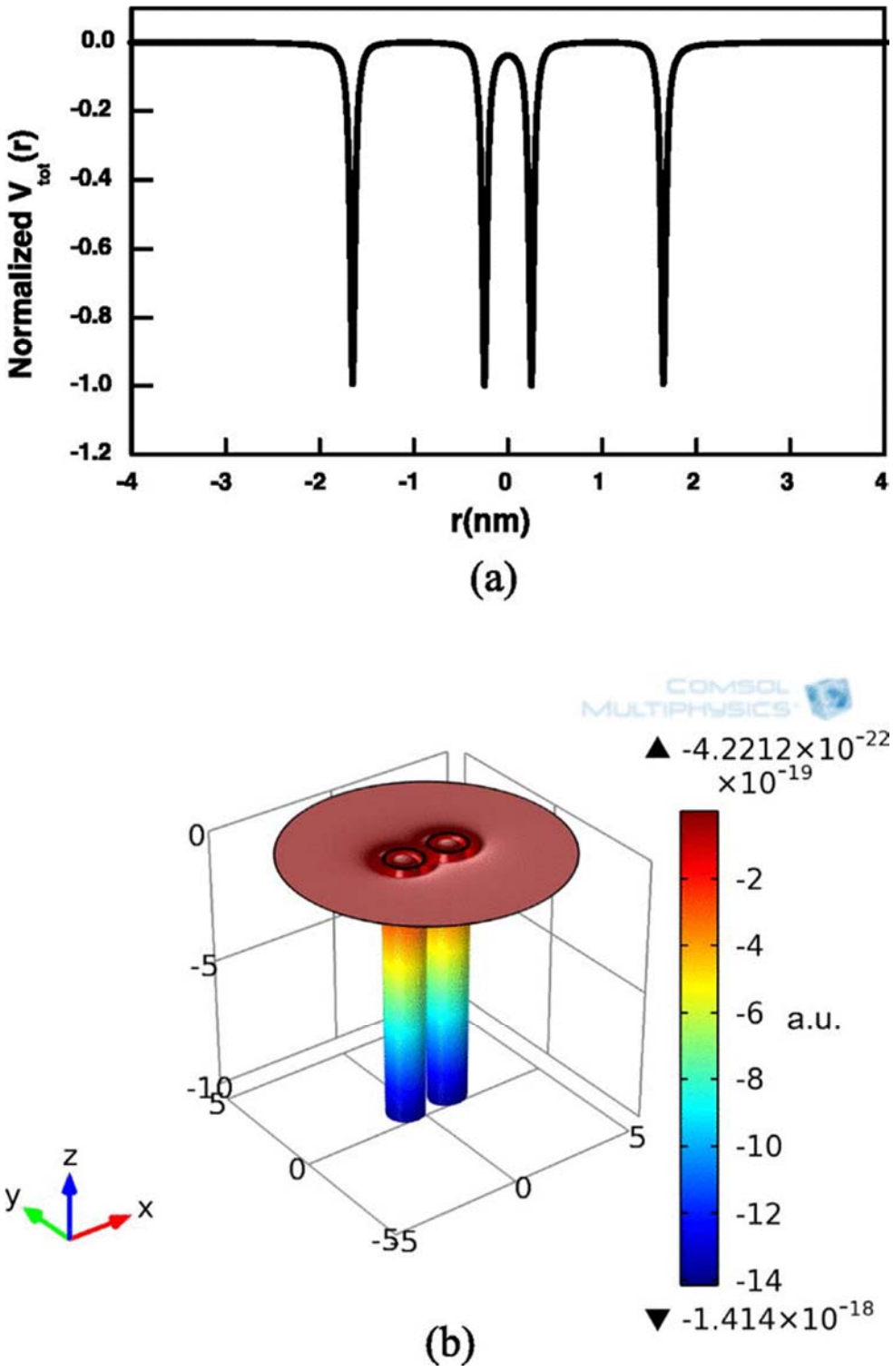

Fig. 4 Normalized Potential function V_{eff} for two s-SWCNT (a) 2D shows the distance between the adjacent s-SWCNTs (b) 3D plot obtained by COMSOL Multiphysics simulator (a.u.) ($R_{t1} = R_{t2} = 0.7\,nm\ and\ d = 0.35\,nm$).

The ground energy state presented in Fig. 5(a) shows direct coupling between s-SWCNTs. However, Fig. 5(b) shows the second level energy state which is across the bundle axis; hence, it does not assist in the coupling between s-SWCNTs. As expected, the coupling between two aligned s-SWCNTs decreases as the distance between them increases. By decreasing the coupling effect, the energy band gap difference ΔE between the coupled nanotubes compared to a single one is reduced as shown in Fig. 6 . The s-SWCNTs used in this work are identical (i.e., they have the same chirality (19, 0); hence, their radius is $R_t = 0.7\,\text{nm}$ and their energy band gap is $E_g(single\ s-SWCNT) = 0.57\,eV$). There is a discrepancy between the analytical and the numerical data in the small distances in the case of no-electric field. It could be induced by the approximations made in the Frobenius series.

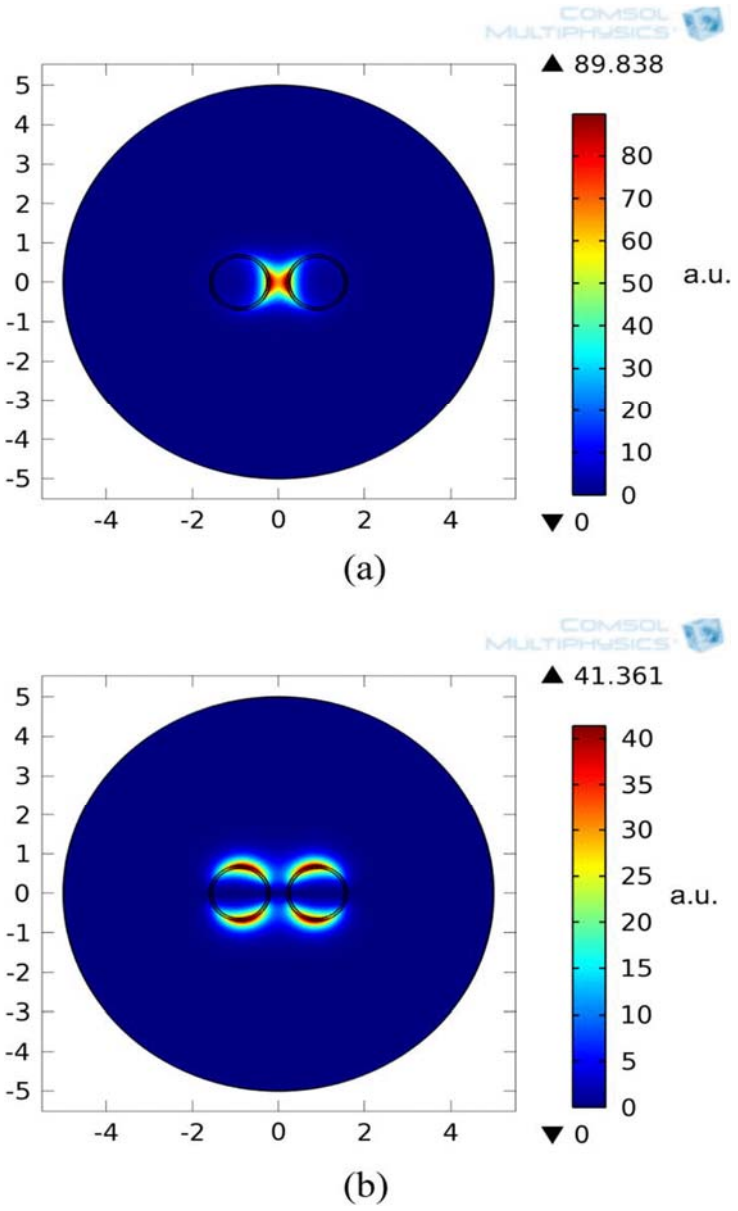

Fig. 5 Probability wave function of the coupled s-SWCNTs (a) ground state (b) second energy level (a.u.) ($R_{t1} = R_{t2} = 0.7\,nm$, $d = 0.35\,nm$, and $E_0 = 0.2825\,eV$, $E_1 = 0.588\,eV$).

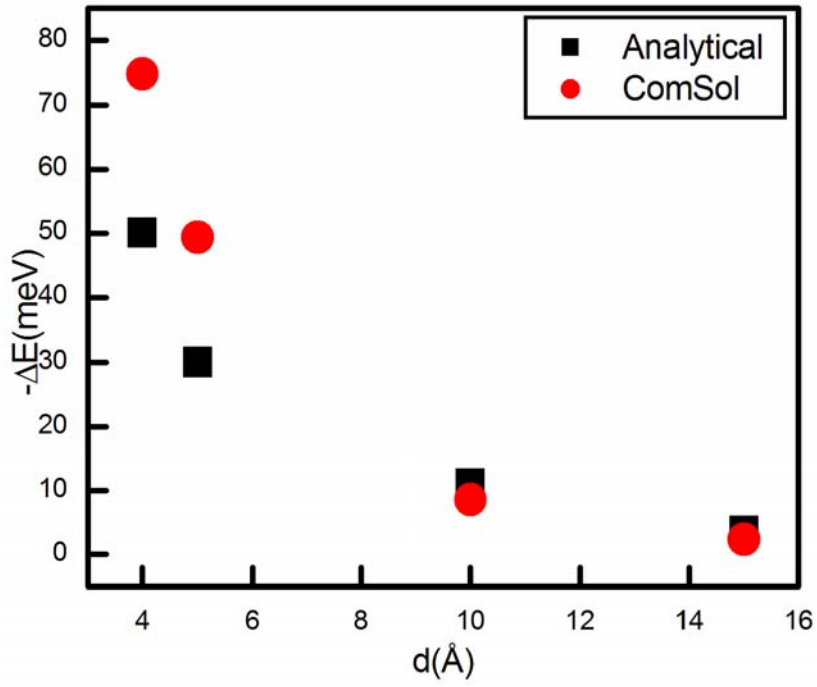

Fig. 6 The reduction in the energy band gap versus the distance between two s-SWCNTs black square curve is calculated using Eq. (10) and red circle curve is calculated using COMSOL simulator.

B. With applied transverse electric field

The contribution of the transverse electric field across one s-SWCNT will change the Hamiltonian of the electron to be

$$H = H_1 - eFr\cos\phi \tag{11}$$

where H_1 is the original Hamiltonian without electric field perturbation, e is the electron charge, and F is the electric field. An additional variational parameter is added to the wave function in order to calculate the energy levels. Following the same approach developed by Vázquez *et al.*[16], the wave function for the ground state is expressed as

$$\Psi_0(r,\phi,z) = y_0(r)cos(\eta\phi)exp(ik_z z) \tag{12}$$

where $y_0(r)$ is the same as Eq. (8) , and η is the variational parameter. The energy of the ground state $E_{0\eta} = \frac{\langle \Psi | H | \Psi \rangle}{\langle \Psi | \Psi \rangle}$ is then minimized with respect to the variational parameter to obtain a lower limit of $E_{0\eta}$. It has been observed that applying an electric field perpendicularly to an individual s-SWCNT reduces its energy band gap [2], [16]. Fig. 7 presents the energy band gap variation as function of the applied electric field. Although the concept of the energy gap reduction by applied electric field is valid for individual s-SWCNT, it requires a high electric field 3×10^9 V/m [2]. Applying the same procedure for a system of aligned s-SWCNTs, the ground state energy of the system is the sum of the electric field's effect on each s-SWCNT added to the coupling between them, as shown in Appendix B. The transverse polarizability of bundle of carbon nanotubes is higher than the isolated carbon nanotube [17] and it is a function of the distance d between the nanotubes [18], which enhances the response of the bundle to an applied electric field with respect to the isolated carbon nanotube. The developed model shows that the applied electric field needed to decrease the energy band gap is lower for aligned s-SWCNTs than for an individual s-SWCNT due to the coupling effect between nanotubes as it has been observed [6]. Fig. 8 shows the energy change for a bundle formed of two identical s-SWCNTs in the existence of applied electric field.

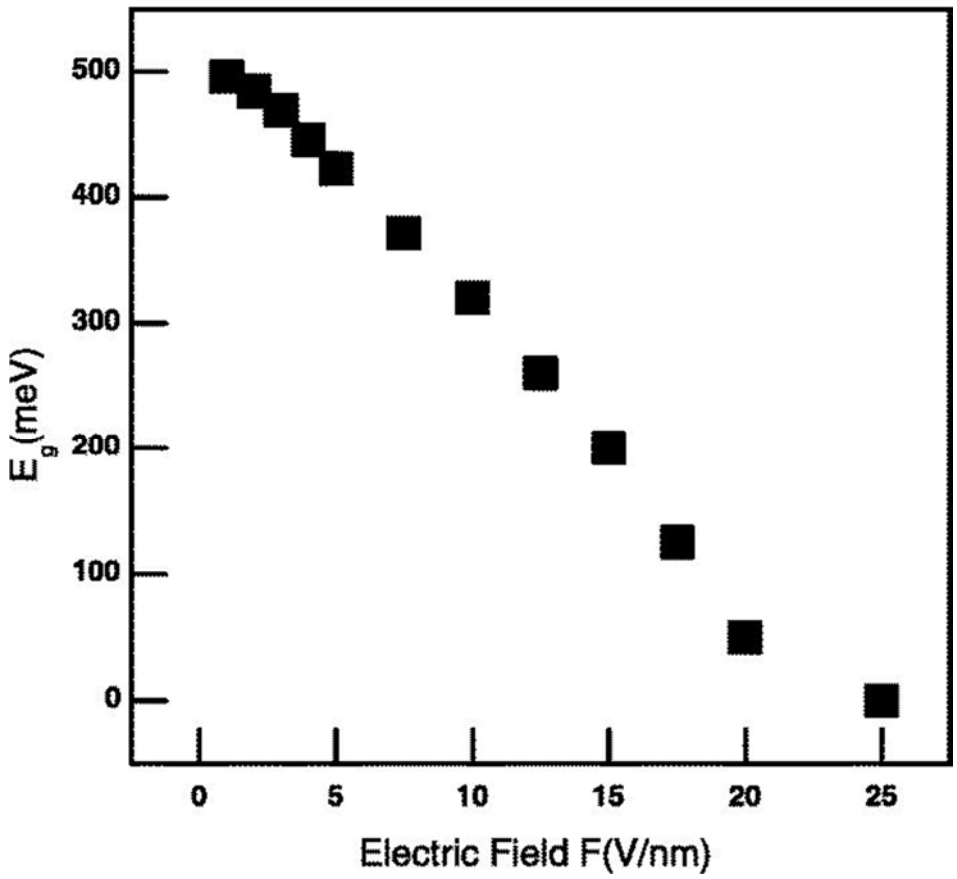

Fig. 7 Energy band gap variation of s-SWCNT versus the applied electric field magnitude.

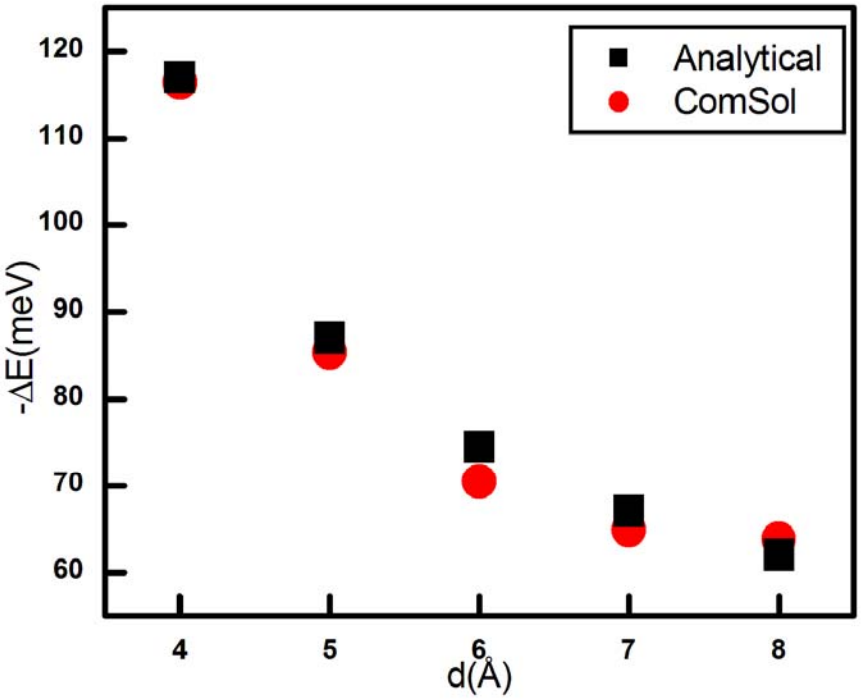

Fig. 8 The reduction in the energy band gap in the case of applying transverse electric field versus the distance between two s-SWCNTs black square curve is calculated using Eq. (10) with the expression of wave function of Eq. (12) and red circle curve is calculated using COMSOL simulator. (The electric field magnitude is $F = 0.1$ V/nm applied across the axis of single SWCNT.)

5. Conclusion

An analytical potential function is introduced to describe the charge density of s-SWCNTs. Schrödinger's equation is then solved by implementing the proposed analytical potential function. The wave function of an individual s-SWCNT as well as multi s-SWCNTs organized inside a bundle is obtained from the semi-analytical approach. The energy band gap reduction due to the coupling in aligned s-SWCNTs is investigated as a function of the distance between s-SWCNTs in the absence and in the presence of transverse electric field. The energy band gap change reaches

10% due to coupling while in the case of applied transverse electric field it increases as much as 22%. The proposed closed-form potential function offers significant reduction in the computation time. Hence, this model can be easily generalized to incorporate a large number of aligned nanotubes. Finally, this study provides innovative approaches for terahertz or far-infrared frequency components requiring a small energy band gap semi-conducting material.

Appendices

APPENDIX A: Frobenius method

The Frobenius method assumes that the solution for Ordinary Differential Equations (ODE) is expressed as a power series [19]. This method begins by assuming the solution for ODE

$$\left(\frac{d^2}{dr^2}+\frac{1}{r}\frac{d}{dr}+K^*(E)+\frac{Bc^2r^2K^*}{r^4+(c^2-2R_t^2)r^2+R_t^4}-\frac{m^2}{r^2}\right)y \tag{A1}$$

to be a power series

$$y=\sum_{n=0}^{\infty}A_n r^{n+\nu} \tag{A2}$$

The first and the second derivatives with respect to r are derived as

$$\frac{dy}{dr}=\sum_{(n=0)}^{\infty}A_n r^{n+\nu-1}(n+\nu) \tag{A3}$$

$$\frac{d^2y}{dr^2}=\sum_{n=0}^{\infty}A_n r^{n+\nu-2}(n+\nu)(n+\nu-1) \tag{A4}$$

By substituting Eqs. (A2)–(A4) in Eq. (A1) , the following expression is obtained:

$$\begin{aligned}\sum_{n=0}^{\infty}A_nR_t^4((n+\nu)^2-m^2)r^{n+\nu}+\sum_{n=2}^{\infty}A_{n-2}\left(K^*(E)R_t^4+((n+\nu-2)^2-m^2)\right)r^{n+\nu}+\\ \sum_{n=4}^{\infty}A_{n-4}(K^*(Bc^2+(c^2-2R_t^2)(E))+((n+\nu-4)^2-m^2))\,r^{n+\nu}\ +\\ \sum_{n=6}^{\infty}A_{n-6}K^*(E)Er^{n+\nu}\ =0\end{aligned} \tag{A5}$$

The coefficients A_n are computed by equating both sides of Eq. (A5) ; hence, the following recursion equations are obtained:

$n = 0 \rightarrow A_0 R_t^4((0+\nu)^2 - m^2) = 0 \rightarrow \nu^2 = m^2$

$n = 1 \rightarrow A_1 = 0,$

$n = 2 \rightarrow A_2 = -\frac{K^* E}{((2+\nu)^2 - m^2)} A_0,$

$n = 3 \rightarrow A_3 = 0,$

$n = 4 \rightarrow A_4 = -\frac{K^* E}{((4+\nu)^2 - m^2)} A_2 \; + -\frac{K^* B\left(\frac{c^2}{R_t^4}\right)}{(4+\nu)^2 - m^2} A_0,$

$n = 5 \rightarrow A_5 = 0,$

$n = 6 \rightarrow$

$A_6 = \frac{-K^* E}{(6+\nu)^2 - m^2} A_4 + \frac{-K^* B\left(\frac{c^2}{R_t^4}\right)}{(6+\nu)^2 - m^2} A_2 - -K^* B\left(\frac{c^2}{R_t^8}\right)(c^2 - 2R_t^2)((6+\nu)^2 - m^2) A_0.$

Substituting all coefficients in Eq. (A1), the solution is a summation of Bessel function of the first order and approximated terms.

$$y(r) = J_\nu(k_r r) + C_1\left(\frac{K^* B c^2}{k_r^2 R_t^4}\right) J_{\nu+4}(\alpha k_r r) - C_2 J_{\frac{\nu}{2}+2}(\beta\sqrt{K^* B c^2}\left(\frac{r}{R_t}\right)^2) \qquad \text{(A6)}$$

The second term in Eq. (A6) is due to the hollow shape of the s-SWCNT. The third term represents the finite depth of the potential function. In other words, if an infinite depth of the potential function is considered, then the third term is neglected. C_1 and C_2 are normalization constants while α and β are calculated using the least square method to satisfy the boundary conditions: The wave function has a zero derivative at $r = 0$, and it vanishes at infinity. The constants α and β are

added to achieve the highest possible accuracy. They are calculated using the least square method by comparing the zeros of Eq. (8) to the zeros of the power series of Frobenius method. The same approach is applied to calculate C_1 and C_2 to ensure the integration of absolute value of wave function squared is the unity ($\int \infty - \infty \mid\mid y(r) \mid\mid 2 = 1$). Hence, to obtain the wave function for the ground state, it is substituted by $= m = 0$.

APPENDIX B: Coupling equations

For coupled s-SWCNTs, the Hamiltonian can be expressed as

$H_t = H_1 + H_2 - F_1 r\, cos\, \phi = (H_1 - F_1 r\, cos\, \phi) + (H_2 - F_2 r\, cos\, \phi)$,

$\Psi_t = A_1\Psi_1 + A_2\Psi_2$,

where Ψ_t, H_t are the wave function and the Hamiltonian for all the system, respectively. F_1 and F_2 are the proportion of the applied electric field on each individual carbon nanotube

$Et = \frac{\langle \Psi t|Ht|\Psi t\rangle}{\langle \Psi t|\Psi t\rangle}$,

$$\begin{aligned}\langle \Psi t|Ht|\Psi t\rangle = {} & \langle A_1\Psi_1|H_1 - F_1 r\, cos\, \phi|A_1\Psi_1\rangle + \langle A_1\Psi_1|H_1 - F_1 r\, cos\, \phi|A_2\Psi_2\rangle \\ & + \langle A_1\Psi_1|H_2 - F_2 r\, cos\, \phi|A_1\Psi_1\rangle + \langle A_2\Psi_2|H_1 - F_1 r\, cos\, \phi|A_2\Psi_2\rangle \\ & + \langle A_2\Psi_2|H_2 - F_2 r\, cos\, \phi|A_1\Psi_1\rangle + \langle A_2\Psi_2|H_2 - F_2 r\, cos\, \phi|A_2\Psi_2\rangle\end{aligned}$$

$Et = \frac{E_{1\eta 1} + 2V_1 + 2V_{12} + E_{2\eta 2}}{2}$,

where $E_{1\eta 1}$ and $E_{2\eta 2}$ are the contribution of the applied electric field to the energy band gap in first and second s-SWCNTs, respectively. It is that the total effect of applying electric field across aligned s-SWCNTs is assisted by the interaction between the s-SWCNTs.

References

[1] A. Jorio, G. Dresselhaus, and M. Dresselhaus, *Carbon Nanotubes: Advanced Topics in the Synthesis, Structure, Properties and Applications* (Springer, 2008), Vol. 111.

[2] S. Rotkin and S. Subramoney, *Applied Physics of Carbon Nanotubes: Fundamentals of Theory, Optics and Transport Devices* (Springer, 2005).

[3] L. Ren, C. Pint, L. Booshehri, W. Rice, X. Wang, D. Hilton, K. Takeya, I. Kawayama, M. Tonouchi, R. Hauge *et al.*, " Carbon nanotube terahertz polarizer," *Nano Lett.* **9**, 2610–2613 (2009).

[4] E. Decrossas, A. Elkadi, and S. El-Ghazaly, " Carbon nanotube based prototype as THz time domain sources/detectors," in*37th International Conference on Infrared, Millimeter, and Terahertz Waves (IRMMW-THz)* (IEEE, 2012), pp. 1–2.

[5] A. Elkadi, E. Decrossas, S.-Q. Yu, H. A. Naseem, and S. M. El-Ghazaly, " Controlling the energy band gap of aligned semiconducting single-walled carbon nanotubes for THz modulator," in *7th European Microwave Integrated Circuits Conference (EuMIC)* (IEEE, 2012), pp. 270–273.

[6] G. Kim, J. Bernholc, and Y. Kwon, " Band gap control of small bundles of carbon nanotubes using applied electric fields: A density functional theory study," *Appl. Phys. Lett.* **97**, 063113 (2010).

[7] Y. Wang, S. K. R. Pillai, and M. B. Chan-Park, " High-performance partially aligned semiconductive single-walled carbon nanotube transistors achieved with a parallel technique," *Small* **9**, 2960–2969 (2013).

[8] P. J. Burke, " Luttinger liquid theory as a model of the gigahertz electrical properties of carbon nanotubes," *IEEE Trans. Nanotechnol.* **1**, 129–144 (2002).

[9] Software COMSOL Multiphysics version 4.2.0.150, 2011, see http://www.comsol.com for information.

[10] J. Zuloaga, " Hydrodynamic modeling of dielectric response in graphene and carbon nanotubes," M.S. thesis (University of Waterloo, 2006).

[11] C. Bender and S. Orszag, *Advanced Mathematical Methods for Scientists and Engineers I: Asymptotic Methods and Perturbation Theory* (Springer, 1999), Vol. 1.

[12] T. Vodenitcharova and L. Zhang, " Effective wall thickness of a single-walled carbon nanotube," *Phys. Rev. B* **68**, 165401 (2003).

[13] F. Leys, C. Amovilli, I. Howard, N. March, and A. Rubio, " Surface charge model of a carbon nanotube: Self-consistent field from Thomas–Fermi theory," *J. Phys. Chem. Solids* **64**, 1285–1288 (2003).

[14] K. El Shabrawy, K. Maharatna, D. Bagnall, and B. Al-Hashimi, " Modeling SWCNT bandgap and effective mass variation using a monte carlo approach," *IEEE Trans. Nanotechnol.* **9**, 184–193 (2010).

[15] O. Manasreh, *Semiconductor Heterojunctions and Nanostructures* (McGraw-Hill, Inc., 2005).

[16] G. Vázquez, M. del Castillo-Mussot, J. M. - Aldrete, H. Spector, and C. Mendoza, " Transverse stark effect of electrons in a hollow semiconducting quantum wire," *Physica E* **33**, 240–243 (2006).

[17] B. Kozinsky and N. Marzari, " Static dielectric properties of carbon nanotubes from first principles," *Phys. Rev. Lett.* **96**, 166801 (2006).

[18] E. N. Brothers, A. F. Izmaylov, G. E. Scuseria, and K. N. Kudin, " Analytically calculated polarizability of carbon nanotubes: Single wall, coaxial, and bundled systems," *J. Phys. Chem. C* **112**, 1396–1400 (2008).

[19] R. Borrelli and C. Coleman, *Differential Equations: A Modeling Perspective* (John Wiley and Sons, USA, 1998).

AIP PUBLISHING LLC LICENSE

TERMS AND CONDITIONS

Mar 30, 2015

All payments must be made in full to CCC. For payment instructions, please see information listed at the bottom of this form.

License Number	3507160783852
Order Date	Nov 13, 2014
Publisher	AIP Publishing LLC
Publication	Journal of Applied Physics
Article Title	Aligned semiconducting single-walled carbon nanotubes: Semi-analytical solution
Author	Asmaa Elkadi, Emmanuel Decrossas, Shui-Q. Yu, Hameed Naseem, Samir El-Ghazaly
Online Publication Date	Sep 18, 2013
Volume number	114
Issue number	11
Type of Use	Thesis/Dissertation
Requestor type	Author (original article)
Format	Electronic
Portion	Excerpt (> 800 words)
Will you be translating?	No
Title of your thesis / dissertation	Single-Walled Carbon Nanotube Arrays for High Frequency Applications
Expected completion date	Dec 2014
Estimated size (number of pages)	120
Total	**0.00 USD**

Terms and Conditions

AIP Publishing LLC -- Terms and Conditions: Permissions Uses

AIP Publishing LLC ("AIPP"") hereby grants to you the non-exclusive right and license to use and/or distribute the Material according to the use specified in your order, on a one-time basis, for the specified term, with a maximum distribution equal to the number that you have ordered. Any links or other content accompanying the Material are not the subject of this license.

1. You agree to include the following copyright and permission notice with the reproduction of the Material:"Reprinted with permission from [FULL CITATION]. Copyright [PUBLICATION YEAR], AIP Publishing LLC." For an article, the copyright and permission notice must be printed on the first page of the article or book chapter. For photographs, covers, or tables, the copyright and

permission notice may appear with the Material, in a footnote, or in the reference list.

2. If you have licensed reuse of a figure, photograph, cover, or table, it is your responsibility to ensure that the material is original to AIPP and does not contain the copyright of another entity, and that the copyright notice of the figure, photograph, cover, or table does not indicate that it was reprinted by AIPP, with permission, from another source. Under no circumstances does AIPP, purport or intend to grant permission to reuse material to which it does not hold copyright.
3. You may not alter or modify the Material in any manner. You may translate the Material into another language only if you have licensed translation rights. You may not use the Material for promotional purposes. AIPP reserves all rights not specifically granted herein.
4. The foregoing license shall not take effect unless and until AIPP or its agent, Copyright Clearance Center, receives the Payment in accordance with Copyright Clearance Center Billing and Payment Terms and Conditions, which are incorporated herein by reference.
5. AIPP or the Copyright Clearance Center may, within two business days of granting this license, revoke the license for any reason whatsoever, with a full refund payable to you. Should you violate the terms of this license at any time, AIPP, AIP Publishing LLC, or Copyright Clearance Center may revoke the license with no refund to you. Notice of such revocation will be made using the contact information provided by you. Failure to receive such notice will not nullify the revocation.
6. AIPP makes no representations or warranties with respect to the Material. You agree to indemnify and hold harmless AIPP, AIP Publishing LLC, and their officers, directors, employees or agents from and against any and all claims arising out of your use of the Material other than as specifically authorized herein.
7. The permission granted herein is personal to you and is not transferable or assignable without the prior written permission of AIPP. This license may not be amended except in a writing signed by the party to be charged.
8. If purchase orders, acknowledgments or check endorsements are issued on any forms containing terms and conditions which are inconsistent with these provisions, such inconsistent terms and conditions shall be of no force and effect. This document, including the CCC Billing and Payment Terms and Conditions, shall be the entire agreement between the parties relating to the subject matter hereof.

This Agreement shall be governed by and construed in accordance with the laws of the State of New York. Both parties hereby submit to the jurisdiction of the courts of New York County for purposes of resolving any disputes that may arise hereunder.
Questions? customercare@copyright.com or +1-855-239-3415 (toll free in the US) or +1-978-646-2777.
Gratis licenses (referencing $0 in the Total field) are free. Please retain this printable license for your reference. No payment is required.

UNIVERSITY OF ARKANSAS
College of Engineering
Department of Electrical Engineering

April 10th, 2015

To whom it may concern,

I certify that Ms. Asmaa Elkadi is the first author of the paper titled "Aligned semiconducting single-walled carbon nanotubes: Semi-analytical solution "published in Journal of Applied Physics in Sept. 2013. Ms. Elkadi completed majority (more than 51%) of this research and writing this paper.

Prof. Samir M. El-Ghazaly
Distinguished Professor
Electrical Engineering
Office: 3169 Bell Engineering Center
Phone: 479-575-6048
E-mail: elghazal@uark.edu

Chapter III. A. Electronic Properties of Double-Walled Carbon Nanotube

Abstract

In this paper, a new method of investigating the electronic properties of double-walled carbon nanotube is introduced. The method is based on dealing with it as two concentric single-walled carbon nanotubes. The results confirm that double-walled carbon nanotubes can be classified as semi metallic, from the electronic conductivity point of view, regardless the electronic type of the two concentric tubes.

1. Introduction

Carbon nanotubes have attracted the attention of researchers due to their electrical properties such as one dimensional confined carriers and photon along their axis; high tensile strength; large thermal and electrical conductivities [1]. A single-walled carbon nanotube (SWCNT) can be regarded as a rolled graphene sheet. Considering its electric conductivity, a SWCNT is either semiconducting or metallic based on its chiral angle determined by rolling indices (m,n). A semiconducting single-walled carbon nanotube has a typical diameter of 0.5 to 2 nm and its energy gap is in the range of 0.5 to 1 eV.

Studying multi-walled and single-walled carbon nanotubes is theoretically a complex problem because the potential function is not well defined. Two adjacent semiconducting carbon nanotubes (s-SWCNTs) were studied by Kim *et. al* [2] using first principle ab intio method. Kim *et al.* mentioned they could extend their calculations to three aligned s-SWCNTs. There are two ways to describe Multi-walled nanotubes (MWNT), either Russian Doll model or Parchment model. The Russian Doll model describes MWNTs as sheets of graphene rolled to form concentric multiple SWCNTs. Whereas the Parchment model describes it as a single sheet of graphite rolled around itself. The interlayer distance in multi-walled nanotubes is close to the distance between graphene layers in graphite, approximately 3.4 Å. A double-walled carbon nanotube (DWNT) is a special case of MWNT as it has just two carbon nanotubes.

In this paper, an analytical approach is adapted to obtain the potential function of DWNT. Section 2 presents the expression for the potential function of DWNT's carrier charge density. Having a well-defined potential function facilitates solving the problem as cylindrical quantum wells. Hence, it enables introducing the potential function expressions into Schrodinger's equation. In this research, Schrodinger model is built in ComSol Multiphysics simulator. Therefore, the probability wave functions are obtained and the energy band gap is calculated in section 3.

2. Analytical Potential Function

Elkadi *et al.* [3] developed the analytical expression for the potential function of single-walled carbon nanotubes shown in (1).

$$V_{eff}(r) = \frac{B \times c^2 r^2}{\left(r^2 - R_t^2\right)^2 + c^2 r^2} \qquad (1),$$

where R_t is the nanotube's radius, $c = \frac{R_t}{11.446}$ represents the effective SWCNT's wall thickness [4], and $B = 8.25\,\mathrm{eV}$ is the potential well depth. This expression facilitates understanding the properties of different configurations of carbon nanotubes. Any configuration can be considered as a superposition of several individual SWCNT. Hence, the overall potential can be derived as the sum of the individual potentials of each tube. A typical distribution of the potential function is presented in Fig. 1.

A DWNT is analysed as two concentric carbon nanotubes of different radii. Hence, its overall potential function is defined as:

$$V_{eff-total} = V_{eff1} + V_{eff2} \qquad (2),$$

where V_{eff-1}, and V_{eff-2} are the effective potential functions of concentric nanotubes of $R_{t1}$and R_{t2} , respectively.

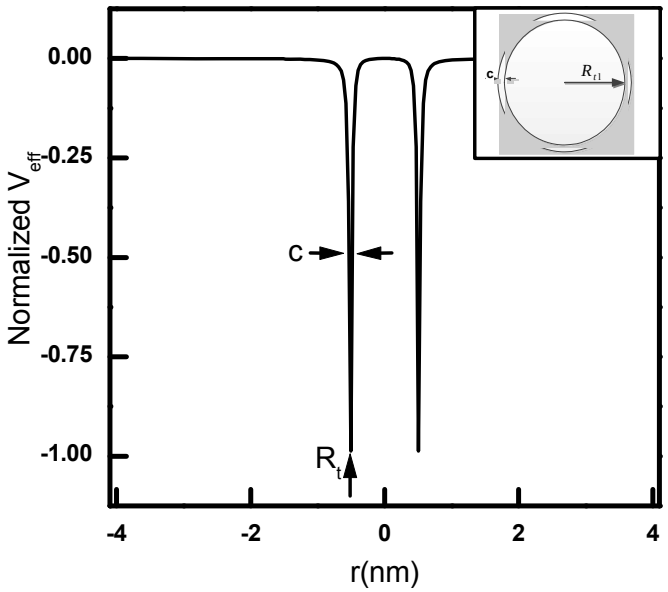

Fig. 1 Potential function of semiconducting single walled carbon nanotube of radius R_t=0.7nm

The resulting overall effective potential of DWNT is shown in Fig. 2. The graph displays the overall potential function of DWNT is similar to that of a larger carbon nanotube with larger effective wall thickness. The larger the diameter of the carbon nanotube, the smaller its energy band gap is.

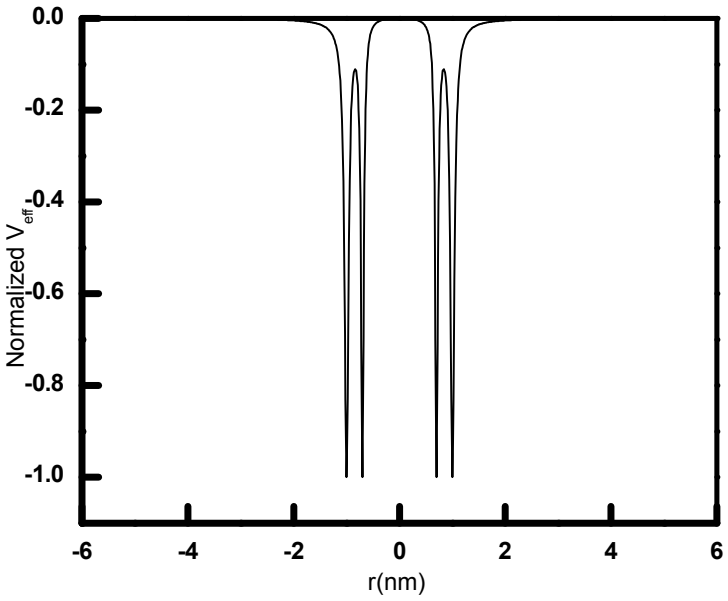

Fig. 2 Potential function of double walled carbon nanotube of radii R_{t1}=0.7nm, and R_{t2}=1nm

3. Simulations and Results

The total potential function $V_{eff\text{-}total}$ is then imbedded in a Schrodinger model. The solution of Schrodinger model in ComSol simulator provides the probability wave functions. Fig. 3 demonstrates the first two principle wave functions which are the ground state and the first energy level. They behave as a carbon nanotube with a larger radius and hence a larger effective wall thickness. From the ground state, the energy band gap is calculated. It depicts semi-metallic characteristics. In other words, the calculated energy band gap of DWNT is on the order of few mili-electron Volts which is significantly less than the energy band gap of a s-

SWCNT. The results are in a good agreement with established characteristics of DWNT with semi-metallic properties.

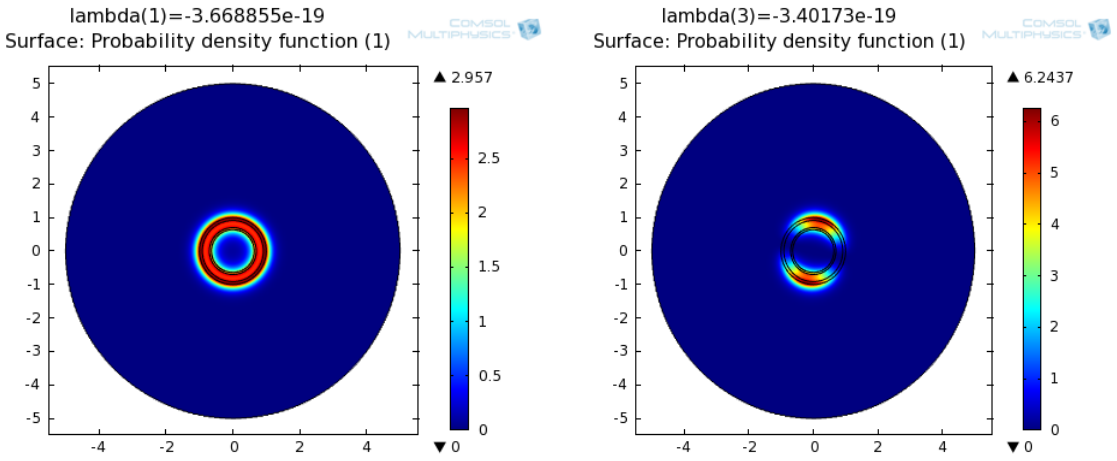

(a) (b)

Fig. 3 Probability wave function (a) ground state (b) second energy level

One of the challenges to testing carbon nanotubes is their dimensions; a typical diameter of a carbon nanotube is around 1-2 nm and its length is around few micrometres. Fig. 4 shows a prototype device fabricated to test carbon nanotubes. The device consists of four probes. Carbon nanotubes are deposited between Electrode2 and Electrode4 using AC dielectrophoresis process. Different measurements setup can take place between the four electrodes (e.g., I-V characteristics measurements along the carbon nanotubes.) Fig. 4 shows scanning electron microscope (SEM) pictures of the fabricated device consisting of four palladium (Pd) nano-elecrodes to realize ohmic contacts at the metal-carbon nanotube interface.

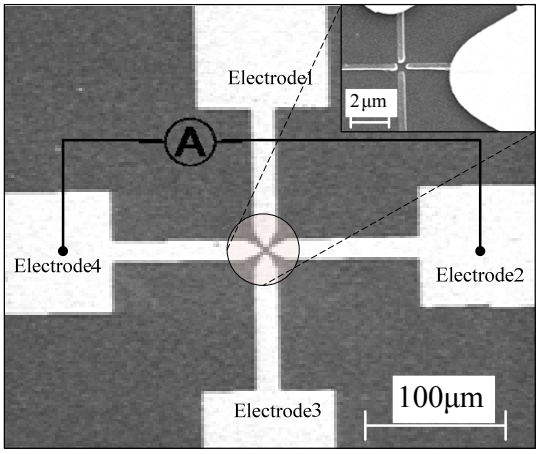

Fig. 4 Scanning electron microscope (SEM) pictures of the fabricated device (the electrode's width is 17μm with gap of around 4μm) and the inset shows SEM picture of Electron Beam lithography fabricated nano-electrodes overlapped with the electrodes made by Photolithography

4. Conclusion

An analytical potential function is introduced to describe double walled carbon nanotubes. A Schrodinger-based model is solved to provide a comprehensive quantum solution. The calculated results are inn good agreement with published data. This paper confirms that double-walled carbon nanotubes are semi-metallic regardless the electronic type of its composing carbon nanotubes.

References

[1] A. Jorio, G. Dresselhaus and M. S. Dresselhaus. *Carbon Nanotubes : Advanced Topics in the Synthesis, Structure, Properties, and Applications* 2008

[2] G. Kim, J. Bernholc and Young-Kyun Kwon. Band gap control of small bundles of carbon nanotubes using applied electric fields: A density functional theory study. *Appl. Phys. Lett. 97(6),* pp. 063113 (3 pp.). 2010

[3] A. Elkadi, E. Decrossas, S.-Q. Yu, H. Naseem, and S. El-Ghazaly, Controlling the Energy Band Gap of Aligned Semiconducting Single-Walled Carbon Nanotubes for THz

Modulator, European Microwave Integrated Circuits Conference 2012, Amsterdam, pp. 270-273.

[4] T. Vodenitcharova and L. C. Zhang. Effective wall thickness of a single-walled carbon nanotube. *Physical Review B (Condensed Matter and Materials Physics) 68(16),* pp. 165401-1. 2003.

UNIVERSITY OF ARKANSAS
College of Engineering
Department of Electrical Engineering

April 10th, 2015

To whom it may concern,

I certify that Ms. Asmaa Elkadi is the first author of the paper titled "Electronic Properties of Double-Walled Carbon Nanotube "presented in IEEE Middle East Conference on Antennas and Propagation, Dec. 2012. Ms. Elkadi completed majority (more than 51%) of this research and writing this paper.

Prof. Samir M. El-Ghazaly
Distinguished Professor
Electrical Engineering
Office: 3169 Bell Engineering Center
Phone: 479-575-6048
E-mail: elghazal@uark.edu

Chapter III. B. Energy Band Gap Study of Semiconducting Single Walled Carbon Nanotube Bundle

Abstract

The electronic properties of multiple semiconducting single walled carbon nanotubes (s-SWCNTs) considering various distribution inside a bundle are studied. The model derived from the proposed analytical potential function of the electron density for an individual s-SWCNT is general and can be easily applied to multiple nanotubes. This work demonstrates that regardless the number of carbon nanotubes, the strong coupling occurring between the closest neighbours reduces the energy band gap of the bundle by 10%. As expected, the coupling is strongly dependent on the distance separating the s-SWCNTs. In addition, based on the developed model, it is proposed to enhance this coupling effect by applying an electric field across the bundle to significantly reduce the energy band gap of the bundle by 20%.

1. Introduction

Carbon Nanotubes (CNTs) consists of a rolled mono-atomic sheet of carbon also known as graphene. Nanotube physical properties including high thermal and electrical conductivities, great tensile strength, and elastic modulus have certainly attracted researchers in the last two decades [1]. For instance, the chiral angle pair of indices (*n,m*) which defines how the graphene sheet is wrapped and the diameter of a single-walled carbon nanotube (SWCNTs) also determine the semiconducting or conducting nature of the nanotube [1].

Although those physical properties have extensively been studied over the years based on the structural carbon atoms assembly, experimental data still lack to reach such theoretical values. Consequently, to enhance the performance of future carbon based devices, it is essential to improve simulated model closer to experiments. Thus, two different approaches can be considered to develop new models. First, experiments are performed to extract the electrical properties of carbon nanotube that are directly implemented in simulation software. For instance, Decrossas et al. built a measurement setup to extract the frequency dependence of the complex permittivity of carbon nanotube in a powder form to engineer novel composite material for high frequency applications [2],[3]. An accurate model predicting the behaviour of the complex nano-powder mixture including both semiconducting and metallic nanotubes entangled together was developed. Second, more efficient model based on experimental observations considering fabrication technique, nanotube defects, parasitic effects are developed by imposing new constraints. This is the approach utilized in this work. In fact, with the emergence of new technologies and growth techniques, semiconducting carbon nanotube highly uniform can now be produced allowing models to predict the behaviour of a device more accurately justifying this approach. The developed model at high frequency considers either metallic or semiconducting nanotubes depending on the applications.

For instance, Sarto *et al.* predicted the coupling effect occurring between conducting nanotubes in a bundle based on a hybrid transmission line quantum mechanical model for signal integrity purposes [4]. In this work instead, semiconducting SWCNTs are studied due to their unique property: the energy band gap is inversely proportional to their diameter leading to potential future terahertz (THz) devices [5]. However, fabrication techniques and experimental observations show that highly dense aligned s-SWCNTs are organized in bundles [6] in a device. Understanding the alignment of carbon nanotubes plays a vital role in designing electronic devices and optimizing their operation. Ren et. al. have developed THz polarizer using aligned metallic SWCNT. THz signals polarized parallel to the carbon nanotubes are absorbed, while signals polarized perpendicular to the alignment direction are transmitted [7]. Wang et. al. have developed a FET transistor based on partially aligned s-SWCNTs where the performance is a function of the number of nanotubes per device [8].

Aligned carbon nanotubes have been used in many devices and measured. The obtained results were not adequately correlated to electron transport physics in carbon nanotubes due to the lack of comprehensive theoretical model (i.e. asymmetrical separation distance between nanotubes, partial alignment,…etc.). Modelling carbon nanotubes can be done either based on electromagnetic theory or based on photonics. Burke et. al. have developed a transmission line model for the carbon nanotubes in the gigahertz range [9]. In the THz range, as all the recent devices are, the transmission line is no longer an efficient tool. Hence, in our model we are applying the photonics properties in modelling carbon nanotubes in order to enhance and synthesize better devices in the THz range.

The presented model predicts the energy band gap of a bundle of aligned s-SWCNTs arranged in semi-random order as shown in Fig. 1 considering different radii and distances separating

nanotube. A typical diameter of s-SWCNT is in the order of 1.4-2.1nm, and the minimum distance between s-SWCNTs is the graphite interlayer distance 0.34 nm [10]. First, a novel proposed analytical potential function of the s-SWCNT is introduced and generalized to the bundle. Then, the potential function is implemented in the Schrödinger equation to determine the ground state wave function and the energy band gap variations. Finally, the energy band tuning is demonstrated after applying an external electric field across the bundle.

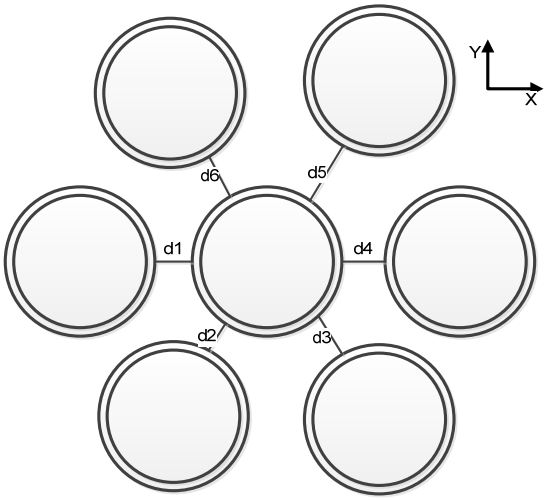

Fig. 1. Geometrical configuration of the semi-conducting single wall carbon nanotube bundle where parallel nanotubes are randomly distant from a centred one (d1, d2, …, d6). (not to scale).

2. Analytical Potential Function

The analytical potential function describes the electron carrier concentration localized around the tube wall due to the tube's cylindrical geometry. Having a well-defined potential function facilitates the study of the electrical and optical properties of a single nanotube as well as the interaction occurring in a bundle. The potential function expression of s-SWCNT was first proposed in [5] as:

$$V_{eff}(r) = \frac{B \times c^2 r^2}{\left(r^2 - R_t^2\right)^2 + c^2 r^2} \qquad (1)$$

where R_t is the nanotube radius, $c = \frac{R_t}{11.446}$ represents the effective SWCNT's wall thickness [11], and $B = 8.25\,\text{eV}$ is the potential well depth is calculated from the general energy dispersion of SWCNT [12] . From (1), the potential function of a single s-SWCNT plotted in Fig. 2 clearly shows that the free carrier electrons are localized on the surface wall of the nanotube.

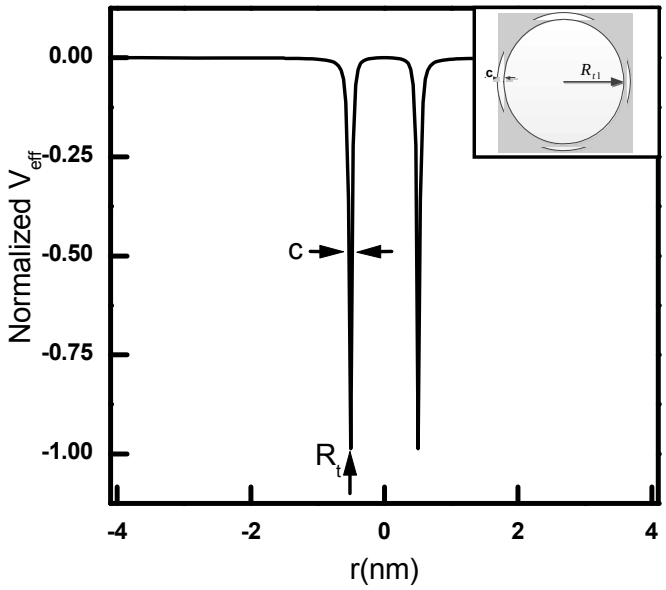

Fig. 2. Normalized potential function across a single s-SWCNT as shown in the inset. R_t is the nanotube radius and c the wall thickness.

The random configuration can be considered as a superposition of several individual s-SWCNTs. Hence, the overall potential is derived as the sum of the individual potentials of each tube.

$$V_{eff-total} = V_{eff1} + V_{eff2} + \ldots + V_{effn} \qquad (2)$$

where n is the number of nanotubes.

The potential function including the contribution of each individual s-SWCNT is then inserted in the differential Schrödinger's equation:

$$\left(\frac{-\hbar}{2m^*}\nabla^2 + V_{eff\ -total}\right)\Psi(r,\phi,z) = E\Psi(r,\phi,z) \tag{3}$$

where $\hbar$ is the Planck's constant, m^* is the effective mass obtained from [13], ∇^2 is the Laplacian and Ψ is the wave function in cylindrical coordinates.

Schrödinger's equation is then solved using *Multiphysics ComSol Simulator* [14]. An ordinary differential equation (ODE) is defined in the radial direction where the azimuthal dependence is sinusoidal and the longitudinal axis is the propagating direction by considering the high aspect ratio (defined by the length and radius) of s-SWCNT. The potential function is then inserted as the analytical expression in Eq. (1) for individual s-SWCNT or the resultant from Eq. (2) in case of a bundle.

3. Simulations and Discussions

Let's first considers three adjacent tubes as shown in Fig.3. All tubes have a diameter of 1.4nm and are separated by 3.4Å.

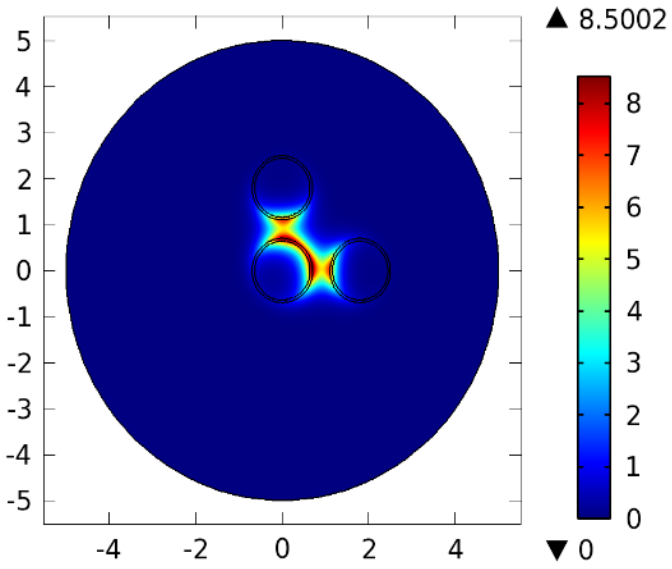
▲ 8.5002
8
7
6
5
4
3
2
1
0
▼ 0
5
4
3
2
1
0
-1
-2
-3
-4
-5
-4
-2
0
2
4

(a)

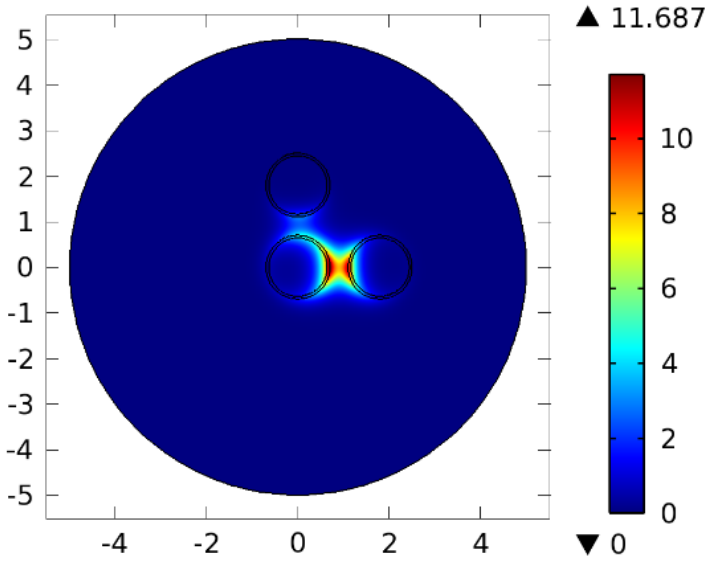
▲ 11.687
10
8
6
4
2
0
▼ 0
5
4
3
2
1
0
-1
-2
-3
-4
-5
-4
-2
0
2
4

(b)

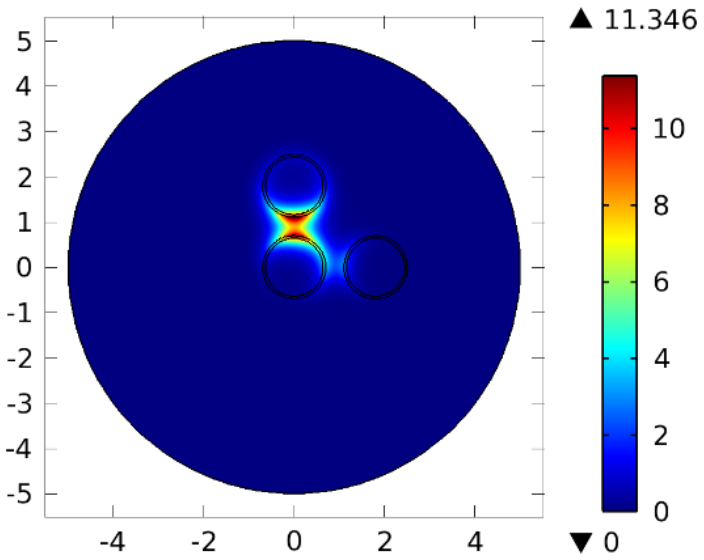

(c)

Fig. 3 Coupling effect occuring between three adjacent s-SWCNT orthogonally localized; (a) uniformly distributed without the presence of an external electric field (b) maximized along the x-axis where the external electric field is applied (c) maximized in the y-axis direction of the applied external electric field .

In this case, the coupling effect between the two adjacent tubes and the centred SWCNT appears to be uniform as presented in Fig. 3(a).

Then an external electrical field of 10^7 V/m is applied in the x direction, the coupling distribution varies with the field direction as shown in Fig.3 (b). It is observed that when applying electric field the coupling is maximized along the tubes in the direction of the electrical field as presented in Fig.3(c) where the electric field is applied in the y-direction.

In the second case, the three nanotubes are now parallel to each other along the x-axis and is referred as configuration A shown in Fig. 4. Similarly to the previous case, all tube diameters are 1.4nm and the distance separating them is fixed to 3.4Å. Again in the absence of an external electric field, the coupling is uniformly distributed, Fig. 4(a). The second case depicted in Fig. 4(b) shows the coupling distribution with the presence of an external electric field along the x-axis

from left to right. It should be noted that the applied electric field greatly enhances the coupling between the two tubes on the left along the field direction.

The third case shows a centred s-SWCNT surrounded by six peripheral s-SWCNTs and is referred as configuration B. Again all tubes 1.4nm wide and equidistant by 3.4Å.

Without external electric field, the coupling effect occurring along the s-SWCNT is equally distributed between

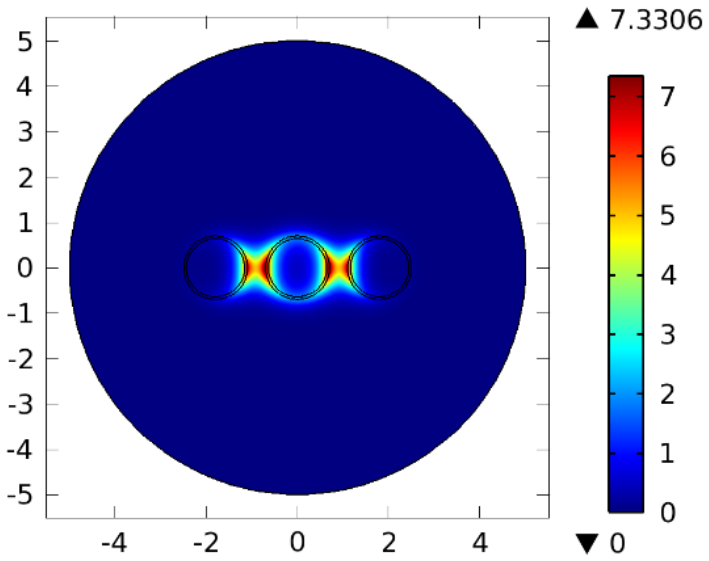

(a)

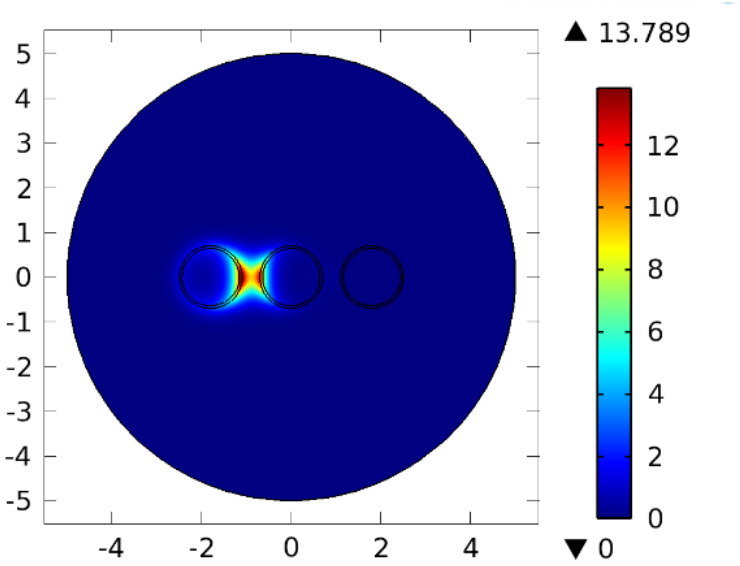

(b)

Fig. 4 Configuration A: Coupling effect distribution between three parallel s-SWCNT; (a) in the absence of an external electric field, (b) with the presence of an external electric field applied along x-axis from left to right.

the nanotube at the centre and its adjacent ones. It should be noted that less coupling occurs among the out-of-centre ones as shown in Fig. 5 (a). Then an external electric field is applied along x-direction from left to right to redistribute the localized coupling among the carbon nanotubes bundle as shown in Fig.5 (b).

In order to clearly understand the effect of the coupling between the adjacent tubes on the electrical and optical properties, the difference of the energy band gap due to the contribution of the coupling effect is calculated:

$$\Delta E = E_g(coupled) - E_g(one\ s - SWCNT) \tag{4}$$

To calculate the energy band gap for the proposed configuration accounting the influence of the electric field, Schrödinger's equation is modified according to [15]:

$$\left(\frac{-\hbar}{2m*}\nabla^2 + V_{eff\ -total} - eFr\cos\phi\right)\Psi(r,\phi,z) = E\Psi(r,\phi,z) \tag{5}$$

where e is the electron charge, F is the electric field applied along the x-axis expressed in cylindrical coordinates.

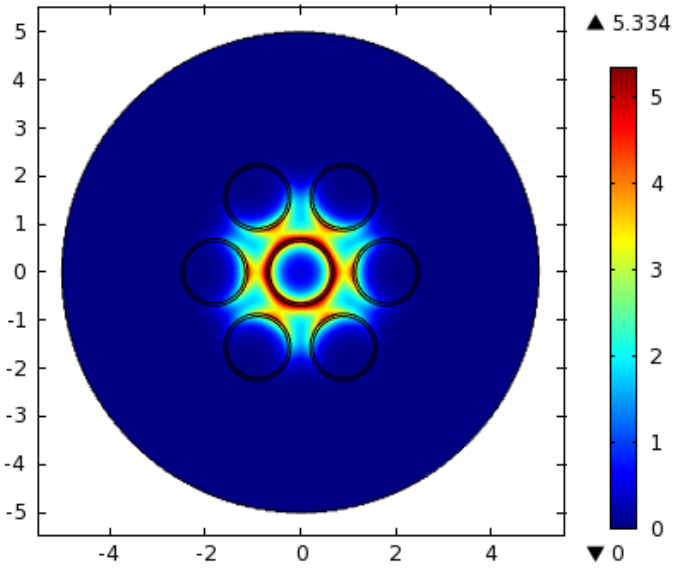

(a)

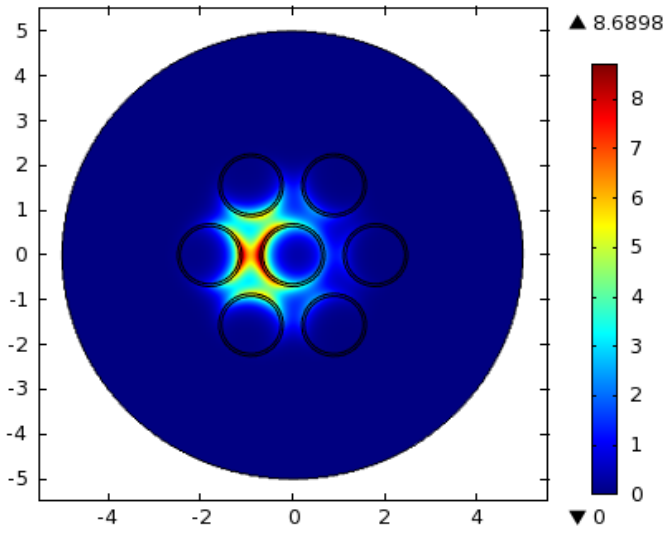

(b)

Fig. 5 Configuration B: Coupling effect distribution between seven adjacent s-SWCNT; (a) in the absence of an external electric field, (b) with the presence of an external electric field applied along x-axis from left to right.

Fig. 6 (a) shows the energy band gap variation versus the distance separating the semi-conducting single-walled carbon nanotubes considering configuration A and B. When the carbon nanotube are close to each other, the contribution of the coupling effect becomes non negligible. As expected the coupling effect is highly dependent of the distance separating the nanotube. The energy band gap is reduced from 50meV to 5meV when the distance between the nanotubes in configuration A and B increases from 3.4Å to 15Å. It should be mentioned that no noticeable effect occurs based on the different configurations. In fact, the coupling effect is equally distributed between the numbers of SWCNTs in the absence of an external electrical field. Fig. 6 (b) presents the energy band gap distinction in the existence of an external applied electric field for both configurations. Applying the electric field clearly enhances the coupling between the s-SWCNTs and; hence, the energy band gap change is 20% more than the case where there no electric field.

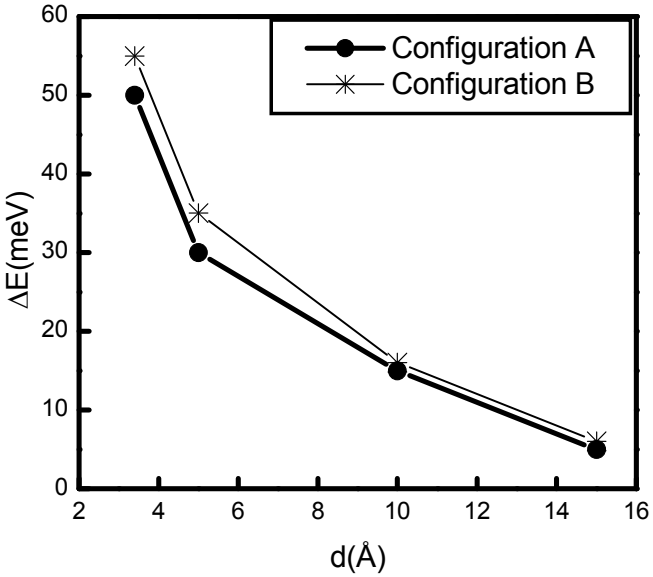

(a)

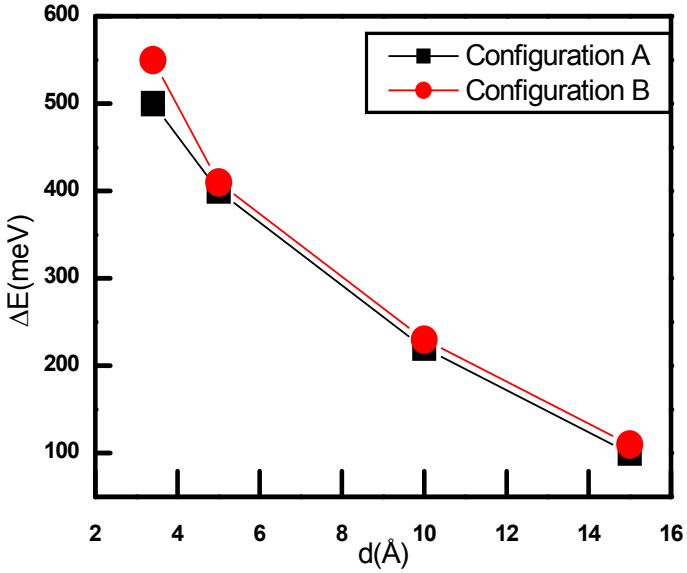

(b)

Fig. 6 the change in the energy band gap for both configurations A and configuration B (a) with no electric field applied, (b) with an electric field applied along x-axis.

4. Conclusion

A comprehensive study of the coupling effect between semi-conducting single-walled carbon nanotube is demonstrated considering different configurations. In the absence of an external electric field, the coupling between the nanotubes is equally distributed among the SWCNT in the bundle. Then by applying an external electric field, our data show that not only the coupling is now localized between the first nanotubes encounter by the electric field along its direction, but also the energy band gap of the bundle is greatly enhance. This is an important property for terahertz or far infrared optical applications where the development of devices in this spectrum is limited by the current semiconductor material properties. Finally, the potential to tune or reduce the energy band gap of semiconducting single-walled carbon nanotube can improve solar cell efficiency by enlarging the absorption spectrum compared to the current technology.

References

[1] A. Jorio, G. Dresselhaus, and M. Dresselhaus, *Carbon nanotubes: advanced topics in the synthesis, structure, properties and applications,* Springer, 2008.

[2] E. Decrossas, M.A. EL Sabbagh, V. Fouad Hanna and S.M. El-Ghazaly, "Rigorous characterization of carbon nanotube complex permittivity over a broadband of RF frequencies," *IEEE Trans. Electromag. Compat.*, vol. 54, no. 1, pp. 81-87, Feb. 2012.

[3] E. Decrossas, M.A. EL Sabbagh, V. Fouad Hanna and S.M. El-Ghazaly, "Engineered Carbon-nanotube Based Composite Materials for RF Applications," *IEEE Trans. Electromag. Compat.*, vol. 54, no. 1, pp. 52-59, Feb. 2012.

[4] M.S. Sarto, A. Tamburrano, and M. D'Amore, "New electron-waveguide-based modeling for carbon nanotube interconnects," IEEE Trans. Nanotechnology, vol.8, no.2, pp. 214-225, Mar. 2009.

[5] A. Elkadi, E. Decrossas, S. F. Yu, H. Naseem, and S. El-Ghazaly, "Controlling the Band Gap of Aligned Semiconducting Single-Walled Carbon Nanotubes for THz Modulator," in IEEE European Microw. Week, Amsterdam, Netherland, 28 Oct.- 3 Nov. 2012.

[6] A. Elkadi, E. Decrossas, and S.M. El-Ghazaly, "Fabrication Technique of Highly Dense Aligned Semiconducting Single-Walled Carbon Nanotubes Devices," in IEEE Photonics conf., Burlingame, CA, 23-27 Sept. 2012.

[7] L. Ren, C.L. Pint, T. Arikawa, K. Takeya, I. Kawayama, M. Tonouchi, R.H. Hauge and J. Kono, "Broadband terahertz polarizers with ideal performance based on aligned carbon nanotube stacks," Nano Letters, vol. 12, pp. 787-790, Jan. 2012.

[8] Y. Wang, S.K.R. Pillai and M.B. Chan-Park, "High-Performance Partially Aligned Semiconductive Single-Walled Carbon Nanotube Transistors Achieved with a Parallel Technique," Small, Feb. 2013.

[9] P.J. Burke, "Luttinger liquid theory as a model of the gigahertz electrical properties of carbon nanotubes," Nanotechnology, IEEE Transactions on, vol. 1, pp. 129-144, Sep. 2002.

[10] Y. Saito, T. Yoshikawa, S. Bandow, M. Tomita and T. Hayashi, "Interlayer spacings in carbon nanotubes," *Physical Review B*, vol. 48, pp. 1907, Jul. 1993.

[11] T. Vodenitcharova and L. Zhang, "Effective wall thickness of a single-walled carbon nanotube" *Physical Review B*, vol. 68, no. 16, pp. 165401. May 2003.

[12] S. V. Rotkin and S. Subramoney. *Applied Physics of Carbon Nanotubes Fundamentals of Theory, Optics and Transport Devices,* Springer, 2005.

[13] K. El Shabrawy, K. Maharatna, D. Bagnall and B. M. Al-Hashimi. Modeling SWCNT bandgap and effective mass variation using a monte carlo approach." *IEEE Trans. on Nanotechnology*, vol. 9, no.2, pp. 184-193, Mar. 2010.

[14] COMSOL Multiphysics, Burlington, MA, Version 4.2.0.150, 2011.

[15] G. Vázquez, M. Del Castillo-Mussot, J. Montemayor-Aldrete, H. Spector and C. I. Mendoza, "Transverse stark effect of electrons in a hollow semiconducting quantum wire," *Physica E: Low-Dimensional Systems and Nanostructures*, vol. 33, no. 1, pp. 240-243, June 2006.

UNIVERSITY OF ARKANSAS
College of Engineering
Department of Electrical Engineering

April 10th, 2015

To whom it may concern,

I certify that Ms. Asmaa Elkadi is the first author of the paper titled "Energy Band Gap Study of Semiconducting Single Walled Carbon Nanotube Bundle "presented in IEEE Symposium on Electromagnetic Compatibility, Aug. 2013. Ms. Elkadi completed majority (more than 51%) of this research and writing this paper.

Prof. Samir M. El-Ghazaly
Distinguished Professor
Electrical Engineering
Office: 3169 Bell Engineering Center
Phone: 479-575-6048
E-mail: elghazal@uark.edu

Chapter IV. Single-Walled-Carbon-Nanotube Contact Resistance: Analysis and RF Performance

Abstract

This paper presents detailed electromagnetic analysis of individual single-walled carbon nanotube-based devices in order to enhance their synthesis and performance. A model is developed using physics-based parameters from measurements to realistically determine the sources of the usual discrepancies that appear between the theory and measurements for nanotube devices. The model is developed for one nanotube calculating the effects of associated parasitic elements on its performance. The proposed electromagnetic model shows good agreement with first-principles calculations and measurements. The model is flexible and could be integrated with quantum transport models.

1. Introduction

Integration of semiconducting nanomaterials such as carbon nanotubes, nano-wires and graphene nano-ribbons into large scale circuits has attracted the attention of many researchers due to their unique 1-D properties [1]. The carbon nanotube's electrical conductivity is anisotropic along its axis while quantified on the perpendicular axis due to the high aspect ratio [2]. Promising electrical and optical 1-D characteristics make carbon nanotubes viable candidates for high frequency devices [3]-[10]. In addition, altering the nanotubes' properties by functionalizing them in the form of composites has been used for photonics applications [11]. Despite the promising theoretical expectations of ballistic high speed transport of single-walled carbon nanotubes (SWCNTs) -based devices, synthesizing and improving their performance is still a challenge [12]-[14].

Observed discrepancies between simulated data and experimental results of fabricated devices obstruct the development of SWCNT-based devices into practical and large-scale integrated circuits[15]. Among key factors that degrade the performance of SWCNT-based devices are the contact resistance and fringe capacitance between nanotubes and metallic electrodes, as they are not well established. Although palladium provides the highest on-current in SWCNT due to its matching work function, carbon-based devices contact resistances have been reported to be on the order of a few KΩ [16]-[20]. These values are higher than the ones for the Ohmic contacts formed in conventional semiconductor devices. A perfect ohmic contact could not be formed at the nano-scale level due to the chemical reactivity between the SWCNT and the metal. Instead, an overlap area of a lower conductivity forms between the SWCNT and the metal which creates an extra barrier due to the hybridization between the carbon atoms and the metal [21].

This paper presents a physical insight to understand this phenomena. In Section II, a scheme for calculating the contact resistance and the fringe capacitance for individual SWCNT-based devices is presented, with full parametric study. The results are presented in Section III, which includes an independent verification of the model.

2. Model

The basic building blocks of an electronic device are the transport medium and contacts. Theoretically speaking, using carbon nanotubes as the transport medium is expected to produce ballistic electron transport. However, there are significant discrepancies between the theory and measurements. One of the main factors behind the discrepancy is the vague understanding of what happens around the contacts and the limitations they introduce. In order to address this problem, this paper takes a close look at the contact areas and performs a parametric study to determine the significant parameters that affect the contacts. This is a considerable step toward enhancing the

overall performance.

A. Electrostatic Analysis

At room temperatures, the charge transport is governed by Luttinger Liquid tunneling for 1-D conductors to describe the electron interactions. Although electrons ballistically transport along the carbon nanotubes due to their long mean free path, they suffer back scattering with optical phonons[19]. The strength of the electron-phonon coupling is defined by the distance an electron travels after the phonon is emitted and before the electron is backscattered. The effect of the backscattering around the contacts is a key factor that controls the overall transport. In this paper, a SWCNT connecting two metallic pads, as shown in Fig. 1(a), can be modeled as a hollow cylinder that has a diameter-dependent effective wall thickness[22]. SWCNTs are either metallic or semiconducting, which determines the material conductivity of the tube. The chemical reactivity between the SWCNT and the metal forms an extra barrier which will be referred to as a chemically-altered resistance (CAR) region due to the hybridization between the $\boldsymbol{dz^2}$ orbitals of the palladium atoms and the ***pz*** orbitals of the carbon atoms in the nanotubes [21]. This barrier is modelled by an overlap area, as shown in Fig. 1(b). In this study, this area is parameterized to develop a correlation between the physical properties and the experimental measurements. The parameters of this region are described as: l_2, the overlap length, is varied from few nanometers to sub-micrometers; t, the overlap thickness, varies as a fraction of the effective wall thickness of the SWCNT [22]; and σ_2, the conductivity of the overlap area, varies from insulating material to high conductivity material in the same order of magnitude as the main conductivity of the SWCNT body. To simplify the model, without any loss of generality, the remaining metallic pads are formed of a lossless conductor. Their resistivity can easily be incorporated, if needed.

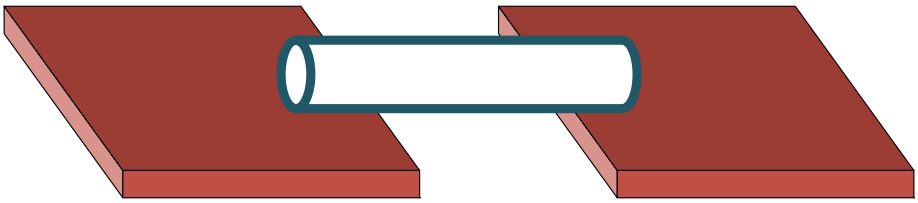

(a)

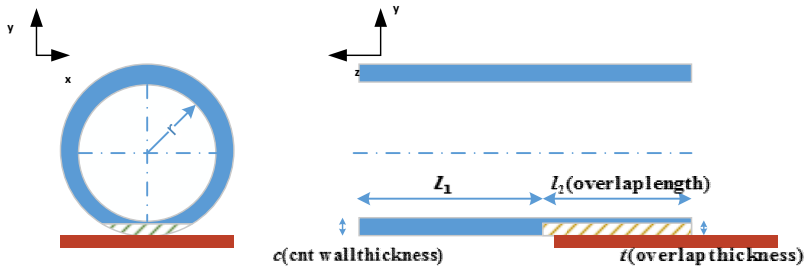

(b)

Fig. 1(a) 3-D schematic of SWCNT touching two metallic contacts, (b) cross-section of the one end of the SWCNT touching the metal.

The electric potential of the structure is governed by Poisson's equation which is solved using a Finite Difference (FD) scheme developed for these structures [23]. For comparison, it is also solved using a commercial Multiphysics simulator [24]. Fig.2 (a) shows a schematic of the boundary conditions applied at the surfaces of the SWCNT. A virtual potential is applied at one end of the tube. The edge of the other end touches the metallic plane, which is grounded. Figs. 2(b)- 2(d) show the electric potential distribution along the SWCNT for different overlap lengths. It is observed that for very short lengths, the electric potential drops too slowly. For long overlap length, the potential drops quickly and the electric charges find a shorter path to the ground plane; hence, a lower resistance is achieved.

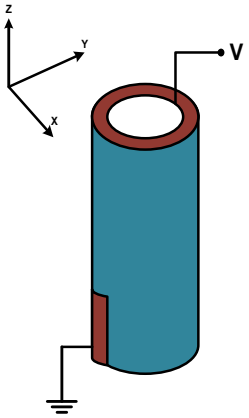

(a)

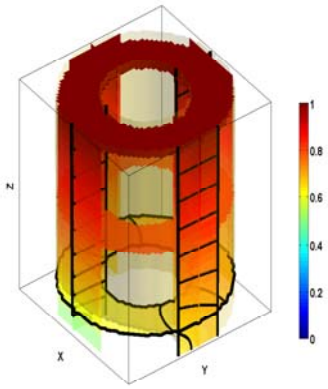

(b)

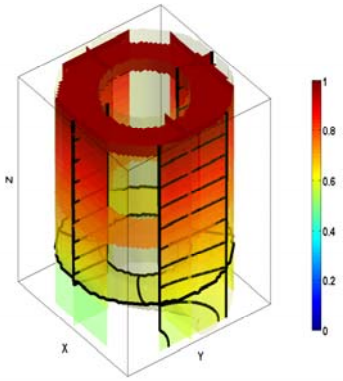

(c)

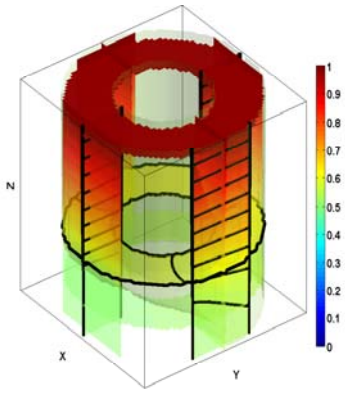

(d)

Fig. 2 (Color online) (a) the schematic of the nanotube boundary conditions for Poisson's equation, (b) the electric potential distribution for overlap length 1 nm, (c) 5 nm, and (d) 10 nm.

The electric field distribution is calculated and depicted in Fig. 3. The three-dimensional distributions of the electric field lines are shown in Fig. 3(a). Their projections in the x-y plane and the z-y plane are presented in Fig. 3(b) and Fig.2(c) respectively.

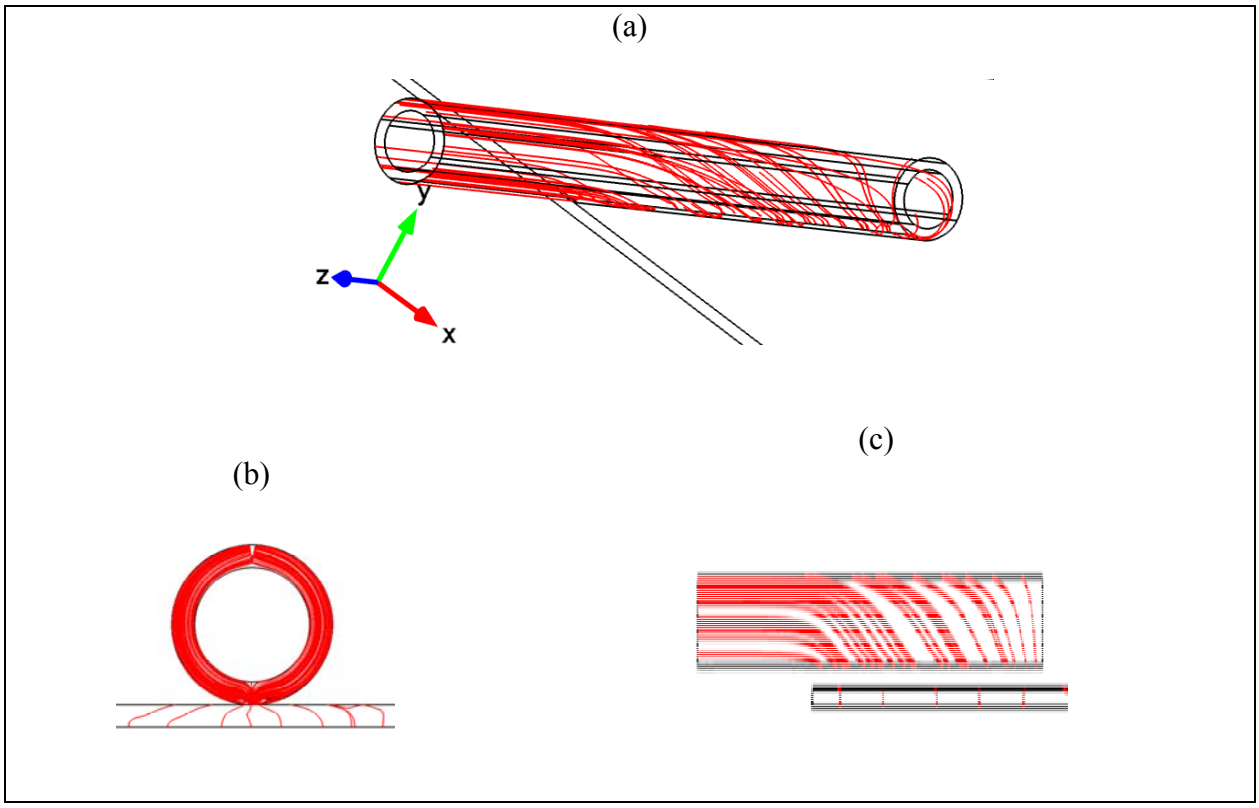

Fig. 3 (a) 3-D Current lines of the SWCNT, (b) Cut projection of the current lines at metallic edge overlap with SWCNT at l_2, (c) Cut projection of the current lines in the middle of the SWCNT wall thickness.

A parametric study has been performed in [25]. This shows that the dominant parameter influencing the contact resistance is the overlap length between the SWCNT and the metallic plane. When the overlap length is very small, the device suffers very high contact resistance regardless of how efficient the metallic electrodes are fabricated or how close their work function is to the carbon nanotubes' work function. The overlap length is then increased to demonstrate the significant improvement of the contact resistance. The study shows that the contact resistance rapidly decreases first, then it reaches an asymptotic minimum value after some characteristic overlap length. This characteristic length may be referred to as the effective length.

To validate the FD results and confirm the previous observation, the parametric study was performed using a Multiphysics simulator. Fig. 4 shows the change of the contact resistance versus

the change in the overlap length for both the Multiphysics simulator and the FD method. The two schemes demonstrate the same trend. They are in a good agreement with the concept of the effective length described earlier. The FD scheme has the advantages of controlling the aspect ratio and mesh size, and offers the possibility of scalability and large scale integration with quantum transport equations.

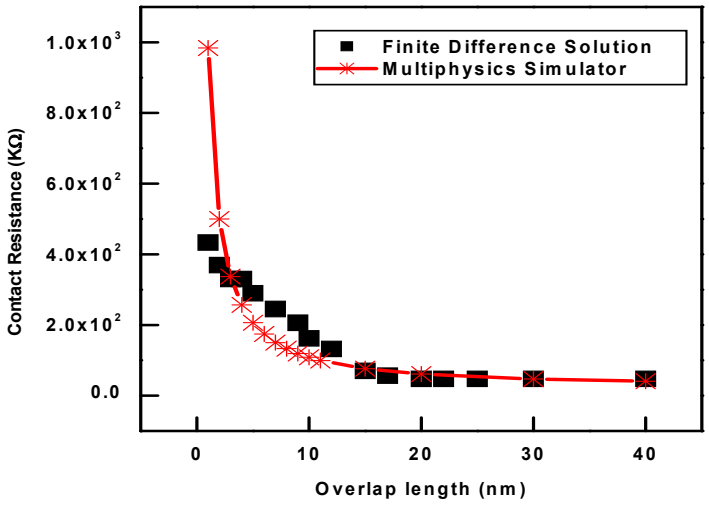

Fig. 4 The contact resistance variation versus the overlap length for both the Multiphysics simulator and the solution obtained by FD (the nanotube radius a=0.7nm; the nanotube bulk conductivity $\sigma_1=10^6$ S/m; the overlap layer conductivity $\sigma_2 = 10^3$; and the thickness of the overlap layer t=0.1nm).

Fig. 5 shows the variation of the contact resistance as a function of the overlap area thickness. The thickness is modeled as a fraction of the SWCNT wall thickness. The contact resistance exhibited a slight increase with the increase of the CAR thickness that is not significant in the device performance with respect to the effect of the overlap length, which concludes that the thickness of the overlap layer is not a governing parameter if the overlap length is less than the effective length [25].

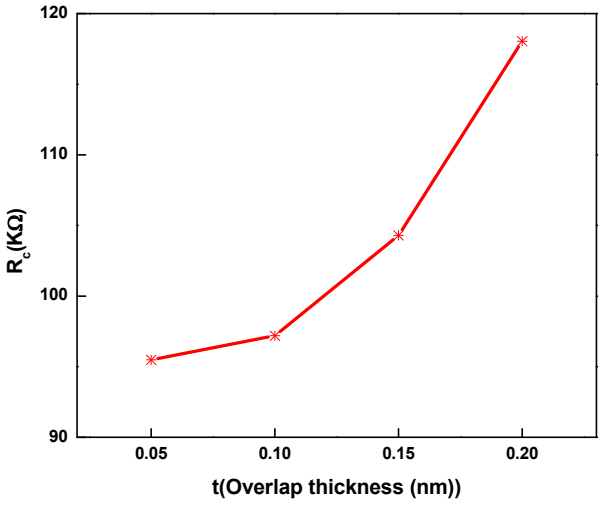

Fig. 5 Contact resistance variation versus overlap thickness (the nanotube radius a=0.7nm; the nanotube bulk conductivity $\sigma_1=10^6$S/m; the overlap layer conductivity $\sigma_2=10^3$; the overlap length l_2=40nm).

In Fig. 6, the contact resistance is studied as a function of the CAR region conductivity for different overlap lengths. The conductivity values are varied ranging from a totally insulating material to a high conductivity, just as the bulk part of SWCNT ($\sigma_1=10^6$). It is demonstrated that as conductivity increases, the overall contact resistance decreases toward ideal Ohmic resistances regardless of the contact overlap length. Hence, if the measured resistance is very high (in the order of 100 MΩ), the first parameter to be checked is the overlap length, followed by the conductivity of the overlap area, ending with the overlap thickness.

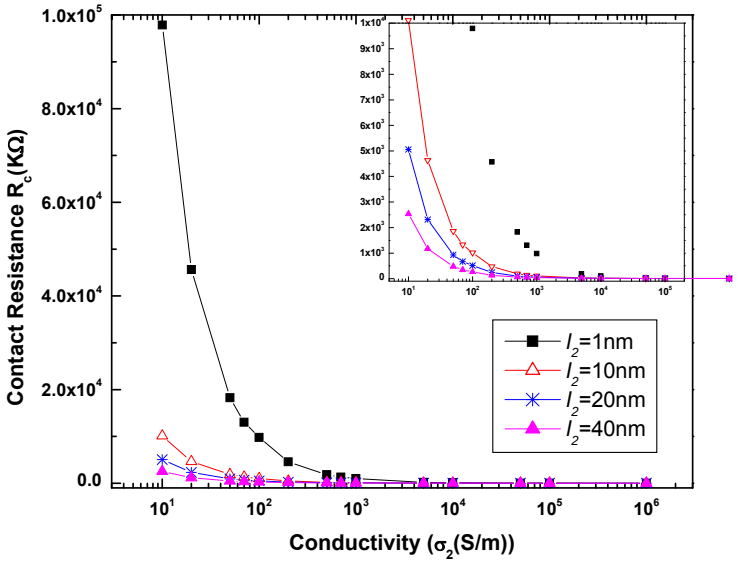

Fig. 6 Contact resistance variation versus overlap conductivity for various overlap length (the nanotube radius a=0.7nm; the nanotube bulk conductivity $\sigma_1=10^6$S/m; the thickness of the overlap layer t=0.1nm).

Some efforts have been made to enhance the contact between the nanotubes and the metallic plane by depositing the metal on top and introducing a graphitic layer as a buffering inter-layer in between to enhance the carrier injection [26]. Adding the metal on top of the nanotubes slightly increases the surface area, while the graphitic layer enhances the conductivity of the area between the nanotube and metal and improves the coupling.

B. RF Analysis

Analyzing the device frequency response gives more information about the other parasitic elements that might limit the device performance. In order to develop the schematic circuit of SWCNT-based devices, one must understand the RF of the tube itself. The nanotube mainly consists of two parts: the non-contacting segment of the SWCNT, and the segment where the SWCNT lays on the metallic pad connected to the ground plane. Fig. 7 shows this schematic of the circuit representation. The non-contacting part deals with quantum quantities R_q and C_q of

values 12.9 KΩ and 82 aF respectively [27]. The contact area quantities R_c and C_c are the contact resistance and capacitance, respectively. The resistance is directly dependent on the conductivity of the overlap-section. The capacitance is dependent on the material permittivity. The conductivity of the carbon nanotubes is position dependent, but the permittivity is independent of position and obtained from experimental data (a very high value, around 80 at low frequencies [28]). The contact resistance is calculated as described before. The capacitance is obtained from the electrostatic analysis of the structure.

The contact reflection coefficient described by the schematic appearing in the inset of Fig. 7 is calculated for different overlap conductivities (the hashed area in Fig.1 (b)) and varied as a function of the overlap length. The results shown in Fig. 7 illustrate that the contact reflection coefficient exhibits direct dependence on the overlap length and the conductivity of CAR. The reflection coefficient has significantly high values for low conductivities, which is expected for the high anticipated contact resistances. However, the reflection coefficient decreases with the increase of the overlap length (l_2) until it reaches an effective length which agrees with the observations and physical explanations provided earlier. The reflection coefficient is also calculated using the equation obtained by ab-initio calculations in [29]:

$$\Gamma = e^{-\frac{l_2}{a_{cc}} * \frac{\Delta}{\gamma}} \tag{1}$$

where Δ is the coupling factor between the overlap area and the nanotube body; a_{cc} is the carbon-carbon bond unit length 0.246nm; γ is the hopping energy between carbon atoms; 2.66eV. The coupling factor Δ is found to be proportional to the ratio between the conductivity of the overlap area and the conductivity of carbon nanotube body. The results of Eq. (1) are plotted in Fig. 7 in addition to those obtained using the model. This RF analysis agrees with the trend calculated using the atomistic approach proposed by Nemec *et al*. [29].

The model could be generalized to include multi-walled carbon nanotube (MWCNT), where the overlap area concept is applied to the outer shell of the MWCNT as shown in the inset of Fig.8. The contact resistances of a multi-wall nanotube is calculated using the model and using the equation developed in [30]:

$$R_c = \sqrt{r_c r_{cnt}}\coth\left(\sqrt{\frac{r_{cnt}}{r_c}}\, l_2\right) \tag{2}$$

where $r_c = 1/(\sigma_2 a * \theta_0)$ (Ω.m) which defines the resistivity of the overlap area, l_2 is the overlap length, $\theta_0$is the angle of the overlap between the metallic plane and the carbon nanotube, and r_{cnt} is the resistance per unit length of main body of the MWCNT nanotube (1KΩ/μm) [30].

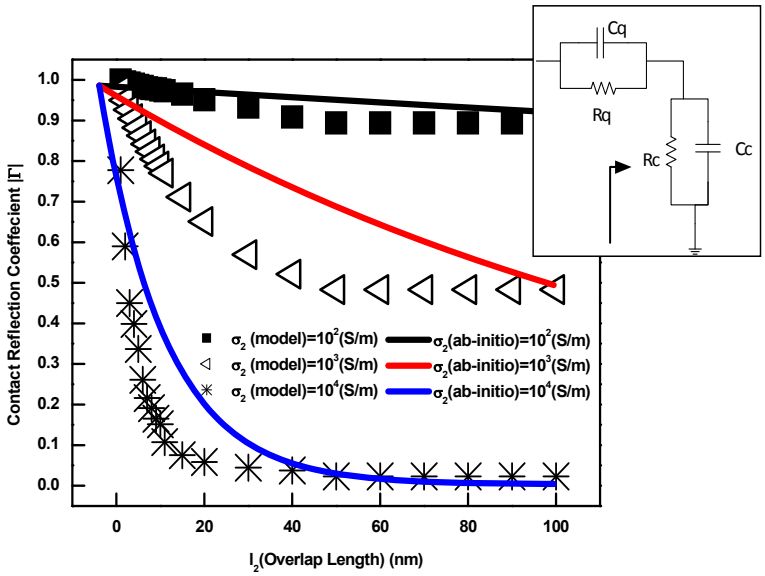

Fig. 7 The contact reflection coefficient versus the overlap length (l_2) with RF schematic model in the inset for the model and ab-initio calculations (the nanotube radius a=0.7nm, the nanotube bulk conductivity σ_1=10^6S/m, the thickness of the overlap layer t=0.1nm).

The contact resistances for MWCNT are plotted versus the overlap length between the nanotube and the metallic plane in Fig. 8. The resistances are calculated using the model and Eq. (2) for

different conductivities of the overlap area. Both methods agree to a great extent in estimating the contact resistance of the MWCNT as well as the good agreement with the measurements [30].

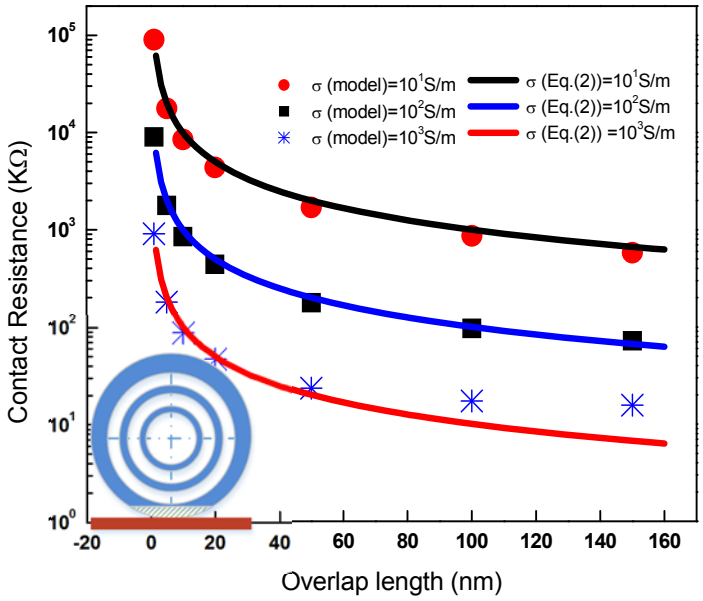

Fig. 8 The contact resistance variation versus the overlap length for both the Multiphysics simulator and the solution obtained by Eq.(2) [30] (the nanotube radius a=2nm; the nanotube bulk conductivity $\sigma_1=10^6$ S/m (inner shells as well); and the thickness of the overlap layer t=0.1nm).

3. Results

In order to correlate the measurements with the model, measurements of an individual SWCNT are extracted from [31] and plotted with the model in Fig. 12. The model parameters for the CAR area for the individual nanotube structure are: the overlap length l_2 = 50 nm, the thickness t = 0.1 nm, and the conductivity σ_2 = 40 S/m. The model predicts an estimated resistance of 132 MΩ, which is in good agreement (within acceptable error range) with the measurements.

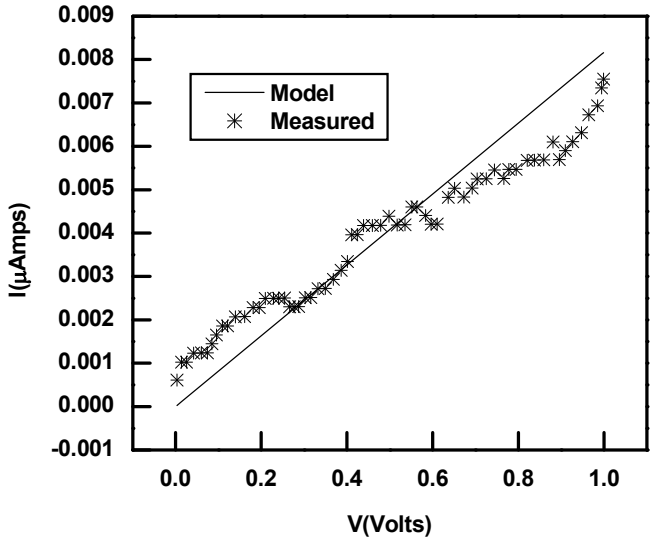

Fig.12 I-V Characteristics of an individual SWCNT device for both the model and the measured data extracted from [31] (the overlap length $l_2 = 50$ nm; the thickness of the overlap area $t = 0.1$ nm; and the conductivity of the overlap area $\sigma_2 = 40$ S/m).

Enhancing the contact resistance could be achieved for a single SWCNT by ensuring that the overlap section between the tube and the contact pad is higher than the effective length studied earlier. The parasitic elements could also be affected by additional post processing (e.g., thermal annealing, RF induction heating, Electron beam irradiation…etc.)[32].

4. Conclusion

A comprehensive model has been developed for SWCNT-based devices. The model incorporates realistic parameters to decrease reported discrepancies between the theory and measurements. The model also provides a physical insight and thorough understanding of the different factors affecting contact resistance values. The model is developed for an individual SWCNT. A parametric study has been performed to demonstrate that the critical factor for improving the device performance and minimizing the contact resistance is ensuring the overlap length between the nanotube and the metallic pad is longer than the effective length. The model results have been compared with

measurements and a good agreement has been observed. This study provides an understanding of key parameters and limitations that degrade the SWCNT-based devices and suggest techniques to enhance their performance.

References

[1] A. Jorio, G. Dresselhaus, and M. Dresselhaus, *Carbon nanotubes: advanced topics in the synthesis, structure, properties and applications,* Vol. 111 (Springer, 2008).

[2] T. Jeon, K. Kim, C. Kang, S. Oh, J. Son, K. H. An, D. J. Bae and Y. H. Lee. "Terahertz conductivity of anisotropic single walled carbon nanotube films," *Appl. Phys. Lett. 80(18),* pp. 3403-3405. Apr. 2002.

[3] P. J. Burke. "AC performance of nanoelectronics: Towards a ballistic THz nanotube transistor." *Solid-State Electronics 48(10),* pp. 1981-1986. June 2004.

[4] A. Elkadi, E. Decrossas, S. Yu, H.A. Naseem and S.M. El-Ghazaly, "Controlling the energy band gap of aligned semiconducting single-walled carbon nanotubes for THz modulator," in 7th European Microwave Integrated Circuits Conference (EuMIC), pp. 270-273, Oct. 2012.

[5] E. Decrossas, A. Elkadi and S. El-Ghazaly, "Carbon nanotube based prototype as THz time domain sources/detectors," in 37th International Conference on Infrared, Millimeter, and Terahertz Waves (IRMMW-THz), pp. 1-2, Sept. 2012.

[6] J. Chaste, L. Lechner, P. Morfin, G. Feve, T. Kontos, J. Berroir, D. Glattli, H. Happy, P. Hakonen and B. Plaçais. "Single carbon nanotube transistor at GHz frequency." *Nano Letters 8(2),* pp. 525-528. Jan. 2008.

[7] J. Guo, S. Hasan, A. Javey, G. Bosman and M. Lundstrom. "Assessment of high-frequency performance potential of carbon nanotube transistors." Nanotechnology, IEEE Transactions on 4(6), pp. 715-721. Nov. 2005.

[8] C. Kocabas, H. S. Kim, T. Banks, J. A. Rogers, A. A. Pesetski, J. E. Baumgardner, S. V. Krishnaswamy and H. Zhang. "Radio frequency analog electronics based on carbon nanotube transistors." *Proc. Natl. Acad. Sci. U. S. A. 105(5),* pp. 1405-1409. Feb. 2008.

[9] S. Hamieh. "Improving the RF performance of carbon nanotube field effect transistor," *Journal of Nanomaterials 2012*pp. 8. Feb. 2012.

[10] M. A. Wahab, S. H. Jin, A. E. Islam, J. Kim, J. Kim, W. Yeo, D. J. Lee, H. U. Chung, J. A. Rogers and M. A. Alam. "Electrostatic dimension of aligned-array carbon nanotube field-effect transistors," *ACS Nano 7(2),* pp. 1299-1308. Jan. 2013.

[11] J. Wang, Y. Chen and W. J. Blau. Carbon nanotubes and nanotube composites for nonlinear optical devices.*Journal of Materials Chemistry 19(40),* pp. 7425-7443. 2009.

[12] H. E. Unalan, G. Fanchini, A. Kanwal, A. Du Pasquier and M. Chhowalla. "Design criteria for transparent single-wall carbon nanotube thin-film transistors," *Nano Letters 6(4),* pp. 677-682. Feb. 2006.

[13] O. Balci and C. Kocabas. "High frequency performance of individual and arrays of single-walled carbon nanotubes," *Nanotechnology 23(24),* pp. 245202. May 2012.

[14] C. Kocabas, N. Pimparkar, O. Yesilyurt, S. Kang, M. A. Alam and J. Rogers. "Experimental and theoretical studies of transport through large scale, partially aligned arrays of single-walled carbon nanotubes in thin film type transistors," *Nano Letters 7(5),*pp. 1195-1202. Mar. 2007.

[15] S. Bellucci and P. Onorato. *Physical Properties of Ceramic and Carbon Nanoscale Structures,* The INFN Lectures, Vol. II (Springer 2011).

[16] Z. Chen, J. Appenzeller, J. Knoch, Y. Lin and P. Avouris, "The role of metal-nanotube contact in the performance of carbon nanotube field-effect transistors," *Nano Letters,* vol. 5, pp. 1497-1502, June 2005.

[17] F. Xia, V. Perebeinos, Y. Lin, Y. Wu and P. Avouris. "The origins and limits of metal-graphene junction resistance," *Nature Nanotechnology 6(3),* pp. 179-184. Jan. 2011.

[18] E. J. Lee, K. Balasubramanian, R. T. Weitz, M. Burghard and K. Kern. "Contact and edge effects in graphene devices," *Nature Nanotechnology 3(8),* pp. 486-490. June 2008.

[19] Z. Yao, C. L. Kane and C. Dekker. "High-field electrical transport in single-wall carbon nanotubes." *Phys. Rev. Lett. 84(13),* pp. 2941. Mar. 2000.

[20] C. Rutherglen, D. Jain and P. Burke. "RF resistance and inductance of massively parallel single walled carbon nanotubes: Direct, broadband measurements and near perfect 50 Ω impedance matching." *Appl. Phys. Lett.93(8),* pp. 083119-083119-3. Aug. 2008.

[21] N. Nemec, D. Tománek and G. Cuniberti, "Contact dependence of carrier injection in carbon nanotubes: an ab initio study," *Phys.Rev.Lett*., vol. 96, pp. 076802, Feb. 2006.

[22] T. Vodenitcharova and L. Zhang. "Effective wall thickness of a single-walled carbon nanotube," *Physical Review B* 68(16), pp. 165401. Oct. 2003.

[23] R. J. LeVeque. *Finite Difference Methods for Ordinary and Partial Differential Equations: Steady-State and Time-Dependent Problems*, (Siam, 2007).

[24] http://www.comsol.com/

[25] A. Elkadi, S. M. El-Ghazaly, “On the Contact Resistance of Single-Walled Carbon Nanotubes in RF devices,” presented at International Microwave Symposium, Tampa, FL, June 2014.

[26] Y. Chai, A. Hazeghi, K. Takei, H. Chen, P. C. Chan, A. Javey and H. P. Wong. “Graphitic interfacial layer to carbon nanotube for low electrical contact resistance.” Presented at Electron Devices Meeting (IEDM). Dec. 2010.

[27] J. Dai, J. Li, H. Zeng and X. Cui, "Measurements on quantum capacitance of individual single walled carbon nanotubes," *Appl.Phys.Lett*., vol. 94, pp. 093114-093114-3, Mar. 2009.

[28] E. Decrossas, M.A. EL Sabbagh, V. Fouad Hanna and S.M. El-Ghazaly, “Rigorous characterization of carbon nanotube complex permittivity over a broadband of RF frequencies,” *IEEE Trans. Electromag. Compat.*, vol. 54, no. 1, pp. 81-87, Feb. 2012.

[29] N. Nemec, D. Tománek and G. Cuniberti. “Modeling extended contacts for nanotube and graphene devices.”*Physical Review B 77(12),* pp. 125420. Mar. 2008.

[30] C. Lan, P. Srisungsitthisunti, P. B. Amama, T. S. Fisher, X. Xu and R. G. Reifenberger. “Measurement of metal/carbon nanotube contact resistance by adjusting contact length using laser ablation.” *Nanotechnology 19 (12),* pp. 125703. Feb. 2008.

[31] B.K. Sarker, S. Shekhar and S.I. Khondaker, ”Semiconducting enriched carbon nanotube align arrays of tunable density and their electrical transport properties,” *ACS Nano 5* (8), pp 6297–6305, July 2011.

[32] L. An, X. Yang and C. Chang. “On contact resistance of carbon nanotubes”. *International Journal of Theoretical and Applied Nanotechnology 1(2),* pp. 30. Dec. 2013.

Chapter V. A. Fabrication Technique of Highly Dense Aligned Semiconducting Single-Walled Carbon Nanotubes Devices

Abstract

A fabrication technique using dielectrophoresis is demonstrated to align semiconducting single-walled carbon nanotubes (s-SWCNTs) and improve electronic devices performance. The proposed method produces highly dense aligned nanotubes (>40 s-SWCNTs/μm) and low sheet resistance (<10 KΩ/□).

1. Introduction

In the last decades, carbon nanotubes have attracted the attention of researchers due to their extraordinary electrical properties along their axis [1]. The very large scale integration (VLSI) of carbon nanotube based devices is challenging as it requires high devices yield and alignment of the nanotubes to optimize the performance of electronic devices and consider mass production manufacture [2,3]. In this paper, the developed method based on AC dielectrophoresis technique

to align semiconducting single-walled carbon nanotubes (s-SWCNTs) is applied to several devices at once. In addition, the resulting density of s-SWCNTs per device has exceeded the ones reported in the literature and the enhancement of the sheet resistance is observed compared to recent publications [4].

2. Fabrication Technique

The semiconducting single-walled carbon nanotubes furnished by Nanointegris suspended in aqueous solution are deposited and aligned using an AC dielectrophoresis (DEP) technique, [2, 3], across the horizontal electrodes presented in Fig. 1(a). According to the manufacturer the utilized solution consists of 20 μg/ml of 99% pure s-SWCNT with diameter from 1.2 nm to 1.7 nm, and length from 300 nm to 5 μm suspended in aqueous solution consisting of 1% w/v ionic surfactant diluted in deionized (DI) water [5]. The fabricated chip is 1 cm^2 and has 17 devices in the center of the chip with two common electrodes to apply the AC bias voltage across the isolated electrodes to all of them at once. The device consists of a four probes as shown in Fig. 1(b) to verify the alignment conditions. Dielectrophoresis is applied along the horizontal electrodes 2 and 4, while the other two vertical electrodes provide information about the isolation between the different electrodes and the good alignment conditions. The s-SWCNTs are deposited and aligned in the 4 μm gap delimited by the electrodes by applying an AC bias voltage of 4 volts with a 2 MHz frequency.

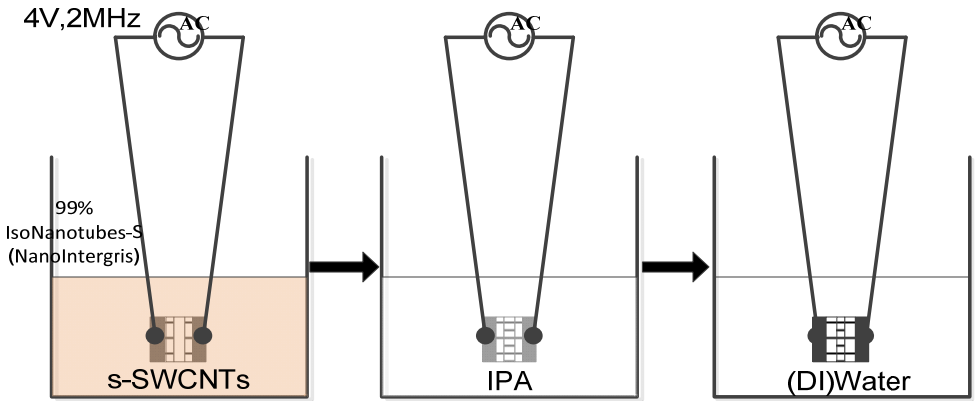

(a)

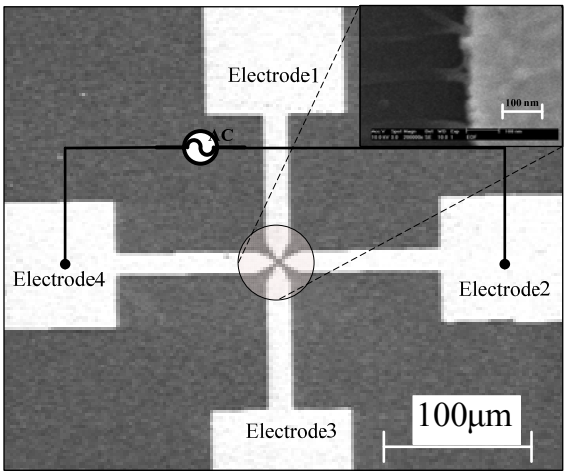

(b)

Fig.1 (a) DEP schematic where the AC source is kept in all the process. (b) Scanning electron microscope (SEM) pictures of the fabricated device(the electrode's width is 17 μm with gap of 4 μm) and the inset shows SEM picture of aligned s-SWCNT bundles

The AC voltage source is connected to the common electrodes of the chip. The chip is then dipped into the s-SWCNTs solution for 1 min. While still applying the AC bias voltage the chip is transferred into an isopropyl alcohol (IPA) solution to remove the remaining surfactant. The ionic surfactant acts as an insulator between the electrodes, so by varying the time of the immerged chip

in the IPA solution from 2 min to 15 min, the electrical resistance measured between the horizontal electrodes is lowered by one fifth. Then the chip is removed to (DI) water to remove the IPA residues and finally dried with nitrogen to remove the remaining liquid particles. A density higher than 40 s-SWCNTs/μm is estimated from the scanning electron microscope (SEM) picture presented in the inset of Fig. 1 (b) exceeding the reported ones in [4,6]. In addition, this technique provides cleaner devices compared to the common DEP techniques which consist of depositing a droplet of suspended CNTs in a an aqueous solution and wait the complete evaporation of the liquid as less residual useless CNTs are observed on the chip [4,6].

3. Results and Discussion

The I-V characteristics along the carbon nanotubes between electrodes 2 and 4 are measured using a Keithley 236 source measure unit. Fig. 2 (a) shows the I-V curve of one of the devices with the inset gives the error bar of the multiple conducted measurements for the same device. It represents a resistance of around 0.4 KΩ with tolerance of 2.5% and a sheet resistance is lower than 10 KΩ/□. Raman spectrum of the devices shown in Fig. 2 (b) highlights the D-, G-, G'-modes that are in a very good agreement with the manufacturer provided data [5]. D-mode represents the disorder bonds; its magnitude is related to the defects in the sample. G-mode represents tangential shear mode of carbon atoms, in SWCNTs it is double peak G+ and G-. G+ location and its value do not change with the type of the SWCNT. G- is strong and separates from G+ by greater than 100 cm^{-1} for metallic ones. So It is apparent that the device is totally semiconducting SWCNTs, the very small D- peak reflects low defects in the sample. G- is 1570cm^{-1} and G+ is 1590cm^{-1} even after processing the DEP.

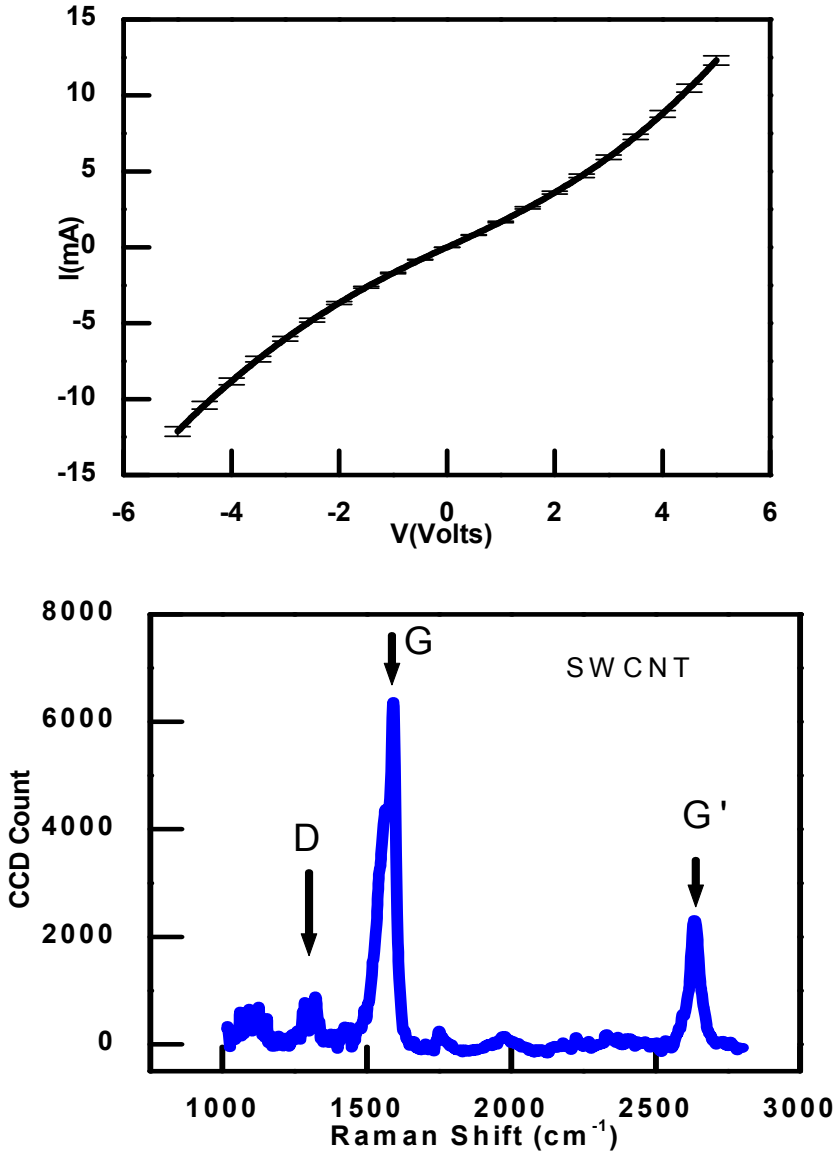

Fig. 2: (a) I-V characteristics of the device presented in Fig.1(b) after s-SWCNTs deposition, (b) Raman spectrum of aligned bundle of semiconducting SWCNTs prototype.

4. Conclusion

A new method for depositing high density s-SWNTs devices is introduced to improve very large scale integration of carbon=based electronic devices. High number of yield with high aligned high density of higher than 40 s-SWCNTs/1μm and sheet resistance less than 10 KΩ/□ is achieved. I-V measurements are realized to show the low electric resistance achieved with 2.5% tolerance.

Raman Spectroscopy is carried out and it shows typical spectrum for highly pure and uniforms-SWCNTs sample.

References

[1] A. Jorio, G. Dresselhaus, and M.S. Dresselhaus, *Carbon Nanotubes: Advanced Topics in the Synthesis, Structure , Properties and Applications*, Eds., Springer: Berlin, 2008.

[2] J. Li, Q. Zhang, D. Yang and J. Tian,"Fabrication of carbon nanotube field effect transistors by AC dielectrophoresis method," *Carbon*, vol. 42, no. 11, pp. 2263-2267, 2004.

[3] J. Li, Q. Zhang, N. Peng and Q. Zhu, "Manipulation of carbon nanotubes using AC dielectrophoresis," *Appl. Phys. Lett*., vol. 86, pp. 153116, 2005.

[4] B.K. Sarker, S. Shekhar and S.I. Khondaker," Semiconducting enriched carbon nanotube align arrays of tunable density and their electrical transport properties," *ACS Nano*, 2*011.*

[5] Available: http://www.nanointegris.com/en/semiconducting

[6] Emmanuel D**e**crossas, " High Frequency characterization of carbon nanotube networks for device applications", Ph.D. Dissertation, Department of Electrical Engineering, University of Arkansas, Fayetteville, May 2012.

UNIVERSITY OF ARKANSAS
College of Engineering
Department of Electrical Engineering

April 10th, 2015

To whom it may concern,

I certify that Ms. Asmaa Elkadi is the first author of the paper titled “Fabrication Technique of Highly Dense Aligned Semiconducting Single-Walled Carbon Nanotubes Devices “presented in IEEE Photonics Conference, Sept. 2012. Ms. Elkadi completed majority (more than 51%) of this research and writing this paper.

Prof. Samir M. El-Ghazaly
Distinguished Professor
Electrical Engineering
Office: 3169 Bell Engineering Center
Phone: 479-575-6048
E-mail: elghazal@uark.edu

Chapter V. B. Arrays of Single-Walled Carbon Nanotubes in RF Devices: Analysis and Measurements

Abstract

This paper presents a detailed model of devices utilizing many nanotubes and the coupling between them based on the electromagnetic model of a device using one nanotube. Empirical equations are proposed to link the device conductance with the number of nanotubes per device. Then, a circuit model is developed to predict the effect of the number of nanotubes per device on the overall conductance, capacitance, and the frequency response of the device. A prototype structure is fabricated and its performance is tested and compared with the proposed model and it shows promising agreements. The model is flexible and can be integrated with quantum transport models.

1. Introduction

Nanomaterials like carbon nanotubes, graphene nano-ribbons, and nano-wires have attracted many researchers because of their unique and promising properties [1],[2]. For example, carbon nanotubes offer the following interesting properties: high mechanical strength, high-temperature

operation, electromigration robustness, and electrically- tunable properties. In addition to the intrinsic material properties of carbon-carbon bonds in the nanotubes, the fact that they could be fabricated in 1-D nano-scale dimensions with very low defects gives them advantage over other materials [3]. Their electrical, optical, and mechanical properties are promising for analog, digital, biomedical, and optical applications [4]-[7]. From theoretical point of view, their electron transport properties are expected to be mostly ballistic, which is very promising for high-speed device applications. Nevertheless, it is still a challenge to synthesize and optimize carbon-nanotube-based devices [8]-[12]. Discrepancies between theoretical calculations, simulation data and experimental results of fabricated devices are among the main obstacles that delay applications and full exploitations of single-walled carbon nanotubes (SWCNT) in electronic devices and large-scale integrated circuits. Estimating the values of parasitic circuit elements, such as contact resistances and fringe capacitances, between nanotubes and metallic electrodes are still among the major challenges. The complete understanding of the physical processes affecting their values is necessary. The parameters limiting the formation of ohmic contacts on the nano-scale include matching of work functions, chemical reactivity, and limited conducting channels. Metals such as palladium (Pd), and rhodium (Rh) should be used to fabricate the contacts because their work function approximately match that of SWCNTs [13]. Although Pd provides the highest on-current in carbon-based devices due to its matching work function, contact resistances have been reported to be on the order of a few KΩ [14-16]. These values are higher than the ohmic contacts formed for conventional semiconductor devices. A perfect ohmic contact could not be formed at the nano-scale level due to the chemical reactivity between the SWCNT and the metal. An overlap area of a lower conductivity forms between the SWCNT and the metal, which forms an extra barrier [17].

This paper presents a physical insight into the processes affecting the contact resistance and the fringe capacitance of an individual SWCNT-based device. In Section II, a method to calculate their values is presented.

Understanding arrays of nanotubes is one of the key contributions of this paper. Thanks to their ability to retain their interesting quantum properties, nanotube arrays may provide a large current carrying capacity and low impedances [3].

The resultant parasitic-element models of the individual nanotube are embedded into a model for multiple SWCNT-based devices using a quantitative physics-based RC model to estimate the frequency dependence of such a device. Section III shows a fabricated prototype structure with a verification of the model followed by discussion and future insight.

2. Model

Electronic devices basically consist of a transport medium and contacts. Theoretically speaking, the use of carbon nanotubes as the transport medium is expected to provide ballistic transport. However, there are significant discrepancies between theoretical and experimental results. One of the main factors contributing to the discrepancy is the incomplete understanding of what happens around the contacts. From devices point of view, the contact properties are among the figures of merit that characterize the device's performance. In order to address this problem we are taking a close look at the contact areas and preforming a parametric study to determine the significant parameters that affect the contacts and hence take a step toward enhancing the overall performance.

A. Individual SWCNT

An individual SWCNT connecting two metallic pads, as shown in Fig. 1(a), is modeled as a hollow cylinder that has a diameter-dependent effective wall thickness [18]. SWCNTs are either metallic or semiconducting, which is the parameter that determines the material conductivity of the tube.

The metallic pads are formed of a lossless conductor. Due to the chemical reactivity between the SWCNT and the metallic pads, an extra area is introduced as shown in Fig. 1(b). The parameters of this area are variables to correlate the physical properties to the experimental measurements. The parameters l_2, the overlap length, varies from few nanometers to sub-micrometers; t, the overlap thickness, varies as a fraction of the effective wall thickness of the SWCNT; and σ_2, the conductivity of the overlap area, varies from insulating material to high conductivity material in the same order of magnitude as the main conductivity of the SWCNT body. The electromagnetic model takes into account the resistance of the bulk section of the nanotube, the solid blue area in Fig. 1(b), and the chemically-modified high-resistance region of the overlap area to obtain the equivalent contact resistance.

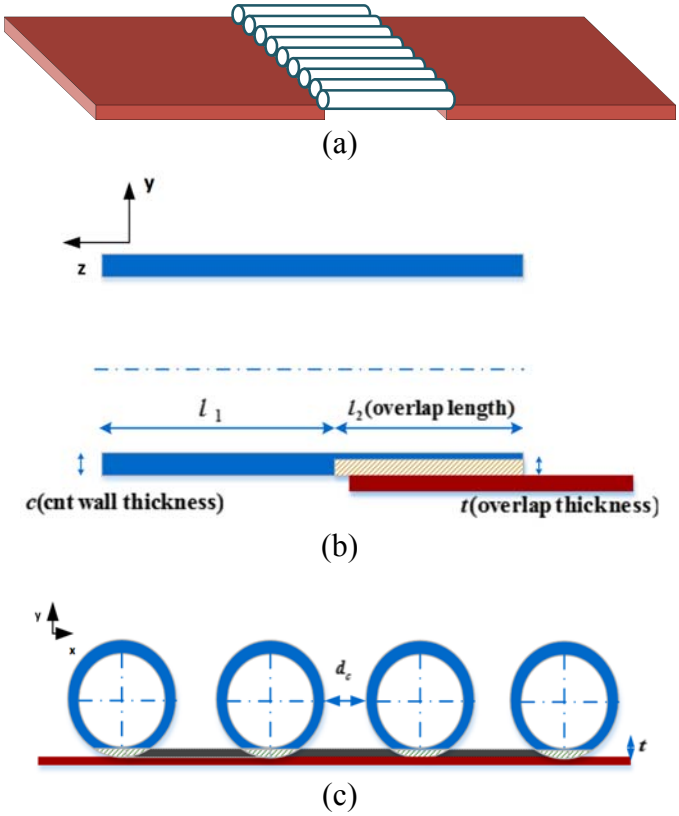

Fig.1 3-D schematic of N SWCNT touching two metallic contacts, (b) cross-section of SWCNT touching the metal z-y plane, (c) cross-section SWCNT touching the metal z-y plane where it shows the separation distance d_c and the dotted black is the coupling layer.

The Poisson's equation of the structure is solved using Multiphysics simulator [19]. A parametric study has been performed in [20]; it shows that the most influential parameter on the contact resistance is the overlap length between the SWCNT and the metallic plane. When the overlap length is very small, the device suffers very high contact resistance regardless of how efficient the metallic electrodes are fabricated or how close their work function is to that of the carbon nanotubes. The overlap length is then increased to show a significant improvement to the contact resistance that decreases drastically to reach its minimum after an effective length. The boundary conditions are applied to one SWCNT by applying a virtual potential at one end of the tube, and the edge touching the metallic plane is connected to ground. The electric field lines along the main body of the nanotube are mostly along the z-axis. The field lines are then get crowded around the metallic plane. For very short overlap length, small percentage of the field lines reach the ground. However, for long overlap length, most of the field lines reach the ground. Hence, a lower resistance is achieved.

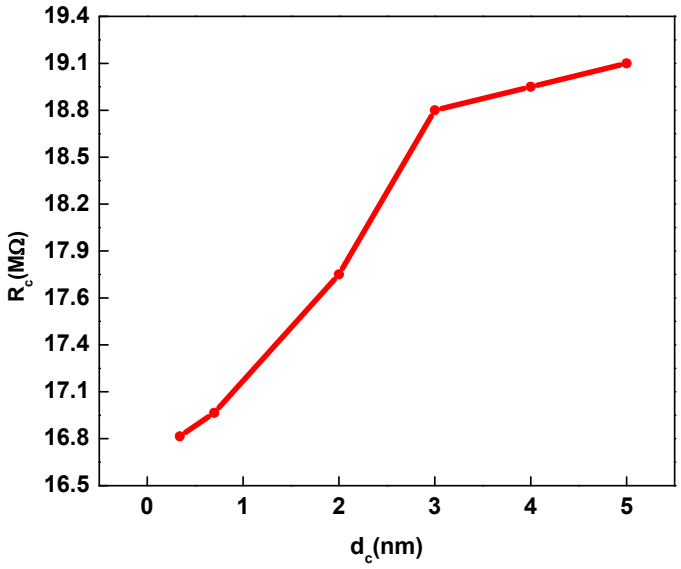

Fig.2 The contact resistance of one side of the device that has 5 SWCNTs for different separation distance d_c.

The model has shown very close agreement with individual SWCNT device measurements in [21]. The parameters extracted for an individual SWCNT are then used to establish a model for multiple-nanotube devices.

B. Arrays of SWCNTs

1. Resistive Elements

For many SWCNTs (Fig. 1 (c)), they are placed at a distance $\boldsymbol{d_c}$ apart from each other. Fig. 2 indicates that the contact resistance increases with the increase of distance $\boldsymbol{d_c}$. This demonstrates that the coupling between the nanotubes decays with the increase of the separation between them to reach a case where the SWCNTs are considered isolated and could be dealt as parallel conductors [21]. In order to implement the coupling between the nanotubes, intersection layers are introduced as shown in Fig. 1 (c) as the black dotted areas with physical parameters that represent the coupling. The layers' thickness is in the same order of the overlap areas' thickness,

and their lengths are the same as the SWCNTs' length. The conductivity of these layers may vary from air's conductivity, which represents no coupling at all between the SWCNT (used when they are far apart) to the quantum conductivity of a graphene layer ($2e^2/h$) 7.775×10^{-5}(S/M) (used when they are so close). The conductance of nanotube based devices has an exponential increase behavior rather than linear. This could be due to the fact that the coupling between the nanotubes influences the overall band structure and it widens the potential function [8]. Hence, it increases the number of conducting channels dramatically. The barrier between one SWCNT and metallic electrode could be described as a triangular barrier. The transmission probability across this barrier is [22]

$$T(E) = \exp\left(\frac{-4\sqrt{2m^*}}{3e\mathcal{E}\hbar}\left(e\phi - \left(E - E_f\right)\right)^{\frac{3}{2}}\right) \quad (1)$$

where m^* is the electron effective mass, e is the electron charge, E is the electron energy, E_f is Fermi level energy, ϕ is the difference between the SWCNT work function and the metal work function, and $\mathcal{E}$ is the magnitude of the electric field (the potential divided by the overlap length l_2). The current in one nanotube is a function of the transmission probability [22]:

$$I = -\frac{2e}{h}\sum_{m=1}^{N_c}\int f\left(E, E_f\right)T(E)dE \quad (2)$$

where N_c is the number of conducting channels, in the case of semiconducting nanotubes of small radii it will have a single subband and hence $N_c=1$, and f is Fermi-Dirac distribution.

In order to obtain the overall current for a different number of nanotubes, the transmission probability of the new system should replace the individual SWCNT one:

$$T_N(E) = T_1(E) * T_2(E) * \ldots * T_N(E) \quad (3)$$

where N is the number of nanotubes and * is the convolution operator. Fig. 3 shows the numerical solution of (2) using the transmission probability described in (3). The transmission probability

function (1) is proportional to $\exp(x^{\frac{3}{2}})$, which is not a canonical known distribution function; therefore, there is no closed form solution for (3). Nevertheless, this distribution function is somewhere between an exponential distribution and a normal distribution. The convolution of many exponential distribution functions gives Gamma distribution function, and the convolution of many normal distribution functions gives normal distribution of N dependence mean and deviation. This gives the trend of an exponential dependence on the number of nanotubes from both distributions, which gives the trend that the dependence of our problem's distribution function sum will also follow an exponential dependence on the number of the nanotubes (at least asymptotically). Hence, the overall current and the conductance will be also exponentially dependent on N.

Basic curve fitting equation has been proposed in [21] to describe the relation between the device conductance and the number of SWCNTs. The conductance, G_0, equation:

$$\boldsymbol{G_0(N) = 10^{a_1 * N - b_1}(S)} \tag{4}$$

where N is the number of nanotubes per device, and a_1 and b_1 are curve fitting parameters obtained by the method of least squares; their values are 0.21, and 8.3 respectively. Equation (4) is plotted in Fig.3 shows a good trend with respect to the measurements for low density nanotubes (less than 20/μm). But as the density increases the curve deviates from the measurements. Hence, an additional equation for the conductance expression is proposed here based on the asymptotic exponential behavior of the overall transmission probability explained previously:

$$\boldsymbol{G_0(N) = e^{\left(-\frac{a_2}{N} + b_2\right)}} \tag{5}$$

where a_2, and b_2 are the fitting parameter calculated by the method of least squares; their values are 45 and -9.4 respectively. This equation also agrees with the form the field enhance factor took

for an array of nanotubes in [23] (the field was presented as function of the separation of nanotubes in the array which is inversely proportional to the density of the tubes.)

Both equations (4) and (5) show a close trend to the measured data as shown in Fig. 3. They are used to extract a lot of information about the device and help to build the RF model for many SWCNTs as done for one SWCNT in [20]. The contact resistance of many nanotubes does not follow the direct parallel dependence on the individual nanotube contact resistance. The relation between the individual nanotube resistance, $R_c(1)$, and the resistance of each nanotube in a many-tube device, $R_c(N)$, is proposed to be:

$$\frac{R_c(N)}{R_c(1)} = \frac{G_0(1)}{NG_0(N)} \tag{6}$$

where for highly aligned array of nanotubes, the thickness of the individual- and many-tubes devices is the same. In addition, the nanotubes used are highly purified, and they have uniform length and diameter distributions of average 1 μm, and 1.4 nm respectively. The conductance calculated from (4), (5), and the measured data for different number of nanotubes per device [25] are plotted in Fig.3. As shown, the conductances follow the same trend for low density nanotubes. However, when depositing higher density of nanotubes per device the model deviates from the measurements. Possible explanation for this deviation could be explained that the nanotubes tend to form many layers instead of single layer. Hence, a stochastic model is needed to explore the different possibilities. In this paper, thin film of almost one layer on nanotubes is considered.

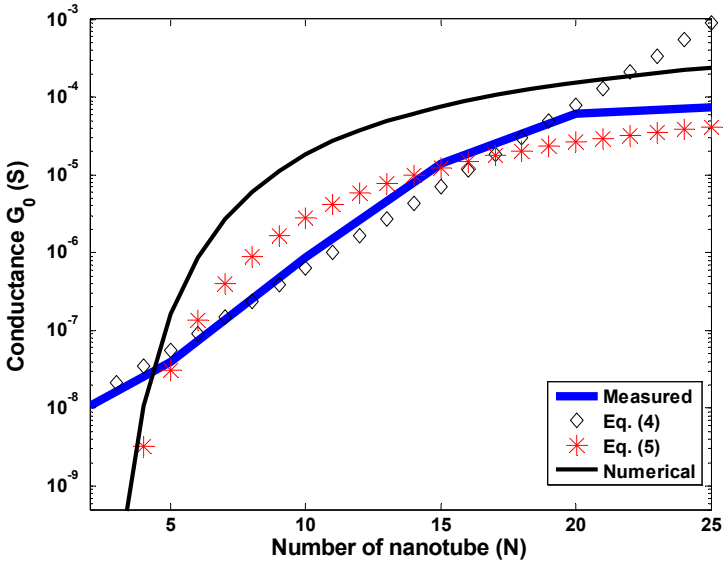

Fig. 3 (Color online) the conductance of the different devices of different number of SWCNTs, the solid blue line is for the measured data obtained from [25] for zero gate voltage, the diamond symbol ◊ is for the conductance calculated using (4), and the star symbol * is for the conductance calculated using (5), solid black line represents the numerical solution for (2) .

2. Capacitive Elements

Analyzing the device frequency response gives more information about the other parasitic elements that might limit the device performance. In order to implement the schematic circuit of SWCNTs-based device, the nanotube mainly consists of three parts: the main body of the SWCNT, the segment where the SWCNT lays on the pad connected to ground, and the coupling between SWCNT and its adjacent tubes. Fig.4 shows the schematic of the circuit that describes the nanotubes-based device. The non-contacting part deals with quantum quantities R_q, and C_q of values 12.9KΩ, and 82aF respectively [24].

The contacting part quantities R_c, and C_c are the contact resistance and capacitance, respectively. The resistance is directly dependent on the overlap-section conductivity and the nanotube number per device N. The capacitance is dependent on the material permittivity.

The contact resistance is calculated as described previously. The capacitances are calculated using two methods; electrostatically across the structure by the Multiphysics simulator, and using the capacitance equation derived in [3]:

$$C_c = \frac{2\pi\varepsilon_r\varepsilon_0}{\left(ln\left(\frac{2a+t}{a}\right) + 2\sum_{m=1}^{N-1} ln\left(\sqrt{1+\left(\frac{2a+t}{m(2a+d_c)}\right)^2}\right)\right)} \tag{7}$$

where a is the nanotube radius, t is the thickness of the overlap area, d_c is the distance between the nanotubes, and ε_r is the relative permittivity extracted in [26].

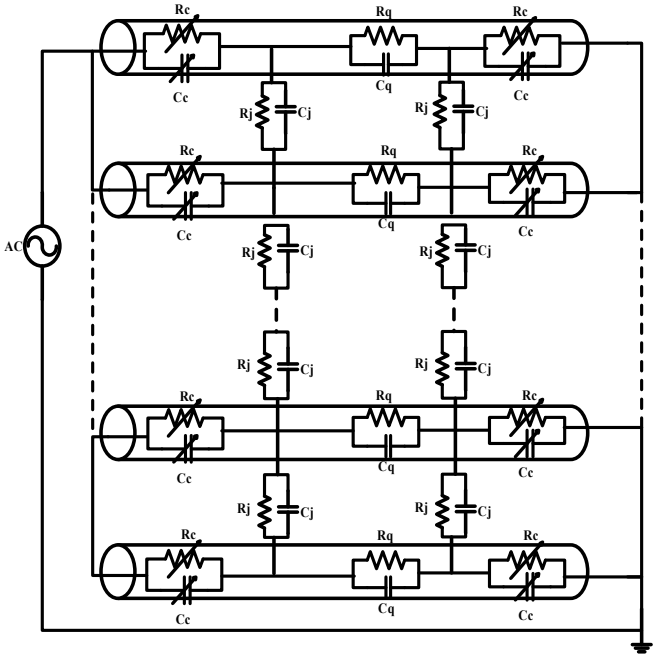

Fig. 4 Circuit schematic of aligned SWCNTs device, R_c is the contact resistance variable of the number of the nanotubes, C_c is the contact capacitance. R_j,and C_j are the coupling resistance and capacitance. R_q, and C_q are the nanotube quantum resistance and capacitance.

Fig. 5 elucidates the capacitance per nanotube versus the number of carbon nanotubes per device. The denser the nanotubes array, the higher the screening effects between them that leads to a decrease in the value of the nanotube capacitance [3], as shown in Fig. 5.

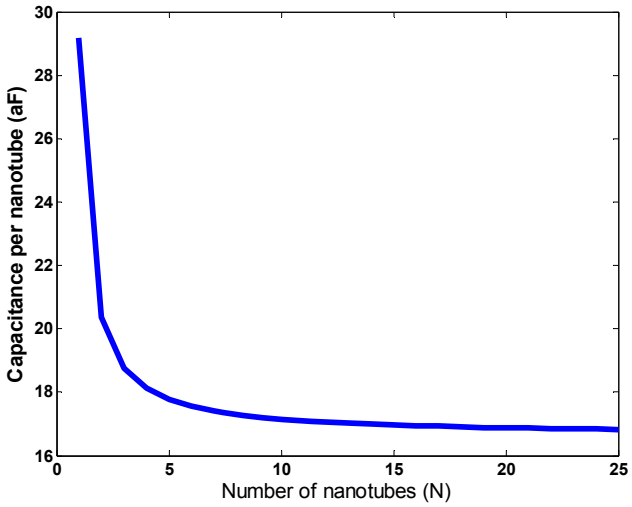

Fig. 5 Contact Capacitance per tube for different number of nanotubes per device

The coupling between the tubes is implemented by R_j and C_j, so they vary with the condition of the nanotubes alignment and the inter-tube distance d_c. In other words, R_j and C_j would vary from the quantum values to the insulating values where the nanotubes are barely coupled to each other. As it will be shown in fabrication (Section III A) when the nanotubes are highly aligned, they distribute 4-5 tubes with $\boldsymbol{d_c}$ less than 1nm every 100±10nm. The microscopic mechanism is not yet fully understood.

The impedance ($Z=R+jX$) of the device's schematic circuit is calculated for one and ten SWCNTs cases. Fig. 6 presents the resistance and the reactance of the impedances of both cases. The maximum of the reactance curve defines the fall off frequency. Below the fall off frequency the charges tend to travel long distance in the same order of the nanotube lengths, while beyond this frequency the charges tend to travel short distances and be more localized [27]. The higher this frequency, the better the performance and the higher the speed of the device. The fall off

frequency shows strong dependence of the number of nanotubes per device. The fall off frequency of ten SWCNTs device is higher than that of the one SWCNT device. This could refer to the significant improvement of the contact resistance of the device. The capacitances are calculated using (7) and the Multiphysics simulator as well. The overall capacitive effect shows a linear increase as function of the number of nanotubes per device. While the overall resistive effect shows an exponential decrease as function of the number of nanotubes per device.

In order to reach the best performance of the device, the parasitic elements of the contacts should be optimized. This could be approached for one SWCNT by ensuring the overlap length between the nanotube and the metallic pad is higher than the effective length studied earlier. The parasitic elements could also be enhanced by some post processing (i.e. thermal annealing, RF induction heating, Electron beam irradiation…etc.) [28], so the fall off frequency could reach to the theoretical values calculated by Bruke [29].

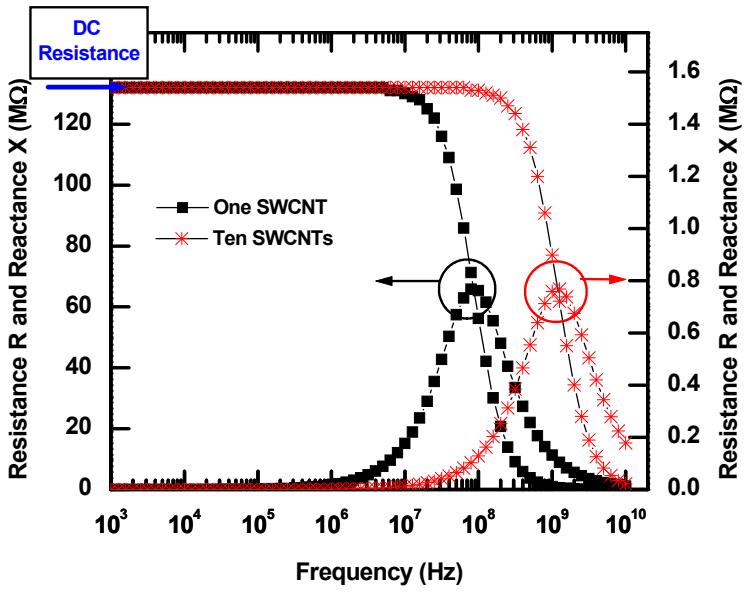

Fig. 6 (Color online) Frequency dependence of the resistance R and reactance X of one SWCNT and ten SWCNTs devices.

3. Measurements and Discussions

A. Fabrication

In order to test the model developed earlier, a prototype structure is designed and fabricated. Two stages of lithography are used to fabricate a structure of metallic electrodes. Photolithography is used to fabricate micrometer scale, then E-beam lithography is used to overlap nano-electrodes with the micrometer ones. The nanotubes used here are semiconducting single-walled carbon nanotubes furnished by Nanointegris suspended in aqueous solution. They are deposited and aligned using an AC dielectrophoresis (DEP) technique [30],[31], across the horizontal electrodes presented in Fig. 7. According to the manufacturer, the utilized solution consists of 20 μg/ml of 99% pure s-SWCNT with diameter from 1.2 nm to 1.7 nm, and length from 0.3 μm to 5 μm. They are dispersed in aqueous solution consisting of 1% w/v ionic surfactant diluted in deionized (DI) water [32]. Fig. 7 shows the scanning electron microscopy (SEM) picture of the device with the inset of higher resolution to ensure the connections between the nanotubes and the metallic electrodes. This high resolution SEM picture of the device after depositing the SWCNTs shows that nanotubes tend to align in groups of 4-5 s-SWCNTs of less than 1nm inter-tube distance. Each group is separated by 100±10nm. There is no clear physical explanation of this behavior yet.

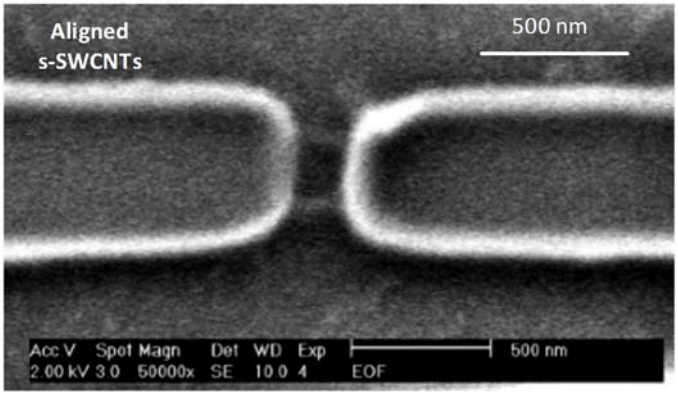

(a)

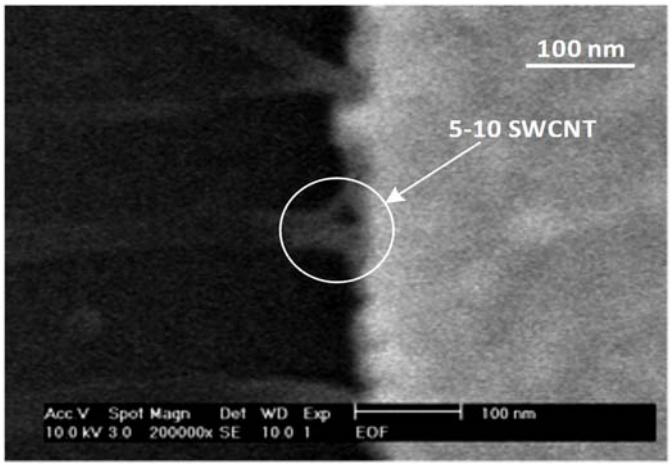

(b)

Fig. 7 SEM picture of (a) two palladium nano-electrodes with aligned s-SWCNTs bundles are deposited using dielectrophoresis (b) zoomed image to estimate the number of nanotubes per device.

B. Measurements

The I-V characteristics are measured for the device, and it is plotted in Fig.8. The model is developed based on the measured resistance and using (4) and (5); one could estimate the number of the nanotubes. For this structure, the estimated number of SWCNTs based on the measured resistance is seven. The I-V characteristics for the model developed for six and seven SWCNTs based device is plotted in addition to the measured data on Fig. 8. The model shows an acceptable estimation of the number of tubes. In addition, referring to the high resolution SEM picture of the device, one could estimate a number of 5-10 nanotubes which is very close to the estimate obtained from the model.

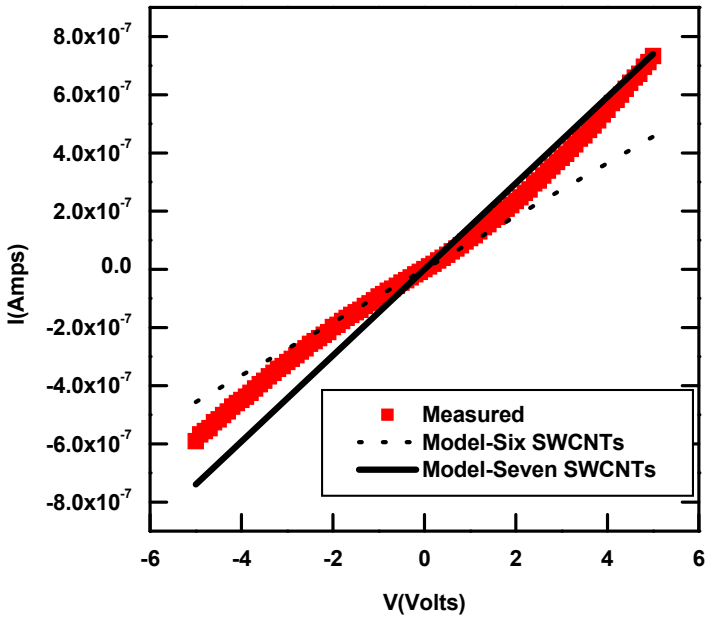

Fig. 8 (Color online) I-V characteristics for the fabricated SWCNTs device and the model of six and seven SWCNTs- devices.

Impedance spectroscopy provides a method to measure the complex impedance of a device and correlate it with some proposed equivalent circuit [33, 34]. Garrett et. al. have measured the impedance of a random network of SWCNTs using impedance spectroscopy [27]. Their capacitance is high with respect to the values calculated in this paper. This could be due to higher density of nanotubes per device. The closer the density is to the percolation limit, the higher the overall permittivity [35]. The drastic increase in the permittivity introduces macroscopic characteristic of the material that dominates the capacitance. Therefore, the fall off frequency of the random network is lower than that of the model due to some more parasitic elements of extra joints between the bundles of the SWCNTs degrading the overall performance. This supports the conclusion that the better the SWCNTs are aligned per device, the better the performance of the device and the lower the contact parasitic elements. Table I summarizes the values of the resistances and capacitances for a various number of nanotubes per device, as well as, the extracted

resistance and capacitance tube. These values are implemented in the circuit model to calculate the frequency response. The fall off frequency of the device is calculated and plotted in Fig. 9.

Table I
PARASITIC ELEMENTS' VALUES FOR VARIOUS NUMBER OF SWCNTS

Number of nanotubes (*N*)	**Resistance**		**Capacitance**	
	Individual (6)	**Overall** (measured)	**Individual** (7)	**Overall**
1	132MΩ	132MΩ	29.2aF	29.2aF
7	1MΩ	23.6MΩ	17.4aF	121.83aF
10	500 KΩ	7.7MΩ	17.15.aF	171.52aF

The overall resistances decrease exponentially, while the capacitances show a linear increase. Hence, the fall off frequency is increasing as shown in Fig.9 (almost linearly). But, as mentioned before, as the density of nanotubes per device increases, the more parasitic elements are introduced. In sum, when increasing the number of nanotubes per device, there is a trade-off between the overall resistances and the overall capacitances that limits the fall off frequency.

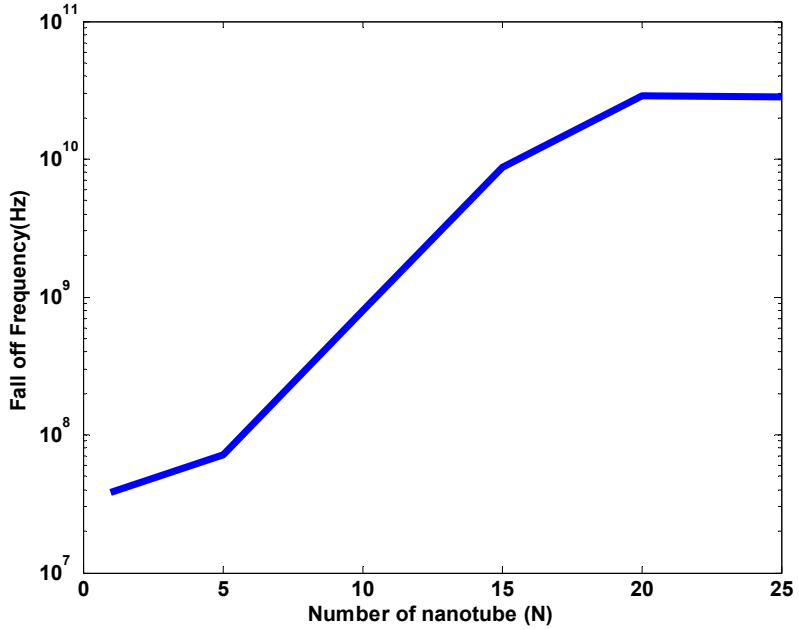

Fig. 9 Fall off frequency as a function of the number of carbon nanotubes per device.

4. Conclusion

A comprehensive model has been developed for SWCNTs-based devices incorporating realistic parameters into the model to decrease the discrepancies between the theory and measurements. The model is developed for individual SWCNT, then it is used to build the model for multiple SWCNTs aligned in a device. The model has included the electrostatic and frequency dependence in a schematic circuit to represent the structure. A prototype structure has been fabricated, tested, and compared to the proposed model, and shows a good agreement. The frequency response has been calculated for various number of nanotubes per device showing linear increase for low density and it saturates with the increase of the number of nanotubes per device. The model helps understand the limitations affecting SWCNTs-based devices followed by some suggested techniques to enhance the performance.

References

[1] A. Jorio, G. Dresselhaus, and M. Dresselhaus, *Carbon nanotubes: advanced topics in the synthesis, structure, properties and applications,* Vol. 111 (Springer, 2008).

[2] T. Jeon, K. Kim, C. Kang, S. Oh, J. Son, K. H. An, D. J. Bae and Y. H. Lee. Terahertz conductivity of anisotropic single walled carbon nanotube films. *Appl. Phys. Lett. 80(18),* pp. 3403-3405. Mar. 2002.

[3] G. W. Hanson, S. McKernan and D. Wang. Analysis of large planar arrays of single-wall carbon nanotubes. *Microwave Theory and Techniques, IEEE Transactions on 59(10),* pp. 2758-2768. Oct. 2011.

[4] A. Elkadi, E. Decrossas, S. Yu, H.A. Naseem and S.M. El-Ghazaly, "Controlling the energy band gap of aligned semiconducting single-walled carbon nanotubes for THz modulator," in 7th European Microwave Integrated Circuits Conference (EuMIC), pp. 270-273, Oct. 2012.

[5] E. Decrossas, A. Elkadi and S. El-Ghazaly, "Carbon nanotube based prototype as THz time domain sources/detectors," in 37th International Conference on Infrared, Millimeter, and Terahertz Waves (IRMMW-THz), pp. 1-2, Sept. 2012.

[6] S. Hamieh, "Improving the RF Performance of Carbon Nanotube Field Effect Transistor," Journal of Nanomaterials, vol. 2012, 724121, 7 pages, Feb. 2012.

[7] M. A. Wahab, S. H. Jin, A. E. Islam, J. Kim, J. Kim, W. Yeo, D. J. Lee, H. U. Chung, J. A. Rogers and M. A. Alam. “Electrostatic dimension of aligned-array carbon nanotube field-effect transistors”. *ACS Nano 7(2),* pp. 1299-1308. Jan. 2013.

[8] A. Elkadi, E. Decrossas, S. Yu, H.A. Naseem and S.M. El-Ghazaly, "Aligned semiconducting single-walled carbon nanotubes: Semi-analytical solution," J. Appl. Phys., vol. 114, pp. 114306, Sept. 2013.

[9] A. Elkadi, E. Decrossas and S. El-Ghazaly, "Energy band gap study of semiconducting single walled carbon nanotube bundle," in IEEE International Symposium on Electromagnetic Compatibility (EMC), pp. 534-538, Aug. 2013.

[10] H. E. Unalan, G. Fanchini, A. Kanwal, A. Du Pasquier and M. Chhowalla. “Design criteria for transparent single-wall carbon nanotube thin-film transistors.” *Nano Letters 6(4),* pp. 677-682. Feb. 2006.

[11] O. Balci and C. Kocabas. “High frequency performance of individual and arrays of single-walled carbon nanotubes.” *Nanotechnology 23(24),* pp. 245202. May 2012.

[12] C. Kocabas, N. Pimparkar, O. Yesilyurt, S. Kang, M. A. Alam and J. Rogers. “Experimental and theoretical studies of transport through large scale, partially aligned arrays of single-walled carbon nanotubes in thin film type transistors.” *Nano Letters 7(5),*pp. 1195-1202. Mar. 2007.

[13] C. Lan, P. Srisungsitthisunti, P. B. Amama, T. S. Fisher, X. Xu and R. G. Reifenberger. “Measurement of metal/carbon nanotube contact resistance by adjusting contact length using laser ablation.” *Nanotechnology 19(12),* pp. 125703. Feb. 2008.

[14] Z. Chen, J. Appenzeller, J. Knoch, Y. Lin and P. Avouris, "The role of metal-nanotube contact in the performance of carbon nanotube field-effect transistors," Nano Letters, vol. 5, pp. 1497-1502, June 2005.

[15] F. Xia, V. Perebeinos, Y. Lin, Y. Wu and P. Avouris. “The origins and limits of metal-graphene junction resistance.” *Nature Nanotechnology 6(3),* pp. 179-184. Jan. 2011.

[16] E. J. Lee, K. Balasubramanian, R. T. Weitz, M. Burghard and K. Kern. “Contact and edge effects in graphene devices.” *Nature Nanotechnology 3(8),* pp. 486-490. June 2008.

[17] Z. Yao, H.W.C. Postma, L. Balents and C. Dekker, "Carbon nanotube intramolecular junctions," Nature, vol. 402, pp. 273-276, Sept. 1999.

[18] T. Vodenitcharova and L. Zhang. Effective wall thickness of a single-walled carbon nanotube. Physical Review B 68(16), pp. 165401. Oct. 2003.

[19] COMSOL Multiphysics® Inc., Burlington, MA, USA (http://www.comsol.com/)

[20] A. Elkadi, S. M. El-Ghazaly, “On the Contact Resistance of Single-Walled Carbon Nanotubes in RF devices,” in International Microwave Symposium (IMS), Tampa, FL, pp. 1-4, June. 2014.

[21] A. Elkadi, S. M. El-Ghazaly, “Modeling of Carbon Nanotube-Metal Contact Losses in Electronic Devices,” presented at IEEE International Symposium on Electromagnetic compatibility, Raleigh, NC, Aug. 2014, pp. 198-202.

[22] G. W. Hanson. *Fundamentals of Nanoelectronics* (Pearson Prentice Hall 2008).

[23] S. Jo, Y. Tu, Z. Huang, D. Carnahan, D. Wang and Z. Ren. “Effect of length and spacing of vertically aligned carbon nanotubes on field emission properties.” *Appl. Phys. Lett. 82(20),* pp. 3520-3522. May 2003.

[24] J. Dai, J. Li, H. Zeng and X. Cui, "Measurements on quantum capacitance of individual single walled carbon nanotubes," *Appl.Phys.Lett., vol. 94*, pp. 093114-093114-3, Mar. 2009.

[25] B.K. Sarker, S. Shekhar and S.I. Khondaker,” Semiconducting enriched carbon nanotube align arrays of tunable density and their electrical transport properties,” *ACS Nano 5 (8),* pp 6297–6305, July 2011.

[26] E. Decrossas, M.A. EL Sabbagh, V. Fouad Hanna and S.M. El-Ghazaly, “Rigorous characterization of carbon nanotube complex permittivity over a broadband of RF frequencies,” *IEEE Trans. Electromag. Compat.*, vol. 54, no. 1, pp. 81-87, Feb. 2012.

[27] M. P. Garrett, I. N. Ivanov, R. A. Gerhardt, A. A. Puretzky and D. B. Geohegan. “Separation of junction and bundle resistance in single wall carbon nanotube percolation networks by impedance spectroscopy.” *Appl. Phys. Lett. 97(16),* pp. 163105. Oct. 2010.

[28] L. An, X. Yang and C. Chang. “On contact resistance of carbon nanotubes.” *International Journal of Theoretical and Applied Nanotechnology 1(2),* pp. 30. Dec. 2013.

[29] P. J. Burke. “An RF circuit model for carbon nanotubes.” Presented at 2nd IEEE Conference on Nanotechnology. pp. 393-396. Aug. 2002.

[30] J. Li, Q. Zhang, D. Yang and J. Tian,”Fabrication of carbon nanotube field effect transistors by AC dielectrophoresis method,” *Carbon*, vol. 42, no. 11, pp. 2263-2267, June 2004.

[31] J. Li, Q. Zhang, N. Peng and Q. Zhu, “Manipulation of carbon nanotubes using AC dielectrophoresis,” *Appl. Phys. Lett*., vol. 86, pp. 153116, Apr. 2005.

[32] NanoIntergris IsoNanotubes-S ™ semiconducting SWCNTs datasheet (Available: http://www.nanointegris.com/en/semiconducting).

[33] I. Dumitrescu, P. R. Unwin and J. V. Macpherson. “Electrochemical impedance spectroscopy at single-walled carbon nanotube network ultramicroelectrodes.” *Electrochemistry Communications 11(11),* pp. 2081-2084. Sept. 2009.

[34] E. Barsoukov and J. R. Macdonald. *Impedance Spectroscopy: Theory, Experiment, and Applications* (John Wiley & Sons 2005).

[35] E. Decrossas, M. A. El Sabbagh, H. A. Naseem and V. F. Hanna. “Effective permittivity extraction of dielectric nano-powder and nano-composite materials: Effects of packing densities and mixture compositions”. In Microwave Conference (EuMC), 2011 41st European. Pp. 956-959, Oct. 2011.

UNIVERSITY OF ARKANSAS
College of Engineering
Department of Electrical Engineering

April 10th, 2015

To whom it may concern,

I certify that Ms. Asmaa Elkadi is the first author of the paper titled "Arrays of Single-Walled Carbon Nanotubes in RF Devices: Analysis and Measurements "published in IEEE Transactions on Electromagnetic Computability, Mar. 2015. Ms. Elkadi completed majority (more than 51%) of this research and writing this paper.

Prof. Samir M. El-Ghazaly
Distinguished Professor
Electrical Engineering
Office: 3169 Bell Engineering Center
Phone: 479-575-6048
E-mail: elghazal@uark.edu

Chapter VI. Tuning the Energy Band Gap of Aligned Arrays of semiconducting single-walled carbon nanotubes for THz Applications[1]

1. Introduction

An individual semiconducting single-walled carbon nanotube (s-SWCNT) has a typical diameter of 0.5 to 2 nm, and its energy gap is inversely proportional to its diameter in the range of 1.4 to 0.35 eV [1]. An array of aligned s-SWCNTs demonstrates promising responses in various devices compared to individual ones. Arrays of aligned s-SWCNTs is a difficult problem to solve due to the lack of a well-defined potential function of individual s-SWCNT.

Alignment of carbon nanotubes plays a vital role in designing electronic devices and optimizing their operation. Ren *et al.* [2] have used aligned metallic SWCNT to develop THz polarizer. THz signals polarized parallel to the carbon nanotubes are absorbed, while signals polarized perpendicular to the alignment direction are transmitted [2]. Wang *et al.* have used partially aligned s-SWCNTs in a FET transistor, where the performance is a function of the number of nanotubes per device [3]. Aligned carbon nanotubes have been used in many devices. The measured results were not highly accurate with respect to electron transport physics in carbon nanotubes due to the lack of comprehensive theoretical model.

This paper is organized as follows: Section 2 discusses the effective potential function of an individual s-SWCNT, this is generalized for aligned arrays of s-SWCNTs. In Section 3, an analogy between Quantum Cascaded Lasers (QCL) and system of aligned s-SWCNTs is discussed and the energy band gap of the system is studied for various number of nanotubes with/out applied transverse electric field. The current-voltage characteristics of an individual nanotube and an array

[1] Parts of this chapter are reprinted with permission from Eu*M*A March 15, 2015 "Controlling the Energy Band Gap of Aligned Semiconducting Single-Walled Carbon Nanotubes for THz Modulator" IEEE European Microwave Integrated Circuits Conference, Oct. 2012.

of nanotubes is discussed in Section 4. The measurements are then compared to the theory in Section 5.

2. Analytical Potential Function

A developed the analytical expression for the potential function of single-walled carbon nanotubes shown in (1).

$$V_{eff}(r) = \frac{B \times c^2 r^2}{\left(r^2 - R_t^2\right)^2 + c^2 r^2} \qquad (1),$$

where R_t is the nanotube's radius, $c = \frac{R_t}{11.446}$ represents the effective SWCNT's wall thickness [4], and $B = 8.25\,\mathrm{eV}$ is the potential well depth. This expression facilitates understanding the properties of different configurations of carbon nanotubes. Any configuration can be considered as a superposition of several individual SWCNT. Hence, the overall potential can be derived as the sum of the individual potentials of each tube.

The effective potential function is inserted in Multiphysics simulator in order to solve Schrödinger equation for a system of many nanotubes. The probability wave functions and energy levels are obtained for various number of nanotubes. Fig.1 demonstrates the ground state probability wave function for different number of adjacent s-SWCNT. The coupling between the wave function is strong for the first neighbor s-SWCNT then it decays for the second neighbor and almost vanishes for the third neighbor s-SWCNT.

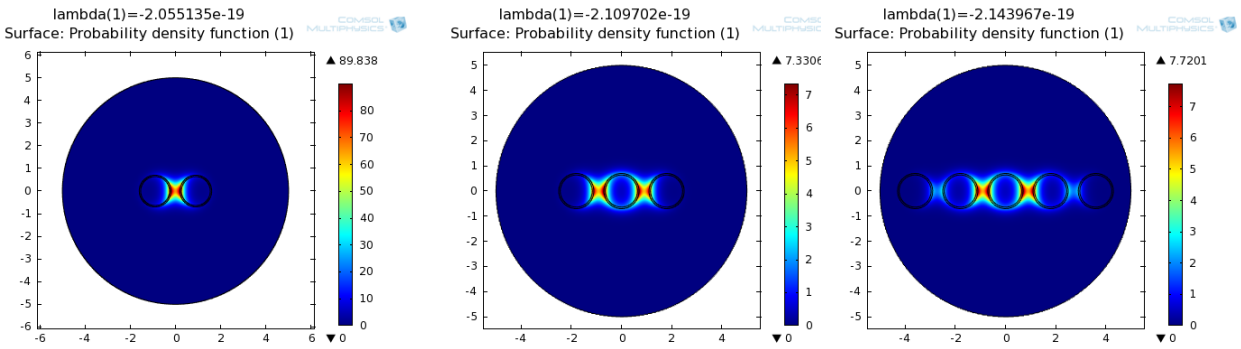

(a) (b) (c)

Fig. 1 Ground state probability wave function (a) two s-SWCNTs, (b) three s-SWCNTs, and (c) five s-SWCNTs.

Fig. 2 shows that the energy band gap decreases with increasing the number of s-SWCNTs due to the coupling between them but it asymptotically reaches to a constant value. This indicates that by placing the nanotubes into proximity arrays, the energy band gap could be altered; hence, it could be tuned as shown in Fig. 2. In the next section applying transverse electric field across these adjacent s-SWCNTs will be studied.

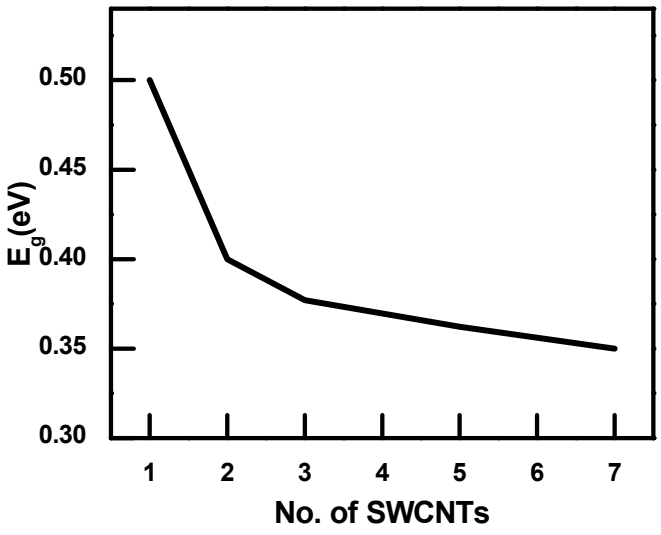

Fig. 2 Energy band gap versus the number of s-SWCNTs

3. Quantum Cascaded Laser Analogy

The quantum cascaded laser (QCL) consists of consecutive quantum wells that interact with each other; hence, this interaction alters the overall system wave functions and energies.

As an analogy, an individual SWCNT represents a cylindrical quantum well. By putting the nanotubes proximately in an array, it will adopt the same behavior as the QCL.

Hence, as it is done in solving QCL the potential function in Schrödinger's equation of many s-SWCNT will be an effective form that represents the overall effective potential function $V_{eff} = V_1 + V_2 + V_3 + \cdots + V_N$, where N is the number of nanotubes per device. As shown in Fig. 3, when applying electric field to quantum cascaded laser the ground state wave function is due to the coupling between the ground state probability wave function of the first and second quantum wells. Then the second level wave function is due to coupling between the ground state function of the second and third quantum well. This pattern varies with the variation of the quantum well width and the value of the applied electric field. If all the quantum wells have the same width, the pattern will repeat itself till the last quantum well.

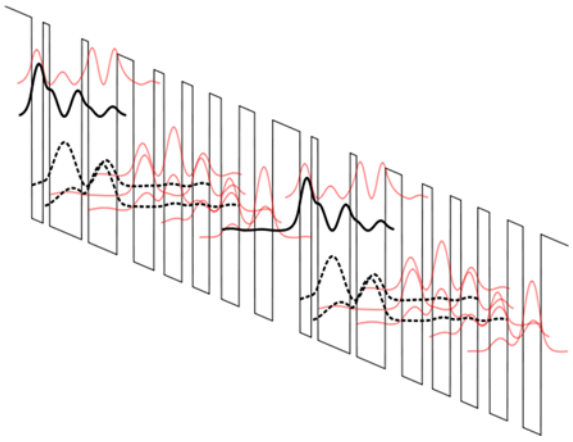

Fig. 3 Probability wave functions in quantum cascaded laser subject to applied electric field [5].

The resultant probability density functions for s-SWCNT system consisting of 5 nanotubes is shown in Fig. 4. It is apparent that it follows the same ideology as the QCL, the ground state energy wave function is mainly the coupling between the first two s-SWCNTs wave functions. The second energy level wave function is the coupling between the next two s-SWCNTs then it repeats itself until it reaches the last nanotube.

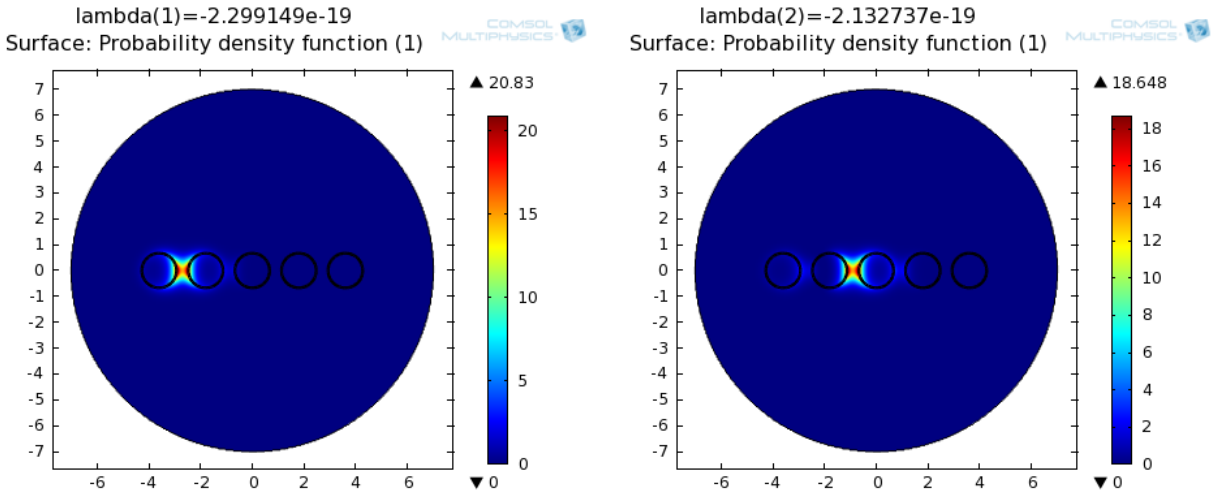

(a) (b)

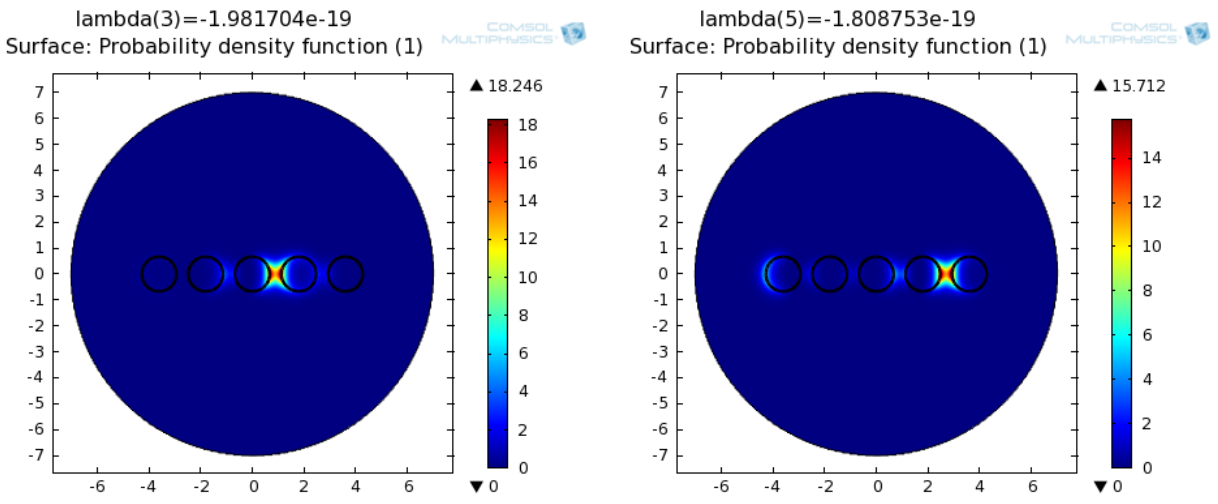

(c) (d)

Fig. 4 Probability wave functions (a) ground state energy level,(b) second energy level, (c) third energy level, (d) fourth energy level.

Correspondingly, the applied transverse electric field is varied to study its effect on various the applied transverse electric field affects the energy sub bands and hence it alters the energy band gap. Fig. 5 presents the change in the energy band gap for various number of nanotubes as a function of the applied transverse electric field. The same applied electric field value the bundle of s-SWCNTs show drastic reduction in the energy band gap. This result illustrates that for higher number of s-SWCNTs, the electric field needed to reduce the energy band gap is less than what is required for a single s-SWCNT.

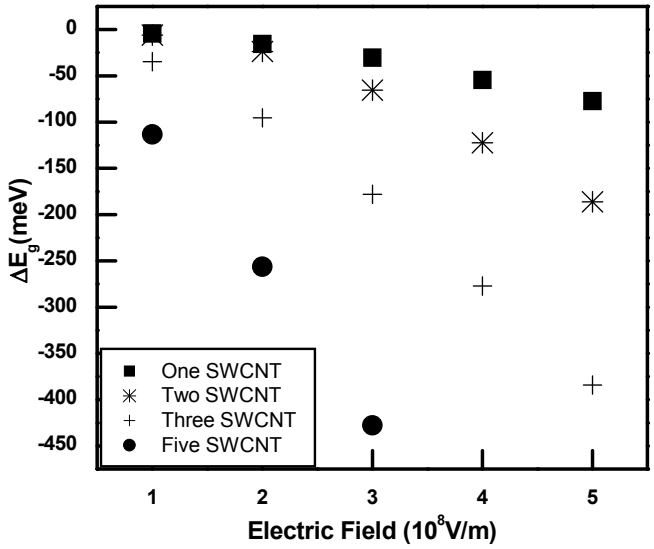

Fig.5 Energy band gap reduction versus applied electric field for different number of s-SWCNTs.

4. The Current

The current along an individual SWCNT body is theoretically ballistic, it follows [6]

$$I = \frac{4ek_BT}{\hbar}\sum_{\forall i} \ln\left(1+\exp\left(\frac{-E_i-eV_s}{k_BT}\right)\right) - \ln\left(1+\exp\left(\frac{-E_i-eV_D}{k_BT}\right)\right) \quad (2)$$

where E_i is the sub band energy levels, i is the number of sub bands contribute to the transport. For the semiconducting nanotubes of small diameters, the ground state is the most contributing to the electron transport. Fig.6 presents the quasi-ballistic current as function of the normalized electric field along the carbon nanotube.

The contact resistance is then included in the current equation:

$$I_{ds} = \frac{V_{ds}}{\frac{V_{DS}}{I}\Big|_{lowfield} + R_c} \quad (3)$$

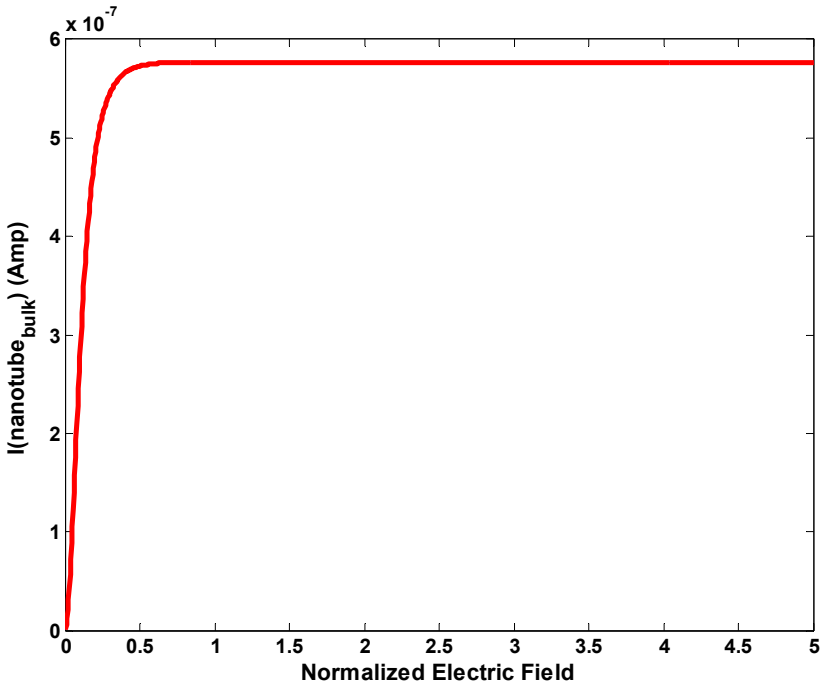

Fig.6

Fig. 7 presents the overall current versus the applied voltage. The current amplitude degrades due to the value of the contact resistance.

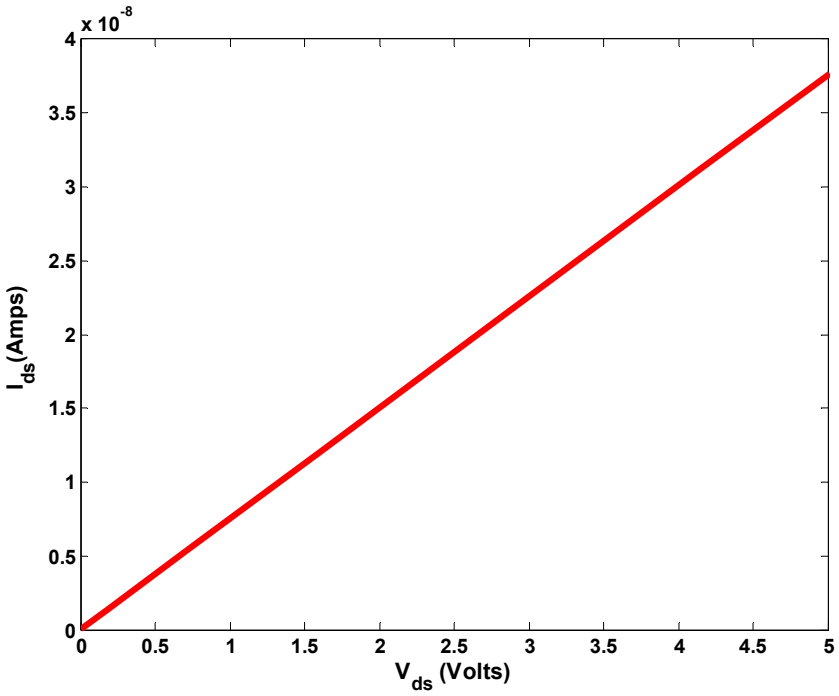

Fig.7

By introducing the coupling between the nanotubes discussed earlier, Fig.8 presents the overall current for an individual nanotube along with the current of many nanotubes. The current of the many nanotubes device is significantly higher due to coupling between the nanotubes and the significant reduction of the overall contact resistance.

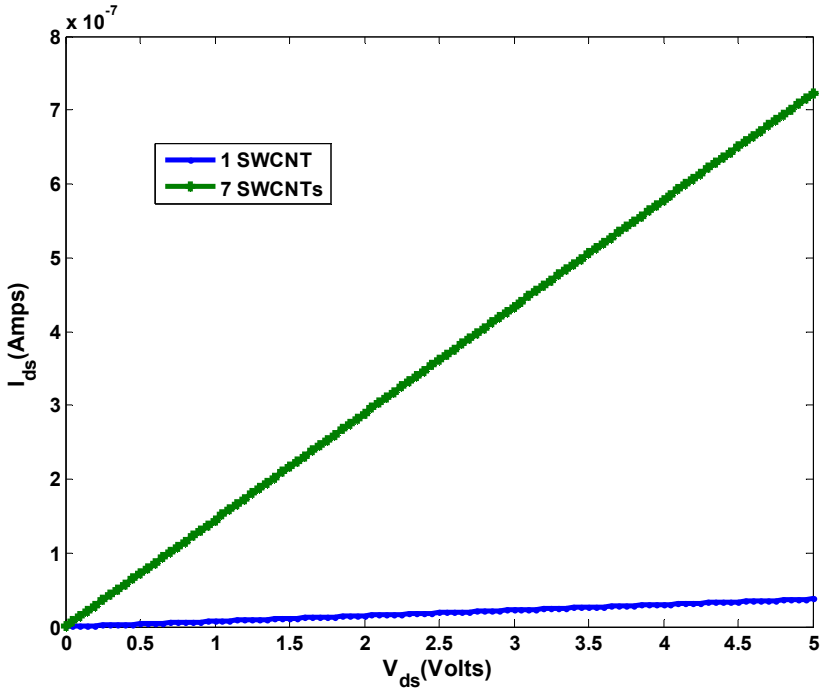

Fig. 8

For many nanotubes, an extra control voltage has been applied to represent the transverse electric field. Fig.9 presents the current with and without applying the voltage control signal across the aligned nanotubes. The current increases by applying the control voltage due to the decrease of the energy band gap of the system.

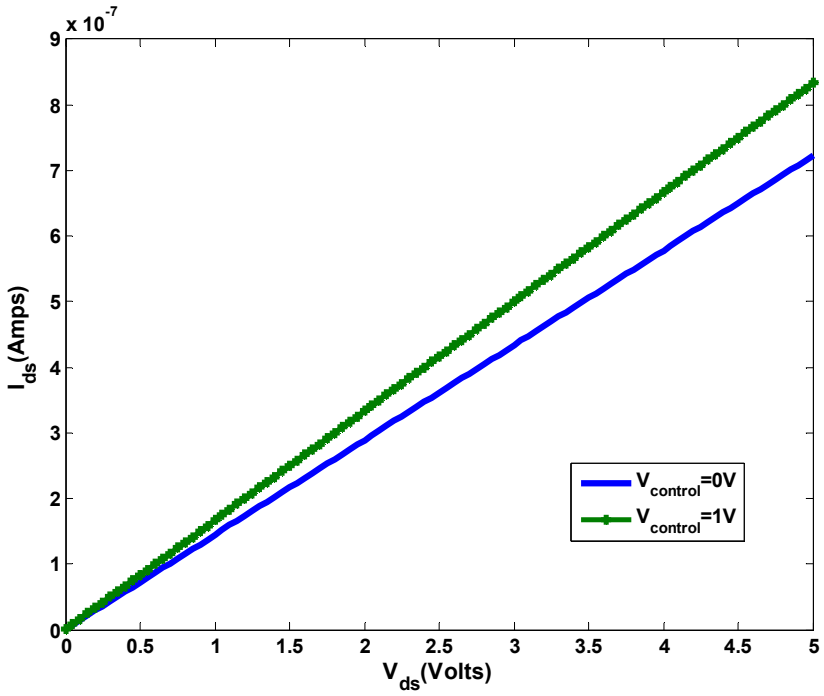

Fig. 9 The current calculated with/out applying transverse electric field ($V_{control}$) for 7 nanotubes device

5. Measurements

In order to verify the theoretical work developed previously, a four-electrode test structure has been fabricated using lithography techniques (photolithography for the micro-dimensions and e-beam lithography for the nano-dimensions). The carbon nanotubes are then deposited between two of the electrodes using the dielectrophoresis method [7]. An electrical field is created by applying a potential difference between the two vertical electrodes. Fig. 10 shows scanning electron microscope (SEM) pictures of the fabricated device consisting of four palladium (Pd) nano-electrodes.

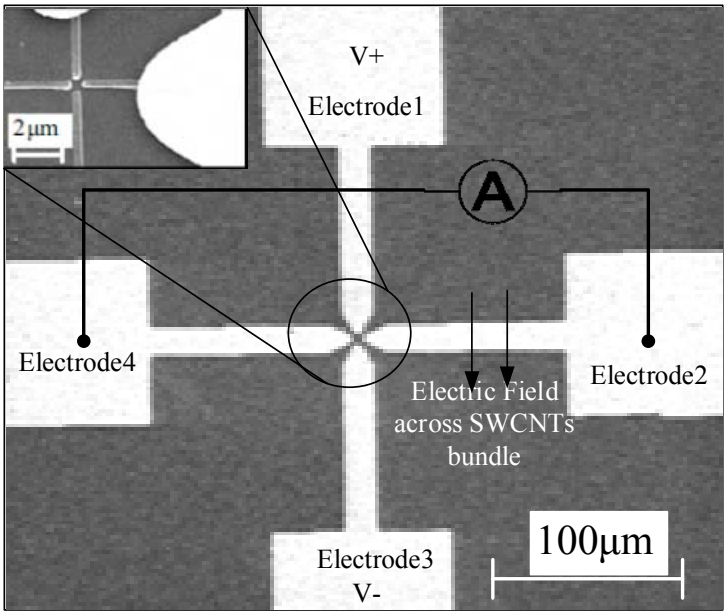

Fig. 10 SEM pictures of the measurement setup where an electrical field is vertically applied while I-V characteristics are realized along the carbon nanotubes axis. The inset zooms in to highlight the nanoscale device where the width of the nano-electrodes is 300 nm and the gap separating them is 500 nm.

An electric field is applied perpendicularly to the semiconducting carbon nanotubes axis by applying a DC voltage between electrodes 1 and 3 as shown in Fig. 10. Then, I-V characteristics along the carbon nanotubes between electrodes 2 and 4 are measured using a Keithley 236 source measure unit. By augmenting the electrical field across the s- SWCNTs, the measured bias current along the carbon nanotubes increases as shown in Fig. 11. In other words, the measured conductance increases due to the energy band gap reduction caused by the applied external electric field. A bias current enhancement is observed when applying control voltage across the bundled SWCNTs equivalent to an Electric Field of $4x10^6$ *V/m* considering the distance between the electrodes and the applied potential. From these measurements, it is obvious that when an electric field is applied across the SWCNT bundle the current increases. This increase in the measured bias current is explained by the idea proposed earlier, that the coupling effect between the SWCNTs

bundle helps generating free carriers. Consequently, these free carriers concentration enhances the conductivity and reduces the energy band gap.

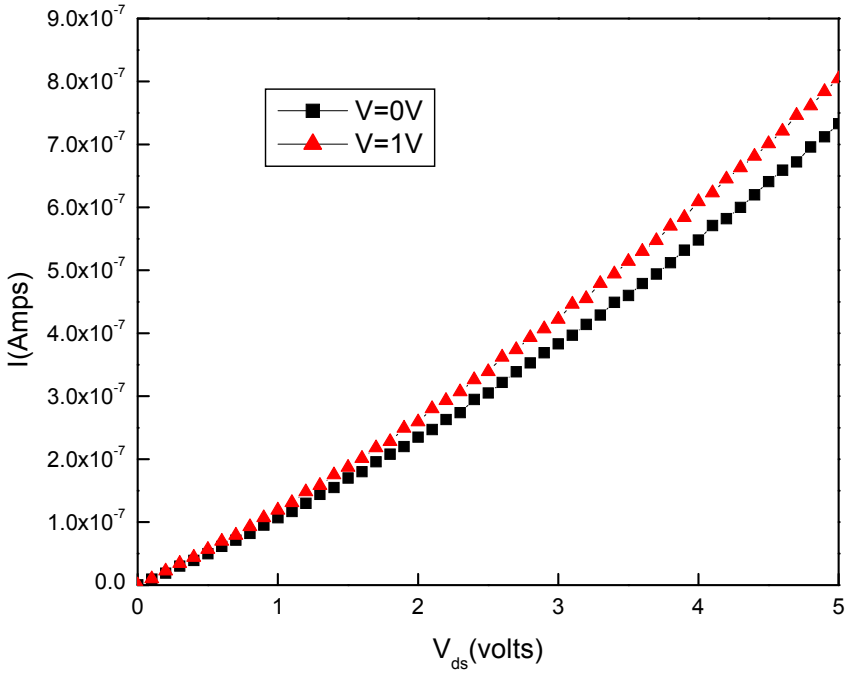

Fig. 11 The current measured with/out applying transverse electric field ($V_{control}$) for 7 nanotubes device

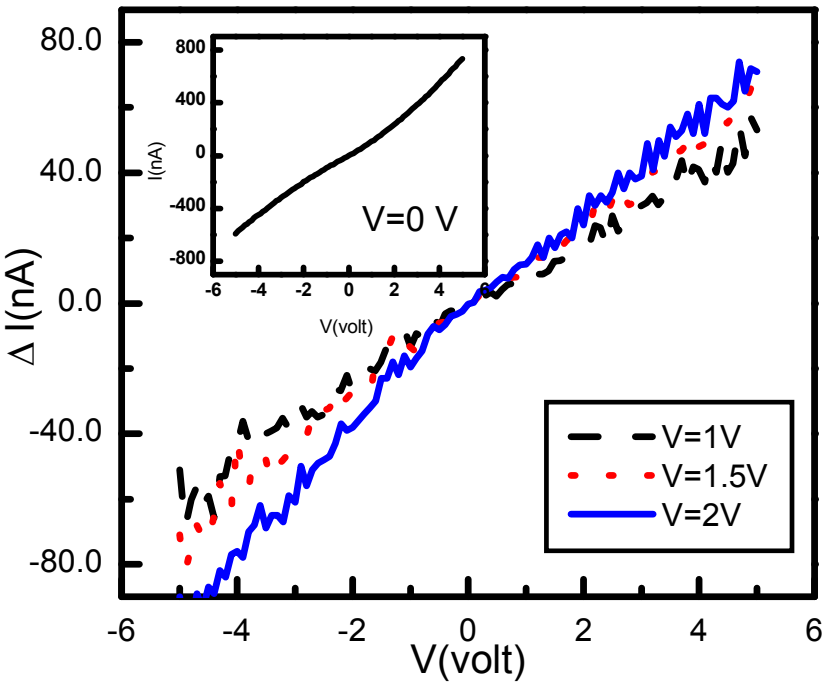

Fig. 12 Variation of the measured bias current along the aligned s-SWCNTs for different DC applied voltage across the bundle; the inset shows the I-V characteristics along the aligned s-SWCNTs without applying DC voltage

The change in the current due to the applied control voltage is plotted in Fig. 13 along with the measured current. The change in the current reflects more than 10% of the original current.

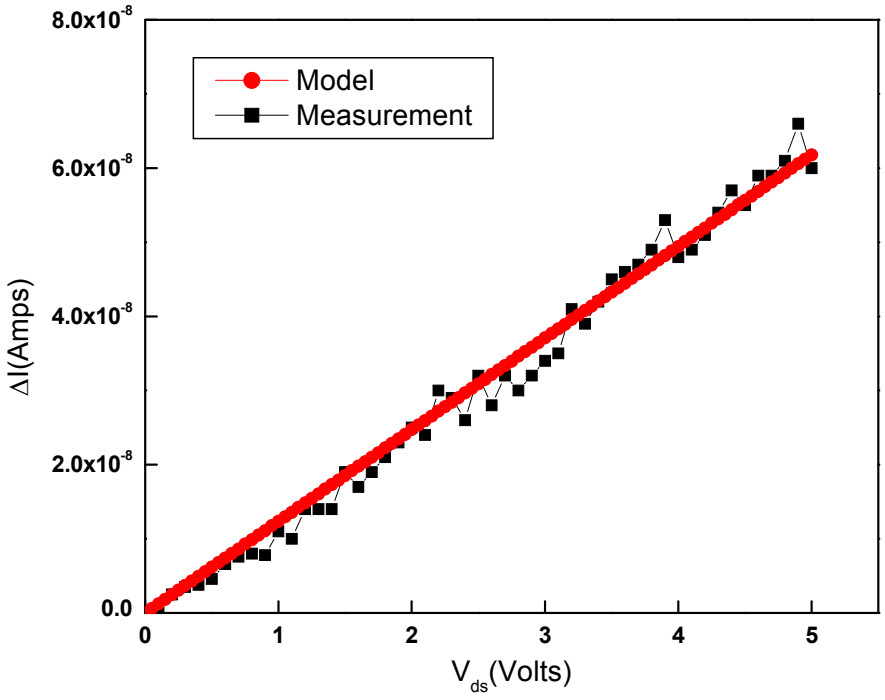

Fig. 13 Comparison between the calculated and measured change of the current due to applied control voltage

Tuning the band gap of this prototype device will enable tuning the operating frequency of the device. Controlling the material energy band gap of the device has a direct impact in THz applications. First the typical semiconducting SWCNT absorption is in the mid infra-red (IR) region. By applying an electric field, the absorption can be tuned to Far IR and even reach the THz frequency band. Second, metallic carbon nanotubes have anisotropic conductance in the THz range. So, by inserting semiconducting carbon nanotubes and tuning their energy band gap, the device will modulate the THz signal.

6. Conclusion

Theoretical and experimental results have demonstrated the possibility to tune the energy band gap by applying an external electrical field across aligned arrays of semiconducting single-walled

carbon nanotubes. The developed analytical model predicts that the coupling effect between semiconducting single-walled carbon nanotubes enhances the energy band gap reduction compared to an individual s-SWCNT. The measurements showed an increase of around 10% in the conductance for $4x10^6$V/m applied transverse electrical field across the aligned bundled carbon nanotubes. The obtained results show promise for s-SWCNTs to be used in THz frequency range.

References

[1] A. Jorio, G. Dresselhaus and M. S. Dresselhaus. Carbon Nanotubes: Advanced Topics in the Synthesis, Structure, Properties, and Applications (Springer 2008).

[2] L. Ren, C. L. Pint, L. G. Booshehri, W. D. Rice, X. Wang, D. J. Hilton, K. Takeya, I. Kawayama, M. Tonouchi, R. H. Hauge and J. Kono. Carbon nanotube terahertz polarizer. *Nano Lett. 9(7),* pp. 2610-2613. 2009.

[3] Y. Wang, S. K. R. Pillai, and M. B. Chan-Park, " High-performance partially aligned semiconductive single-walled carbon nanotube transistors achieved with a parallel technique," *Small* **9**, 2960–2969 (2013).

[4] T. Vodenitcharova and L. C. Zhang. Effective wall thickness of a single-walled carbon nanotube. *Physical Review B (Condensed Matter and Materials Physics) 68(16),* pp. 165401-1. 2003.

[5] J. Faist, F. Capasso, D. L. Sivco, C. Sirtori, A. L. Hutchinson and A. Y. Cho. Quantum cascade laser. *Science 264(5158),* pp. 553-556. 1994.

[6] S. Hamieh, "Improving the RF Performance of Carbon Nanotube Field Effect Transistor," Journal of Nanomaterials, vol. 2012, 724121, 7 pages, Feb. 2012.

[7] J. Li, Q. Zhang, N. Peng and Q. Zhu. Manipulation of carbon nanotubes using AC dielectrophoresis. *Appl. Phys. Lett. 86(15),* pp. 153116 (3 pp.). 2005.

EUROPEAN MICROWAVE ASSOCIATION

Prof. A. Vander Vorst
Rue Louis de Geer 6
B-1348 Louvain-la-Neuve
Belgium
vandervorst@eumw.org

TO WHOM IT MAY CONCERN

Louvain-la-Neuve, March 31, 2015

On behalf of **EuMA**, the European Microwave Association, Prof. André VANDER VORST is granting Mr. Asmaa ELKADI permission to include parts of the paper by A. Elkadi, E. Decrossas, S.Q. Yu, H.A. Naseem, S.M. El-Ghazaly, « Controlling the Energy Band Gap of Aligned Semiconducting Single-Walled Carbon Nanotubes for THz Modulator », *Proc. 7th European Microwave Integrated Circuits Conference*, pp. 270-273, Amsterdam, The Netherlands, October 2012, in his doctoral dissertation at University of Arkansas, Fayetteville, USA. This permission is granted on condition that the source of the material, including authors, date and copyright owner are acknowledged, the copyright owner being the European Microwave Association. **EuMA**.

André VANDER VORST
EuMA Secretary-Treasurer

T+32 (0)10 390 068
F+32 (0)10 390 001

VAT BE 0464.401.356

IBAN BE40 2710 6139 4463
Fortis 271-0613944-63

UNIVERSITY OF ARKANSAS
College of Engineering
Department of Electrical Engineering

April 10th, 2015

To whom it may concern,

I certify that Ms. Asmaa Elkadi is the first author of the paper titled "Controlling the Energy Band Gap of Aligned Semiconducting Single-Walled Carbon Nanotubes for THz Modulator "presented in IEEE European Microwave Integrated Circuits Conference, Oct. 2012. Ms. Elkadi completed majority (more than 51%) of this research and writing this paper.

Prof. Samir M. El-Ghazaly
Distinguished Professor
Electrical Engineering
Office: 3169 Bell Engineering Center
Phone: 479-575-6048
E-mail: elghazal@uark.edu

Chapter VII. Conclusion

An analytical potential function is introduced to describe the charge density of (semiconducting single-walled carbon nanotube) s-SWCNTs. Schrödinger's equation is then solved by implementing the proposed analytical potential function. The wave function of an individual s-SWCNT as well as multi s-SWCNTs organized inside a bundle is obtained from the semi-analytical approach. The potential function is developed to describe different kinds of nanotubes. For instance double walled carbon nanotubes are solved and comprehensive quantum solution is provided. The calculated results are in a good agreement with published data that double-walled carbon nanotubes are semi-metallic regardless the electronic type of its composing carbon nanotubes.

Additionally, a comprehensive study of the coupling effect between s-SWCNTis demonstrated considering different configurations. In the absence of an external electric field, the coupling between the nanotubes is equally distributed among the SWCNT in the bundle. Then by applying an external electric field, our data show that not only the coupling is now localized between the first nanotubes encounter by the electric field along its direction, but also the energy band gap of the bundle is greatly enhanced. This is an important property for terahertz or far infrared optical applications where the development of devices in this spectrum is limited by the current semiconductor material properties.

The model is then developed to incorporate realistic parameters to decrease reported discrepancies between the theory and measurements. The model provides a physical insight and thorough understanding of the different factors affecting contact resistance values. The model is developed for an individual SWCNT. A parametric study has been performed to demonstrate that the critical factor for improving the device performance and minimizing the contact resistance is ensuring the overlap length between the nanotube

and the metallic pad is longer than the effective length. The model results have been compared with measurements and a good agreement has been observed. This study provides an understanding of key parameters and limitations that degrade the SWCNT-based devices and suggest techniques to enhance their performance. A test structure is then fabricated and a new method for depositing high density s-SWNTs devices is introduced to improve very large scale integration of carbon=based electronic devices. High number of yield with high aligned high density of higher than 40 s-SWCNTs/1μm and sheet resistance less than 10 KΩ/□ is achieved. I-V measurements are realized to show the low electric resistance achieved with 2.5% tolerance. Raman Spectroscopy is carried out and it shows typical spectrum for highly pure and uniforms-SWCNTs sample.

The model that was developed for individual SWCNT, is used to build a model for arrays of aligned SWCNTs. The model has included the electrostatic and frequency dependence in a schematic circuit to represent the structure. The proposed model is compared to the measurements, and it shows a good agreement. The frequency response has been calculated for various number of nanotubes per device showing linear increase for low density and it saturates with the increase of the number of nanotubes per device. The model helps understand the limitations affecting SWCNTs-based devices followed by some suggested techniques to enhance the performance.

Theoretical and experimental results have demonstrated the possibility to tune the energy band gap by applying an external electrical field across aligned arrays of semiconducting single-walled carbon nanotubes. The developed analytical model predicts that the coupling effect between semiconducting single-walled carbon nanotubes enhances the energy band gap reduction compared to an individual s-SWCNT. The measurements showed around 10% in the conductance for $4x10^6$V/m applied transverse electrical field across the aligned bundled carbon nanotubes. The

obtained results provide innovative approaches for terahertz or far-infrared frequency components requiring a small energy band gap semi-conducting material.